A Comparison of Conceptual Rainfall-Runoff Modelling Structures and Approaches for Hydrologic Prediction in Ungauged Peatland Basins of the James Bay Lowlands

by

Jean-Sébastien Bouffard

A thesis submitted to the Faculty of Graduate and Postdoctoral Affairs in partial fulfillment of the requirements for the degree of

Master of Science

in

Geography

Carleton University
Ottawa, Ontario

Abstract

James Bay Lowland peatlands are environments with unique hydrologic characteristics that challenge some basic assumptions embedded within many hydrology models, including topographically-driven lateral flows and hydrologic connectivity of all terrestrial landscape elements within the stream network. With increasing resource development in northern lowland regions of Canada, more rigorous and honest appraisal of modelling capabilities and deficiencies is warranted. This study was initiated with the following two objectives: (1) to compare the performance of two popular conceptual rainfall-runoff models, TOPMODEL and HBV, for rainfall-runoff simulation in a James Bay Lowland peatland complex in the James Bay Lowlands, and (2) to compare regionalization methods to maximize the predictive value of available landscape information to improve model calibration using HBV. HBV was found to outperform TOPMODEL, which was altogether unsuitable for this environment. Regionalization analyses and results favoured empirical methods such as artificial neural networks to improve predictive capabilities of the HBV model.

Acknowledgements

I would like to express gratitude to my supervisor, Dr. Murray Richardson, whose guidance, knowledge, and enthusiasm has significantly contributed to both my undergraduate and graduate experience. I appreciate everything that he has done for me throughout the many years we've worked together. He's assisted me in various ways and has provided me with many experiences that I will never forget, such as travelling to James Bay and throughout Europe. Thank you Murray.

Besides my supervisor, I would like to thank members of the Muskeg Crew, specifically Dr. Pete Whittington who has always made himself available for advice and providing me with data.

I must acknowledge members of my committee: Dr. Scott Mitchell, for his counsel.

I would like to thank my family for the support they've provided me over the years. Without them none of this would have been possible. I would like to thank my fiancée, Sam, for her support and encouragement.

Table of Contents

List of Tables

List of Figures

List of Appendices

Chapter 1: Introduction

Peatlands, also known as mires or muskeg, are wetlands largely consisting of peat and encompass an estimated 400 million ha (3%) of the Earth's surface. The largest proportions of peatlands are located in humid climates in the northern hemisphere (Franzen, 2006). Northern peatlands are a significant store of soil carbon (C), sink of carbon dioxide (CO_2), and source of atmospheric methane (CH_4). Additionally, they are a lesser source of nitrous oxide (N_2O) (Strack, 2008). Estimates of carbon stored in northern peatlands range from 120 to 500 Gt (Gorham, 1991; Franzen, 2006; Yu, 2012), accounting for approximately 26% of all terrestrial carbon accumulated during the postglacial period (Smith et al., 2004). At a global scale, peatlands play an important role in stabilizing greenhouse gases (GHG). The importance of this role has long been established in scientific literature, and recognized by the United Nations Framework Convention on Climate Change (UNFCCC) (IPCC, 1997).

This acknowledgement supports advancing research in understanding the role of northern peatlands. One of the prominent scientific disciplines interested in northern peatlands is *peatland hydrology*.

Peatland hydrology is a sub-discipline of hydrology. The prominence of this sub-discipline is attributed to the importance of the water balance in peatland environments. The water balance is a framework for conceptualizing fluxes and stores of water in a system. Different elements of the water balance have a role in various aspects related to peatlands. For example: ecological characteristics (Hilbert et al., 2000; Belyea & Clymo, 2001), geomorphologic characteristics (Ingram, 1982; Siegel, 1983; Glaser et al., 2004), GHG dynamics (Holden, 2005), and dissolved organic carbon (Schiff et al., 1998; Pastor et al., 2003; Worral et al., 2006). The water balance underpins the fundamental processes in peatland hydrology, ecology, geomorphology, or GHG dynamics. Water balance fluxes of a watershed can be obtained through monitoring of streamflow, evapotranspiration, precipitation, etc. In remote northern peatland regions, however, such monitoring is expensive and difficult.

The importance of advancing research in peatland hydrology is indisputable considering the role of peatlands in stabilizing GHGs. The study focuses on rainfall-runoff simulation in northern peatlands in order to address two overarching questions: (1)

do commonly accepted conceptual approaches to rainfall-runoff simulation work effectively in northern lowland regions, and (2) to what extent can landscape information be used to reduce error and uncertainty in rainfall-runoff simulations in these regions, where historical hydrologic monitoring records are limited?

Hydrological models or modelling is the application of formalized mathematical or empirical relationships that describe hydrological processes. These formalized relationships reflect our knowledge of a hydrological system. Each environment has different topographic, land cover, and vegetation characteristics that influence the rainfall-runoff relationship. These characteristics must be considered when selecting an appropriate hydrological model to achieve optimal results.

Hydrologic models fall under two broad categories: deterministic and probabilistic. Deterministic models are those where the parameters and states result in a precise outcome without random variation. Probabilistic models have random variation and express the output in terms of probability. In this study the deterministic approach was taken, with a focus on testing how model structures and landscape-base regionalization of model parameters affect rainfall-runoff simulation results.

There are three main groups of deterministic models: empirical, conceptual, and physical-based. Empirical models establish a link between the input and output often applying approaches like regression that is mathematically simpler than conceptual and physical-based models (Aghakouchchak & Habib, 2010). Conceptual models generalize the governing hydrological processes using simple mathematics. Physically-based models solve partial-differential equations of mass and momentum that describe the hydrological processes in greater detail (Aghakouchchak & Habib, 2010). In this study, the conceptual modeling was favoured over physically-based approaches, for several reasons.

The first reason for choosing the conceptual modelling approach is to generalize complex hydrological relationships (Whitfield et al., 2009). An all-encompassing representation of the hydrological processes in northern peatlands would be difficult, if not impossible (Whitfield et al., 2009; Morris et al., 2011). The second reason is the reduced number of model parameters. Model parameters are values that are adjusted during calibration to improve a model's representation of hydrologic processes. Empirical models generally require the fewest number of parameters. However, empirical

models are not always representative of the hydrological processes and efforts to increase our understanding of northern peatlands require a model with some physical basis. At the other end of the spectrum, most physically-based models require a large number of parameters to represent the entirety of the hydrological processes. Increasing the number of parameters complicates the calibration process (Jakeman & Hornberger, 1993), and often requires a greater volume of data. Conceptual models provide a compromise between simple but baseless and detailed but too complex. They typically require a lower number of parameters than physically-based while maintaining some physical basis through its generalization of the dominant hydrological processes. Within this category it is necessary to identify whether a groundwater model, or a rainfall-runoff model, is most appropriate for the system under investigation.

Conceptual groundwater models focus on simulating recharge and discharge in groundwater systems, whereas conceptual rainfall-runoff (CRR) models focus on simulating rainfall-runoff of surface and near-surface processes. CRR models were selected as the focus of this study for two reasons: (1) surface and near-surface processes account for the majority of runoff in peatlands and specifically at the research site (Metcalfe & Buttle, 2001), and (2) areas of research related to GHG in peatlands focus on surface and near-surface processes (Bubier et al., 1995; Holden, 2005).

In this study, two popular CRR models were selected, both of which have dominated the scientific literature. TOPMODEL (topography based hydrological model) and HBV (Hydrologiska Byråns Vattenbalansavdelning) are CRR models both developed in the mid-1970s that emphasize surface and near-surface hydrological processes (Bergström, 1976; Beven & Kirkby, 1979; Beven et al., 1995; Bergström, 1995). Since the 1970s there have been numerous applications of both models in various research environments. Unfortunately, applications in northern peatland complexes have not been reported with only few studies in similar environments for both TOPMODEL (Lane et al., 2004), and HBV (Engeland & Hisdal, 2009). This scarcity warrants an examination of both CRR models in northern peatland complexes.

The scarce documentation of TOPMODEL and HBV in this environment is problematic because of the influence of the low-gradient and the highly patterned nature of bog and fen complex on surface flow (Price & Maloney, 1994). Specifically, there are

three notable hydrological characteristics that challenge basic assumptions and structural components of TOPMODEL and HBV: (1) representation of lateral flow, (2) representation of the storage-discharge relationship, and (3) representation of topology. In Richardson et al. (2012), the lateral exchange of water between distinct land cover types was highlighted as a poorly understood aspect of peatland hydrology. This knowledge deficiency implies that formalization of storage and routing processes in these landscapes are probably inadequate (Quinton et al., 2003). Similarly, Whitfield et al. (2009) emphasized the need to better formalize the complex storage-discharge relationship in northern peatlands. Inadequate representation of this complex relationship has hindered the predictive capability of many hydrological models (Davidson & Kamp, 2013). Finally, the topological arrangement of land cover has been recognized as an important factor in the evolution and behaviour of peatlands that influences streamflow characteristics (Quinton & Roulet, 1998; Spence et al., 2013). This challenges the application of TOPMODEL and HBV because they do not consider any complex topological arrangement. This examination of TOPMODEL and HBV will not explicitly assess each listed challenge. Instead, they are assessed as a whole based on the predictive capability of each model.

Both TOPMODEL and HBV require model calibration. The traditional approach to model calibration requires historical data to adjust model parameters. The adjustment of model parameters is necessary to provide adequate model performance. The performance of a model is measured based on its ability to adequately simulate the historical data. The historical data for model calibration of CRR models is streamflow data. Streamflow data is acquired from *in-situ* monitoring sites. To successfully calibrate CRR models five to ten years is the recommended length of the streamflow data (Boughton, 2007). To fulfill this requirement monitoring programs must be implemented. As previously noted, establishing monitoring programs in northern peatlands can be expensive and difficult due to the remoteness of these environments. This brings us to our second overarching question previously listed above: To what extent can landscape information be used to reduce error and uncertainty in rainfall-runoff simulations in these regions, where historical hydrologic monitoring records are limited?

It is necessary to reassess the traditional approach of model calibration to reduce error and uncertainty in rainfall-runoff simulations. The reassessment of traditional model calibration has been an area of interest in hydrology. As such, this interest was prioritized by the International Association for Hydrological Sciences (IAHS) with the inauguration of the Prediction in Ungauged Basins (PUB) initiative. The term ungauged basin refers to a catchment with no streamflow data that requires other available data for model calibration. PUB has been an ongoing international effort to promote dialogue to address specific areas of interest in hydrology, notably efforts in ungauged basins. An area of interest shared between PUB and this study is maximizing the predictive value of available information for ungauged basins (e.g. Pomeroy et al., 2013).

This shared interest is an extensive area of research (Sivapalan et al., 2003) that stems from heterogeneity in space, time, and scale, variability in the available information, differing model structures, and many other factors. From the items above, spatial heterogeneity is perhaps the most important factor to consider when considering variability of the dominant hydrological processes. The combination of characteristics of the hydrological processes and of the environment is directly reflected in the model parameters (Beven, 2000). To address the issue of spatial variability a non-traditional calibration approach known as *regionalization* is applied (Pilgrim, 1983; Kleeberg, 1992; Bloschl & Sivapalan, 1995).

Regionalization is a model calibration technique that transfers information from gauged (well-monitored) to ungauged (poorly monitored or unmonitored) basins to improve model effectiveness and reduce predictive uncertainty (Kleeberg, 1992; Bloschl & Sivapalan, 1995; Parajka et al., 2005). The quality of the predictive capability of the ungauged site is dependent on prior analysis to determine a suitable *donor*(s) or to adequately estimate model parameters. Donor refers to a gauged site considered a candidate to transfer information to an ungauged site. To determine a suitable donor(s) or estimate model parameters, an array of regionalization techniques is available (Bloschl, 2005; Parajka et al., 2005; Oudin et al., 2008).

Regionalization techniques often rely on landscape analysis as a basis to determine suitable donor(s) or model parameter values. This approach has been effective in linking landscape elements as first-order controls on hydrological behaviour (Marechal

& Holman, 2005; Mazvimavi et al., 2004, 2005; Pallard et al., 2009; Cheng et al., 2012; Lyon et al., 2012). The application of landscape analyses is often dependent on data acquired using remote data acquisition techniques. These acquisition techniques significantly reduce cost and have received considerable attention (Huisman et al., 2003; Lunt et al., 2005; Parajka & Bloschl, 2006; Jones et al., 2008; Parajka & Bloschl, 2008; Schumann et al., 2008; Aghakouchak et al., 2010). The extent of regionalization efforts in the last decade as a result of PUB has greatly advanced the field of hydrology (Hrachowitz et al., 2013). Despite these advances, regionalization efforts in northern peatlands remain limited to non-existent.

The lack of documentation on CRR models and regionalization applications in James Bay Lowland peatlands is problematic due to the unique characteristics of the landscape, such as the low-gradient and the highly patterned nature of bog and fen complex. Following the key outcomes of this review, the research questions have developed around two main objectives:

- assess and compare the predictive capability of both TOPMODEL and HBV in a northern peatlands complex; and
- evaluate regionalization methods to maximize the predictive value of information acquired from landscape analysis.

Chapter 2 describes the study site and outlines the data applied in the research. Chapter 3 outlines the methods that are central to both objectives, the model structures of both TOPMODEL and HBV, the methods applied in the first objective, and the methods applied in the second objective. Chapter 4 presents the results. Chapter 5 is a discussion of the results, and Chapter 6 presents overall conclusions of the study.

Chapter 2: Study Site & Data

2.1 Study Site

The study site is in proximity to the De Beers Victor Diamond Mine (52° 49' 15", 83° 53' 00") 90 km west of Attawapiskat, Ontario, Canada. Construction of the Victor Diamond mine began in February 2006 and it was operational in 2008. The mine is open-pit and covers a surface area of approximately 15 hectares. The site is in the interior of the James Bay Lowland (JBL) ecoregion, which is part of the world's third largest wetland complex (Riley, 2011). This portion of the ecoregion is almost entirely covered by patterned bog and fen systems (Riley, 2011). In both systems, common vegetation groups are coniferous trees, mosses, sedges, sphagnums, and shrubs. Permafrost is relatively absent, and is categorized as sporadic and discontinuous.

The study site is in a subarctic region that has a humid continental climate regime. This climate regime is described as humid with severe winters, no dry season, and warm summers. The climate normals of the surrounding areas for the 1971 to 2000 period are listed in Table 2.1-1.

Table 2.1-1. Climate normals from 1971 to 2000 of regions in proximity to the study site (Environment Canada, 2013).

Location	Daily Average (C°)	Rainfall (mm)	Snowfall (cm)	Wind Speed (Km/h)	Distance from Study Site (Km)
Lansdowne House	-1.3	488.7	241.6	14.2	~300 West-South-West
Moosonee	-1.1	493.9	212.9	11.3	~250 South-East
Cochrane	0.6	583.2	296.8	N/A	~460 South-East
Timmins	1.3	558.1	313.4	11.9	~510 South-East

The structure of the geological stratification has three strata. The first stratum is a mixture of peat and silt. This stratum has an average depth of 1.5 m in fens and 2 - 2.5 m in bogs. The second stratum is composed of marine clay sediment and has an average

depth of 20 m. The third stratum is limestone that has an average depth of 180 – 200 m. Mining activities in the region have resulted in the depressurization of the upper-portion of the limestone stratum. The effect of the depressurization has created a cone of depression resulting in a drawdown area of ~65 km^2 (Itasca, 2011; Whittington & Price, 2012; Whittington, 2013).

The study site includes eight headwater catchments that cover an extent of ~1600 km^2. They are hereafter labeled as follows: North-North Granny Creek (NNGC), South-North Granny Creek (SNGC), North Granny (NG.001), South Granny (SG.001), Tributary 3 (Trib 3), Tributary 5 (Trib 5), Tributary 5A (Trib 5A), and Tributary 7 (Trib 7). The catchments contribute to the Nayshkootayaow River that flows into the Attawapiskat River. The average elevation of the eight catchments is 92 m above mean sea level. The study region is characterized as a low-gradient environment with an average slope of 0. 1%. The catchments span a relatively large range in gross drainage area (GDA) from ~12 km^2 to ~215 km^2 (Table 2.1-2).

Table 2.1-2. Gross drainage area (GDA) and perimeter of catchments included in this study.

Catchment	GDA (km^2)	Perimeter (km)
NNGC	12.40	38.40
SNGC	19.80	37.90
Trib 3	105.60	94.30
Trib 5	215.70	145.00
Trib 5A	27.70	46.90
Trib 7	88.00	81.70
NG-001	42.90	61.40
SG-001	34.80	64.40

NNGC, SNGC, NG.001, and SG.001 are in close proximity to the De Beers Victor Diamond Mine and are within a *cone of depression*. The cone of depression is the area surrounding the mine where the water table drops and forms a cone due to pumping. To prevent streams from drying up or any other unwanted effect, a pumping station has been supplementing water from ~8,200 m^3 per day to ~85,000 m^3 per day (Whittington, 2013). The other catchments are not within the cone of depression. The boundaries of each catchment are illustrated in Figure 2.1-1 to 2.1-6.

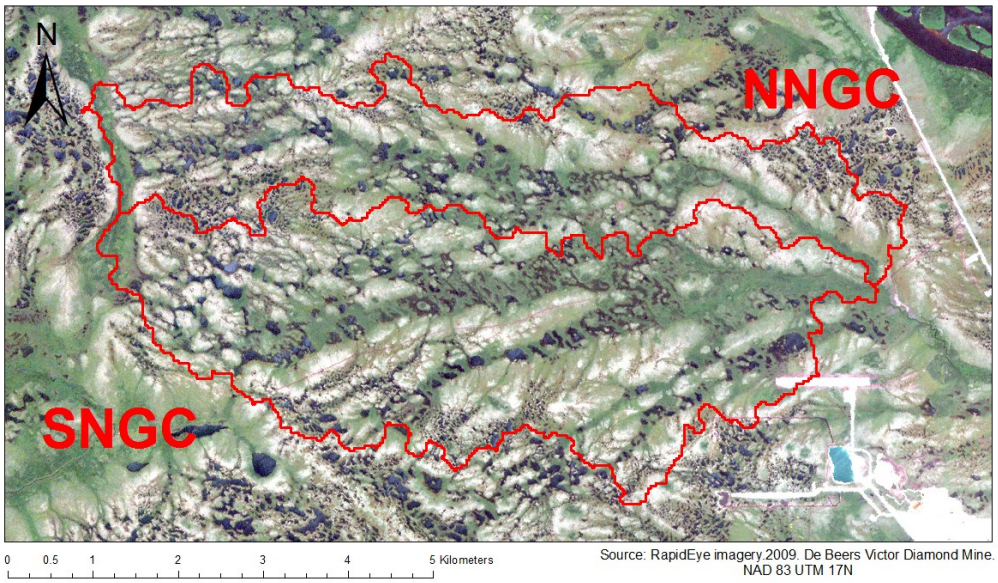

Figure 2.1-1. Boundaries (in red) of catchments NNGC (12.40 km^2) and SNGC (19.80 km^2).

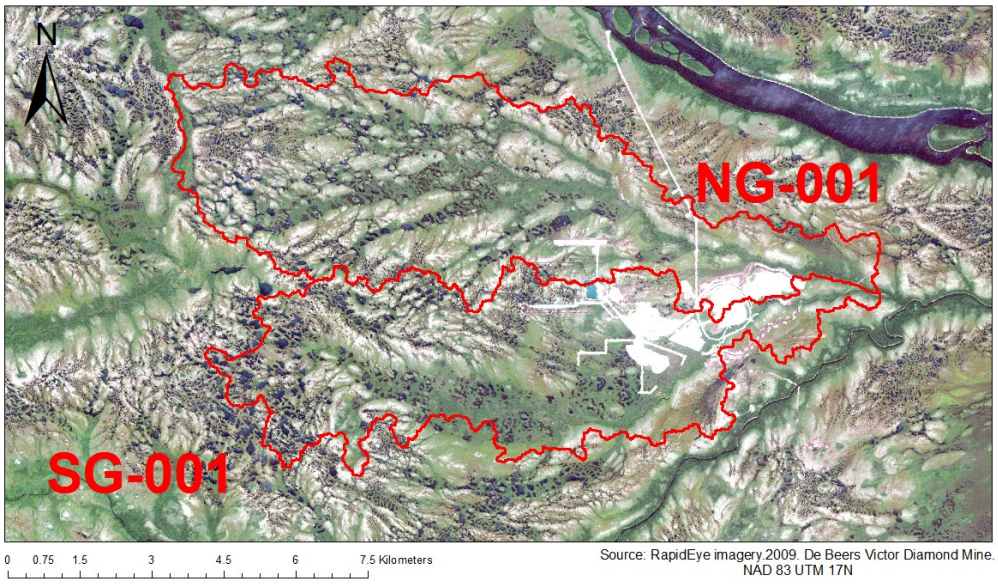

Figure 2.1-2. Boundaries (in red) of catchments NG.001 (42.90 km^2) and SG.001 (34.80 km^2).

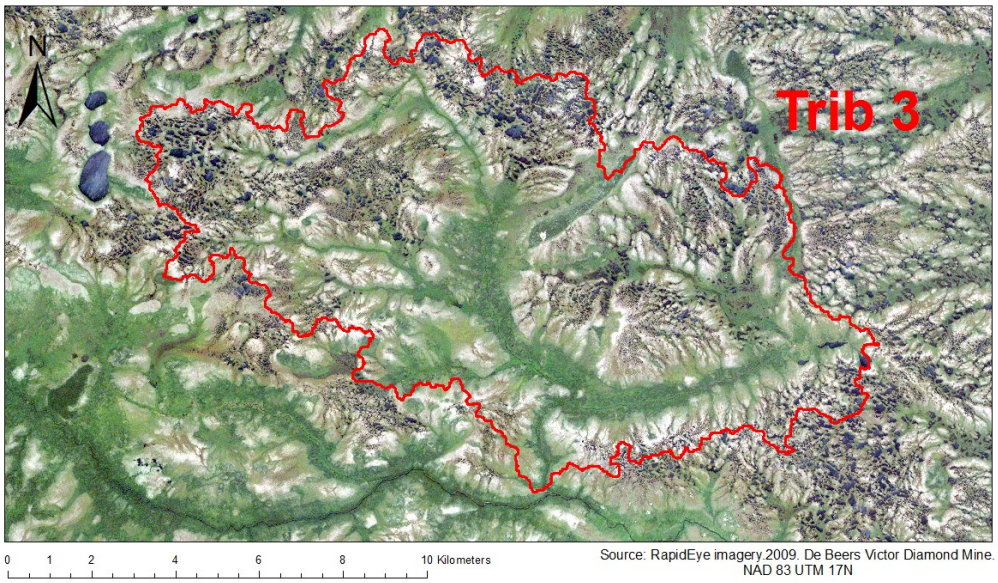

Figure 2.1-3. Boundary (in red) of catchment Trib 3 (105.60 km^2).

Figure 2.1-4. Boundary (in red) of catchment Trib 5 (215.70 km^2).

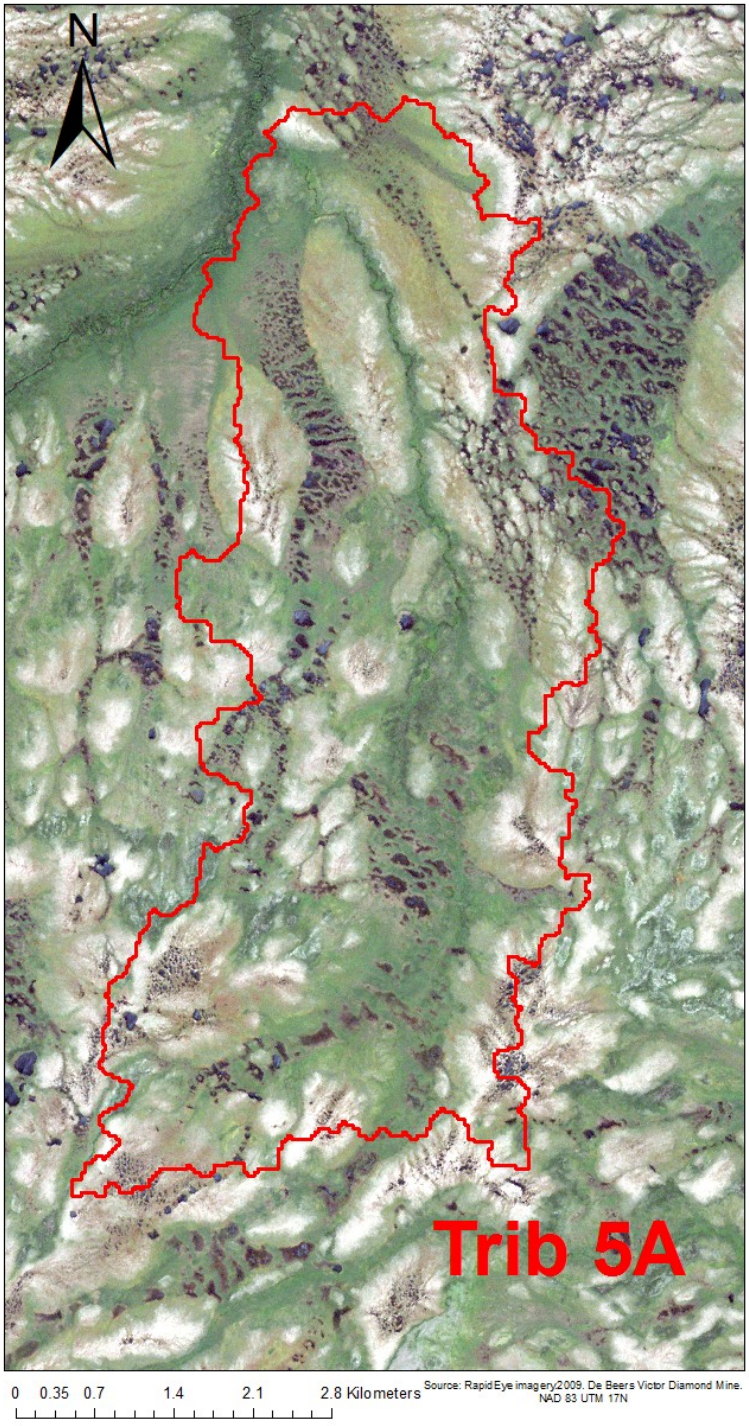

Figure 2.1-5. Boundary (in red) of catchment Trib 5A (27.70 km^2).

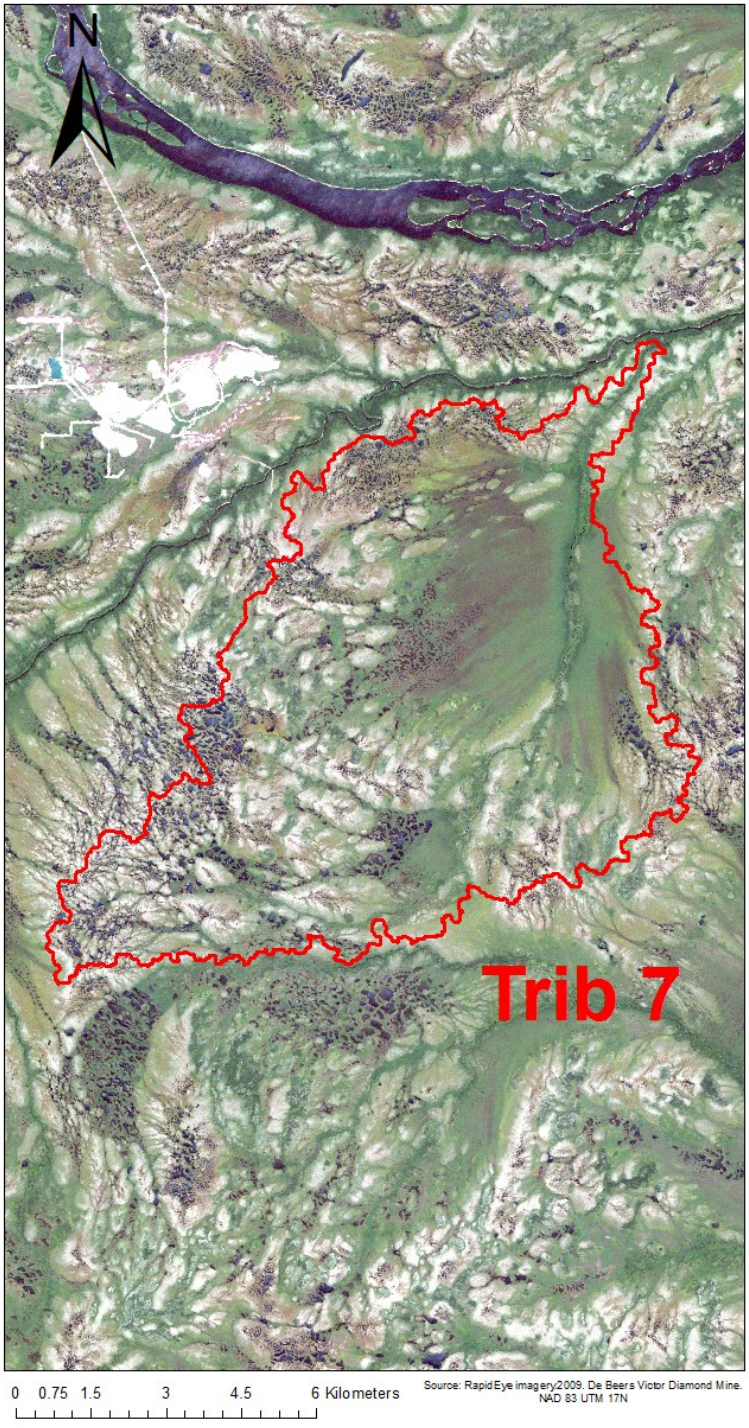

Figure 2.1-6. Boundary (in red) of catchment Trib 7 (88.00 km^2).

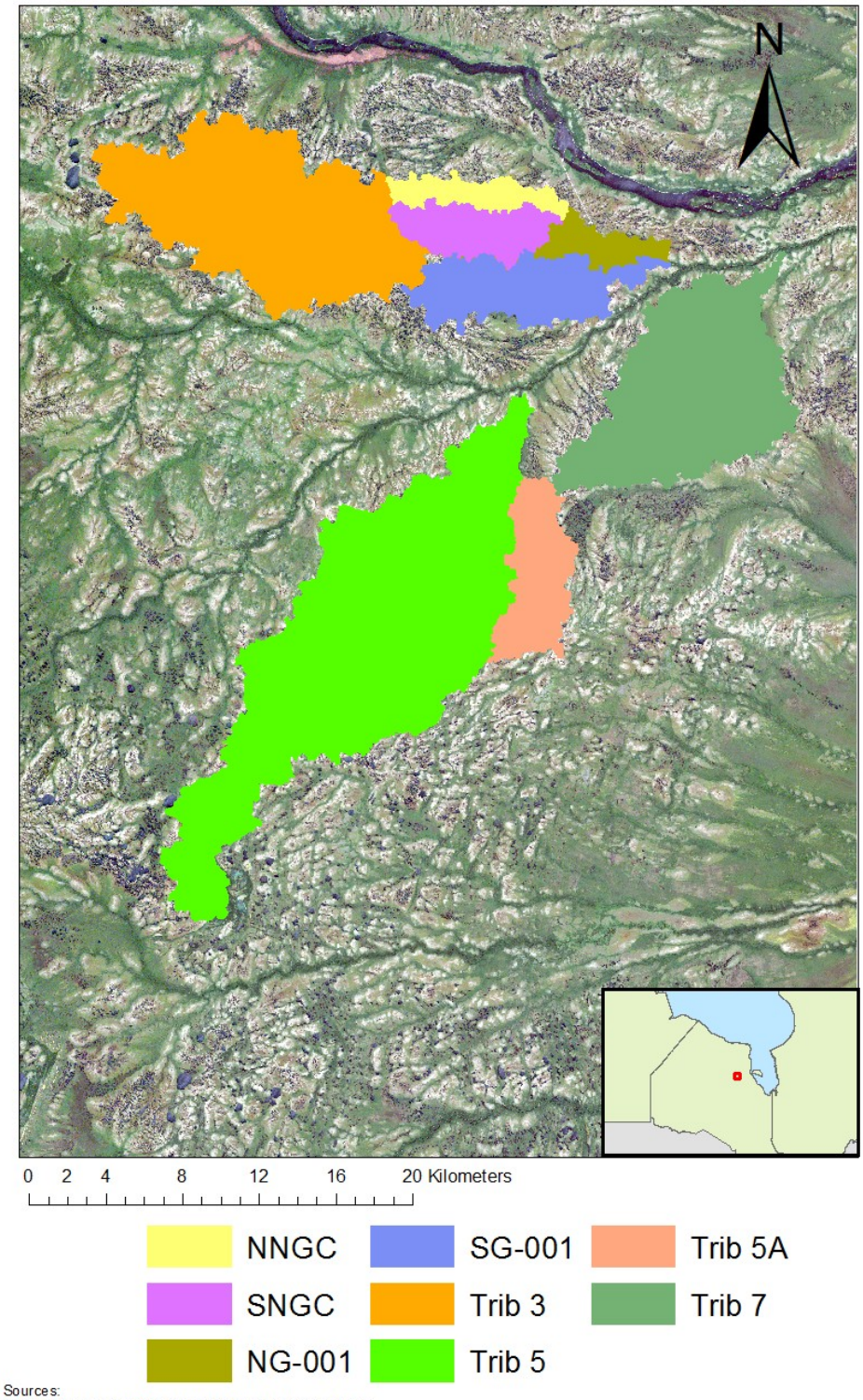

2.1-7. Boundaries of all catchments at study site, within the study region near Attawapiskat, ON, in the James Bay lowlands.

2.2 Meteorological Data

In-situ meteorological data has been collected since 2000 from four meteorological stations that cover different time periods. The initial meteorological station entitled *Victor* is located directly in the mining camp. The Victor station recorded data from early 2000 to early 2009. The meteorological data collected were wind speed, daily air temperature, relative humidity, and net radiation. Rainfall measurements were recorded using a tipping bucket.

The second meteorological station entitled *Muskeg Crew* (MC) is located in NG.001. The MC station has been operational since early 2009 and continues to record meteorological data, including daily air temperature, wind speed, relative humidity, air pressure, and net radiation. Rainfall measurements were recorded using a tipping bucket.

The third and fourth meteorological stations are entitled *MOE Bog* and *MOE Fen*. Both stations are located in Trib 5 and have been recording meteorological data since early 2011. The stations record latent heat flux, sensible heat flux, methane flux, friction velocity, net radiation, relative humidity, soil temperature, daily air temperature, soil moisture, wind speed, air pressure, and precipitation. The stations are operated by the Ministry of the Environment in cooperation with Dr. Elyn Humphreys at Carleton University. The locations of the four *in-situ* meteorological stations are provided in Figure 2.2-1.

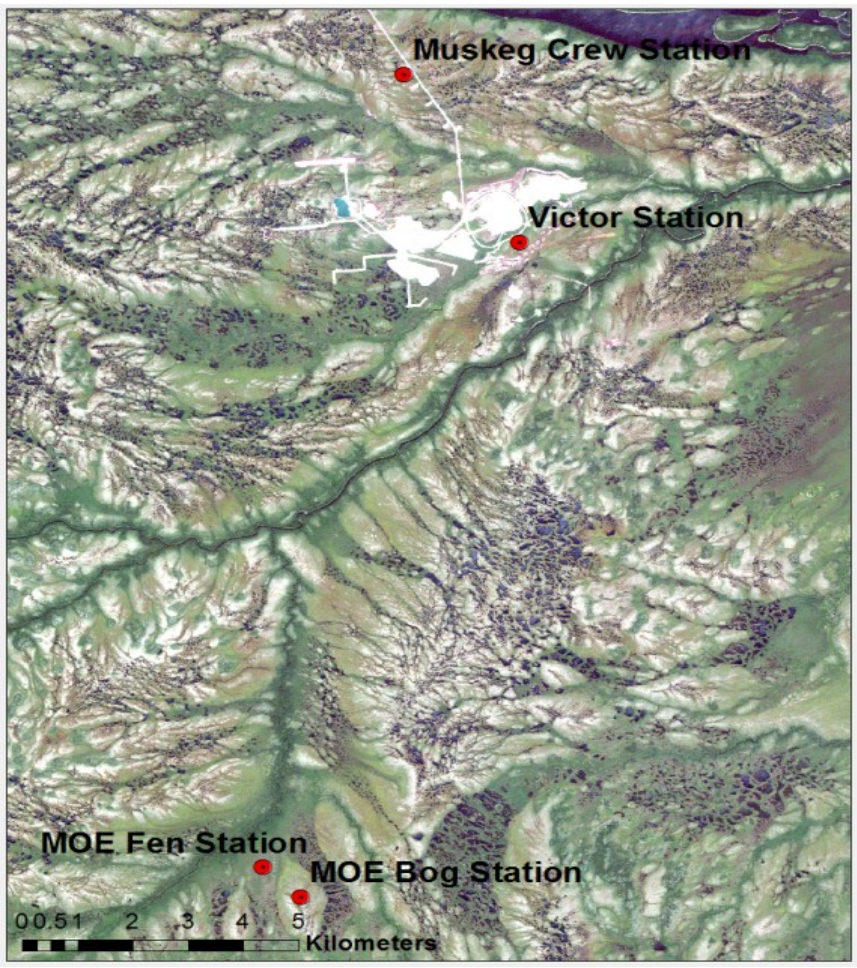

Figure 2.2-1. The location of the four *in-situ* meteorological stations across the study site.

A fifth meteorological station has been included entitled Lansdowne House (LH). The LH station is located in the village of LH approximately 280 km from MC and provides daily air temperature, net radiation, and precipitation measurements. The station has been included as a surrogate to resolve missing data issues within the *in-situ* station network data.

The four *in-situ* meteorological stations have a number of gaps in the data and various corrective measures were undertaken to provide continuous coverage. The corrective measures are detailed in Chapter 3.

2.3 Streamflow Data

Streamflow series were derived from a stage-discharge relationship by AMEC. The stage-discharge relationship originates from recorded spot discharge measurements

using an YSI Flowtracker Acoustic Doppler Velocimeter, and hourly stage measurements using a Schlumberger diver water level logging pressure transducer. The streamflow series vary in length per catchment (Table 2.3-1).

Table 2.3-1. Description of streamflow series per catchment and gaps in the series.

Catchment	Start Date	End Date	Total Days	Number of Missing Measurements
NNGC	25-Jun-08	21-Oct-11	1214	3 (0.001)
SNGC	25-Jun-08	21-Oct-11	1214	71 (0.05)
Trib 3	13-Sep-05	31-Dec-12	2667	36 (0.01)
Trib 5	14-Sep-05	31-Dec-12	2666	138 (0.05)
Trib 5A	24-Jun-07	31-Dec-12	2049	284 (0.14)
Trib 7	15-Sep-05	31-Dec-12	2665	703 (0.26)
NG-001	01-Jan-07	31-Dec-12	2192	543 (0.25)
SG-001	01-Jan-07	31-Dec-12	2192	407 (0.19)

Each catchment varies in the number of missing daily measurements (Table 2.3-1). Certain catchments, notably Trib 5A, Trib 7, NG.001, and SG.001 possess a large number of missing values. However, the larger portion of the missing values is during the winter season. As with the meteorological data, gap filling measures were required to ensure continuous coverage. In addition, it is important that some error exists within the streamflow data which is inevitable due to the use of rating curves (Tomkins, 2014). Environmental and safety conditions on site made it difficult to collecting spot discharge measurements during spring flow conditions and under certain ice conditions. Unfortunately, there is insufficient metadata available to quantify error in the streamflow time series used in this study.

2.4 Topographical Data

Topographical data were acquired from the Ontario Ministry of Natural Resources (MNR). Two datasets of topographical data are provided: a raw digital elevation model (DEM), and a hydrologically enforced DEM. The raw DEM was generated using the Ontario radar digital surface model (DSM). The DSM was created using 1 arc-second spaceborne C-band interferometric radar data. The raw DEM has been projected to a Lambert Conformal Conic projection with an EGM96 and CGVD28 vertical datum at a

spatial resolution of 30 m (MNR, 2013). An accuracy assessment of the data has yet to be completed by the MNR.

The hydrologically enforced DEM originates from the raw DEM and was prepared by MNR. The DEM was hydrologically enforced for the province of Ontario by burning watercourse features (barriers, culverts, and conduits). In addition, a flow direction grid was derived from the hydrologically enforced DEM. The hydrologically enhanced flow direction grid is representative of both the direction of water flow on the landscape surface (Jensen and Domingue, 1988) and the direction of water flow shaped by hydrological or waterbody features (Kenny and Matthews, 2005). Shaping the direction of water flow in this environment is important. This environment is troublesome for maintaining continuous water flow due to: (1) low relief areas: (2) wetland/peatland complex: and (3) the complexity of the drainage system (Kenny and Matthews, 2005). Honouring the topological relationships between hydrological or waterbody features, maintains water flow within the flow-routing algorithms. It is important to note that the hydrologically enforced DEM is not representative of true ground elevation (MNR, 2012).

2.5 Satellite Imagery

GeoEye-1 imagery provided by De Beers through Digital Globe was captured during various periods between 2009 and 2012. GeoEye-1 has a panchromatic band at a spatial resolution of 0.41 m and four multispectral bands at a resolution of 1.65 m. The multispectral bands were pan-sharpened to a resolution of 0.5 m. The spectral ranges of the multispectral bands are in listed in Table 2.5-1 (Digital Globe, ND).

Table 2.5-1. Radiometric information of each band for GeoEye-1.

Bands	Spectral Range (nm)
Red	624-694
Green	506-586
Blue	442-515
NIR	756-901

Chapter 3: Methods

3.1 Data Preparation

This section describes the methods necessary to prepare the data prior to modelling efforts.

3.1.1 Preparation of Meteorological Data

Meteorological data is an integral input to hydrological modelling. Prior to modelling, the preparation, correction, and management of meteorological data and the consolidation of datasets is an important undertaking. This undertaking is instrumental towards the predictive capabilities of hydrological models. To improve the predictive capability it is necessary to reduce the *input uncertainty*. Input uncertainty is the uncertainty in the model parameters that results from input data error (McMillan et al., 2010; Renard et al., 2010). Input data errors may arise from: sampling and measurement errors, the manipulation of data, temporal variations of measured variables, and many more systematic or random sources of errors. To reduce the input uncertainty a number of methods were applied to consolidate datasets and resolve gaps in the data.

The following is divided into three sub-sections. The first sub-section describes the consolidation process, the second sub-section describes the estimation of missing measurements, and the third sub-section describes computing a potential evapotranspiration (PET) time series.

The consolidation process created one master dataset using the MC dataset covering the majority of the study period. The remaining datasets were consolidated to the MC dataset to resolve gaps in the data. During the consolidation process it was important to ensure homogeneity between variables in the datasets. Dubreuil (1974) and Haan (1977) described a series of empirical techniques to assess homogeneity between meteorological variables from multiple datasets. Among those techniques are: basic descriptive statistics, regression and covariance analysis, correlation analysis, and analysis of the cumulative sum of the residuals. The application of descriptive statistics, regression and covariance, and correlation analysis was straightforward and applied to each meteorological variable.

The analysis of the cumulative sum of the residuals from linear regression to assess the homogeneity between two meteorological variables was also performed, using the ellipse test (Allen et al., 1998). The ellipse test determines if a meteorological variable from two datasets is homogenous. This has been performed by plotting the cumulative sum of the residuals of a linear regression between two times series within a parametric ellipse. The meteorological variables are considered homogeneous if the cumulative residuals are contained within the parametric ellipse. The procedure is as follows:

1) The residuals from the linear regression are calculated.
2) The normality of the residuals is evaluated using density plots and quantile-quantile plots.
3) Homoscedaticity of the regression is evaluated to ensure the dependent variable is autonomous of the independent variable. This is performed by inspecting residual diagnostic plots.
4) The standard error of estimates ($S_{y,x}$) is computed as in equation [1] below.

$$S_{y,x} = S_y(1 - r^2)^{1/2} \quad [1]$$

5) The cumulative residuals (E_i) are computed as in equation [*2*] below.

$$E_i = \varepsilon_i + \sum_{j-1}^{i-1} \varepsilon_i \quad [2]$$

6) The shape of the parametric ellipse is determined using equations [*3-6*]. The alpha parameter is the sample size (n) divided in half. The beta parameter is the product of the ratio of the sample size, standard normal variate of probability (Z_p), and standard error of estimates.

$$\alpha = \frac{n}{2} \; [3] \qquad \beta = \frac{n}{(n-1)^{0.5}} \, Z_p S_{y,x} \; [4]$$

$$X = \alpha \cos(\theta) \quad [5] \qquad Y = \beta \sin(\theta) \quad [6]$$

7) The cumulative residuals are plotted within the parametric ellipse, with the x-axis representing the timestep.

The second sub-section in the preparation of the meteorological data was the estimation of missing measurement values in the MC dataset. Missing data results from either instrumentation malfunctions or data logging interruptions. Also, missing data resulted in the MC dataset if a meteorological variable did not have a homogenous equivalent in another dataset. The estimation of missing data was necessary to ensure continuity that is optimal for model calibration. There were various techniques applied for resolving missing data. The main meteorological variables corrected in the MC dataset were daily temperature, precipitation, and net radiation.

Daily temperature measurements in the MC dataset were sporadically missing. The importance of daily temperature is accredited to its role in computing ET and partitioning precipitation. This demonstrates the importance of effectively and carefully interpolating missing values. Kotsiantis et al. (2006) demonstrated that regression tree models provide satisfactory results for filling missing temperature values. An M5 regression tree was trained using mean temperature, maximum temperature, and minimum temperature from the surrogate dataset. The performance of the trained model was evaluated by estimating and comparing against 20% of the observational data.

Missing daily precipitation measurements in the MC dataset were sporadic. Precipitation is the most important *input* variable in rainfall-runoff models. The relationship between rainfall and runoff is dependent on the quality of both datasets. The missing precipitation measurements were filled using values from the surrogate dataset.

Net radiation had a larger number of missing values in the MC dataset. A continuous dataset of net radiation is required to compute ET. Missing net radiation measurements were estimated by training a regression model (Bocco et al., 2009). An M5 regression tree was trained using maximum daily temperature, minimum daily temperature, day length, and extraterrestrial radiation as predictors to estimate daily net

radiation. Both day length and extraterrestrial were calculated based on solar geometry (Bojanowski, 2013). The performance of the trained model was evaluated by estimating and comparing against 20% of the observational data.

The third sub-section was the computation of a daily PET series. PET was calculated using the Penman-Monteith equation [*7*] with the variables: gradient of the saturation vapour pressure curve (Δ), net radiation (R_n), vapour pressure deficit (vpd), aerodynamic resistance (r_a), and surface resistance (r_s) (Allen et al., 1998).

$$PET = 0.408\ \frac{\left(\Delta R_n + \frac{(105.028 * vpd\ )}{r_a}\right)}{\Delta + 0.067\ \left(1 + \frac{r_s}{r_a}\right)} \quad [7]$$

3.1.2 Streamflow Preparation

The streamflow data were missing a number of daily measurements for each catchment as summarized in Table 2.3-1. Maintaining a continuous streamflow series is important for a number of reasons, such as: uninterrupted model calibration, improved analysis of inter-annual variability and streamflow characteristics, better inference of ungauged streams (Peel et al., 2000; Konrad & Voss, 2012). In this research, the issue of missing streamflow measurements was resolved by applying a sequential k-nearest neighbour imputation technique (Kim et al., 2004).

The sequential k-nearest neighbour (SKNN) imputation technique is a cluster-based approach that performs multiple imputations of datasets (Whitfield, 2013). Imputation is an empirical process that replaces missing values by substitution based on probability. Multiple imputations simply substitute multiple data series simultaneously. The SKNN method has two main operations: (1) grouping samples by similarity in expression patterns using correlation and Euclidean distance analysis, and (2) the missing values are then imputed using the weighted average of the corresponding k-nearest sample (Kim et al., 2004).

The imputed measurements were evaluated by estimating and comparing for a known observation period. The imputed streamflow was evaluated against the observation period with the following metrics: Nash-Sutcliff (NS), root mean square error

(RMSE), percent bias (%Bias), coefficient of correlation (r), and coefficient of determination (r^2).

3.1.3 Catchment Boundary Delineation

The delineation of catchment boundaries is another very important element in hydrological modelling applications. There are various methods available to delineate catchment boundaries that often rely on DEMs. As a result, the delineation process is sensitive to DEM quality and resolution. The resolution of a DEM can have an impact on the area of the delineated boundary that subsequently affects model calibration (Teegavarapu et al., 2006). In addition, Krause & Bronstert (2005) highlighted that the resolution of a DEM can be problematic for delineating lowland catchments, because topographic gradients are too small compared to the resolution.

The boundary of each catchment was delineated using the method proposed by Chen et al. (2003) using ESRI ArcInfo. The method applied the hydrologically enhanced flow direction grid to determine the contributing areas of the measurement stations. The enhanced flow direction grid represents the direction of water flow across the landscape (Jensen and Domingue, 1988). Using this grid, a flow accumulation grid was computed that the cell values represent the total number of cells draining into each cell. The flow accumulation grid was then used to determine the stream network and subsequently the drainage area following Maidment, (2002). The boundaries of the catchments were delineated from the measurement sites along the stream network.

The SRTM delineated catchment boundaries were compared visually to catchments delineated from higher-resolution LiDAR data, which were assumed to have higher accuracy since LiDAR surveys capture much finer level of topographic detail suitable for peatland catchments. The delineated boundaries of NNGC and SNGC from both data sources were visually compared. The NNGC and SNGC catchments were chosen due to the spatial overlap between the LiDAR and SRTM datasets.

3.2 Conceptual Rainfall-Runoff Model Structure Methodology

This chapter describes the model structures of TOPMODEL and HBV. These models were selected due to their popularity in the literature and their differences in structure. HBV and TOPMODEL differ for a number of reasons, with completely different formulations of hydrologic processes. However, the main difference is that HBV does not consider surface topography to determine flow rates or any other hydrologic property. The structure of each model is described in the subsequent subsections.

3.2.1 TOPMODEL Model Structure

TOPMODEL is a conceptual rainfall-runoff model that simulates daily discharge from rainfall, temperature, and PET. Daily discharge is determined using an *Explicit Euler* timestep approach. Explicit Euler or forward Euler is a method for solving numerical procedures using past state variables. The TOPMODEL model structure applied in this study was the generic exponential recession structure (Beven et al., 1995). For ease of explanation the model structure is presented in three stages. Each stage is supported by lumped parameters that are representative of the catchment as a whole.

In the first stage the topographical wetness index (TWI) is calculated. The TWI is a topographical-derived hydrologic index that is fundamental to the TOPMODEL approach. The TWI contributes to the simplicity of TOPMODEL by reducing the number of model parameters required in simulations. The TWI concept is an approach that divides a catchment into classes of hydrological similarity (Kirkby & Weyman, 1974; Kirkby 1975). The classes of hydrological similarities represent areas of similar soil moisture conditions that are determined by topography (Burt & Butcher, 1985). In equation [*8*] classes of hydrological similarity (λ) are calculated by dividing the area draining through a point upslope (a) by the local slope angle ($\tan\beta$).

$$\lambda = \ln\left(\frac{a}{\tan\beta}\right) \quad [8]$$

Since the original TWI, a number of new approaches for calculating the TWI have been developed (Barling et al., 1994; Boehner & al., 2002; Ma & al., 2010). Each approach has its advantages and disadvantages, and as Sorensen et al. (2006)

demonstrates no single TWI is optimal for all applications. There have been a number of applications of the original TWI and variants for peatland landscapes (Rodhe & Seibert, 1999; Lane et al., 2004; Richardson et al., 2010; Kleinen et al., 2012; Richardson et al., 2012). For example, in Richardson et al. (2012) the SAGA wetness index (SWI) (Boehner et al., 2002) was applied to examine runoff generation in northern peatlands. This formulation of the TWI was also applied in this study for two reasons: (1) it has previously been applied at this location, and (2) it is thought to provide a better representation of low gradient environments than the original TWI (Boehner et al., 2002; Richardson et al. 2012).

Similar to the TWI, the SWI is based on the calculation of a modified catchment area (SCA_m) shown in equation [*9*].

$$\lambda = \ln \frac{SCA_m}{tan\beta}$$

$$where\ SCA_m = \begin{cases} \left[SCA_m = SCA_{max}\left(\frac{1}{15}\right)^{\beta exp\,(15^{\beta})}\right] \Leftrightarrow \left[SCA < \ SCA_{max}\left(\frac{1}{15}\right)^{\beta exp\,(15^{\beta})}\right] \\ \left[SCA_m \neq SCA_{max}\left(\frac{1}{15}\right)^{\beta exp\,(15^{\beta})}\right] \Leftrightarrow \neg\left[SCA < \ SCA_{max}\left(\frac{1}{15}\right)^{\beta exp\,(15^{\beta})}\right] \end{cases} \quad [9]$$

In equation [*9*] iterative calculations of the modified catchment area continues until the specific catchment area (SCA_m) is less than the locally modified specific catchment (SCA_{max}). Calculations of λ are identical to the original TWI formulation.

In the second stage, both the snow routine and infiltration were calculated. The snow routine is an addition to the model that is identical to the snow routine used in HBV-Light (see HBV-Light model structure). Infiltration is calculated based on the Green-Ampt assumptions (Beven, 1984). In its basic form Green-Ampt infiltration can be described as seen in equation [*10*] below, f is the wetting front, k_s is the saturated hydraulic conductivity, and $\frac{dh}{dz}$ is the hydraulic gradient.

$$f = -K_s \frac{dh}{dz} \quad [10]$$

In the third stage, discharge for each hydrologically similar class is calculated after equation [11]. In equation [*11*] subsurface flow (T) is calculated from the lateral transmissivity (T_{0i}) when the soil is just saturated, the local storage deficit (S_i), and the m parameter applied as an effective storage capacity.

$$T(S_i) = T_{0i} \exp\left(-\frac{S_i}{m}\right) [11]$$

The downslope saturated subsurface flow rate (q_i) is calculated with equation [*12*]. q_I is determined by the local transmissivity, the local slope ($tan\beta_i$), and the $\frac{S_i}{m}$ relationship.

$$q_i = T_{0i} tan\beta_i \exp\left(-\frac{S_i}{m}\right) \quad [12]$$

The storage deficit relationship is defined as the difference between the local and mean storage deficit. In equation [*13*] the relationship is the ratio of the local and mean storage deficit. $\zeta_{\infty i}$ represents the local topographic index and λ_∞ is the spatial average of the topographical index. It is important to note that T_{0i} is normally omitted in catchments with spatially uniform transmissivity.

$$\left(\frac{S_i}{m}\right) - \left(\frac{\bar{S}}{m}\right) = \frac{\zeta_{\infty i}}{\lambda_\infty} = \begin{cases} \zeta_{\infty i} = \ln\left(\dfrac{a_i}{tan\beta_i T_{0i}}\right) \\ \lambda_\infty = A^{-1} \displaystyle\int_A \left(\dfrac{a_i}{tan\beta_i T_{0i}}\right) dA \end{cases} \quad [13]$$

In equation [*14*] the total discharge from the saturated zones $q_s(\bar{S})$ is calculated by summing the subsurface flows. TOPMODELs parameters are listed in Table 3.2-1.

$$q_s(\bar{S}) = Aexp(-\lambda_\infty) \exp\left(-\frac{\bar{S}}{m}\right) \quad [14]$$

Table 3.2-1. List of parameters to calibrate used by TOPMODEL.

Parameter	Description	Unit
qs0	Initial subsurface flow per unit area	m
lnTe	Log of the areal average of transmissivity (T0)	m^2 h
m	Model parameter	m
Sr0	Initial root zone storage deficit	m
Srmax	Maximum root zone storage deficit	m
td	Unsaturated zone time delay per unit storage deficit	h/m
vr	Channel velocity	m/h
k0	Surface hydraulic conductivity	m/h
CD	Capillary drive	N/A

In addition to the model structure, there are two main assumptions underlying TOPMODEL, which are:

1) The hydraulic gradient of the saturated zone can be approximated by the local surface topographic slope (Beven, 1997).

2) Water table dynamics can be approximated by the uniform subsurface runoff production per unit area (Beven, 1997).

The applicability of the first assumption is in question; it is uncertain whether this assumption is applicable in low-gradient environments. The second assumption is

problematic in peatland environments due to the degree of spatiotemporal heterogeneity in the hydraulic properties of peat (Lewis et al., 2011; Branham, 2013). A general conceptual overview of TOPMODEL excluding the snow routine is depicted in Figure 3.2-1.

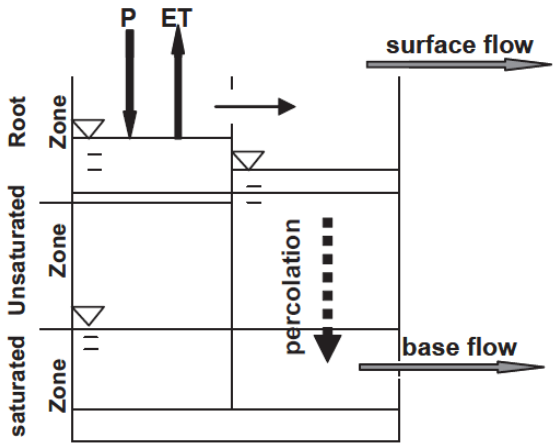

3.2-1. Conceptual overview of TOPMODEL model structure (Kazuo et al., 2013).

3.2.2 HBV Model Structure

The HBV model used in this study was HBV-Light (Seibert, 2005). HBV-Light is a conceptual rainfall-runoff model that simulates daily discharge from rainfall, temperature, and PET. Daily discharge is determined using an Explicit Euler timestep approach. The model structure is composed of four routines: snow, soil moisture, response function, and routing. Each routine is supported by lumped parameters that are representative of the catchment as a whole.

The snow routine is a degree-day model that partitions precipitation to either rainfall or snow, and determines the volume of snowmelt contributions. There are five parameters to the snow routine as listed in Table 3.2-2.

Table 3.2-2. Parameters used by HBV's snow routine.

Parameter	Description	Unit
TT	Threshold temperature	°C
CFMAX	Degree-Δt factor	mm °C^{-1} Δt$^{-1\ Day}$
SFCF	Snowfall correction factor	N/A
CFR	Refreezing coefficient	N/A
CWH	Water holding capacity	N/A

The TT parameter is applied to determine if precipitation is either snow or rainfall. Precipitation is assigned to rainfall if the temperature is greater or equal to TT or to snow if the temperature is less than TT. If the precipitation is assigned as snow the SFCF parameter is applied to correct for snowfall measurement errors. At each time step both meltwater and refreezing meltwater are calculated.

Meltwater is the portion of snow that melted from the snowpack, and is computed using equation [*15*].

$$meltwater = CFMAX\ (Temp - TT) \quad [15]$$

Refreezing meltwater is the portion of meltwater that refreezes before it can contribute to discharge [*16*].

$$refreezing\ meltwater = CFR * CFMAX(Temp - TT) \quad [16]$$

The meltwater is then added to the incoming rainfall for the soil moisture routine.

The soil moisture routine determines the actual evapotranspiration (AET), soil moisture, and groundwater recharge from the rainfall and snowmelt. There are three parameters that apply to the soil moisture routine listed in Table 3.2-3.

Table 3.2-3. Parameters used by HBV's soil moisture routine.

Parameter	Description	Unit
FC	Maximum soil moisture storage (field capacity)	mm
LP	Soil moisture value above which AET reaches PET	mm
BETA	Determines the relative contribution to runoff from rain or snowmelt.	N/A

The first procedure in the soil moisture routine is to partition rainfall and snowmelt contributions to the soil box or groundwater recharge based on equation [*17*].

$$\frac{recharge}{p} = \left(\frac{SM(t)}{FC}\right)^{BETA} \quad [17]$$

AET is then calculated from the contents of the soil box using equation [*18*]. Figure 3.2-2 provides an overview of the soil moisture routine.

$$AET = PET \min\left(\frac{SM(t)}{FC * LP}, 1\right) \quad [18]$$

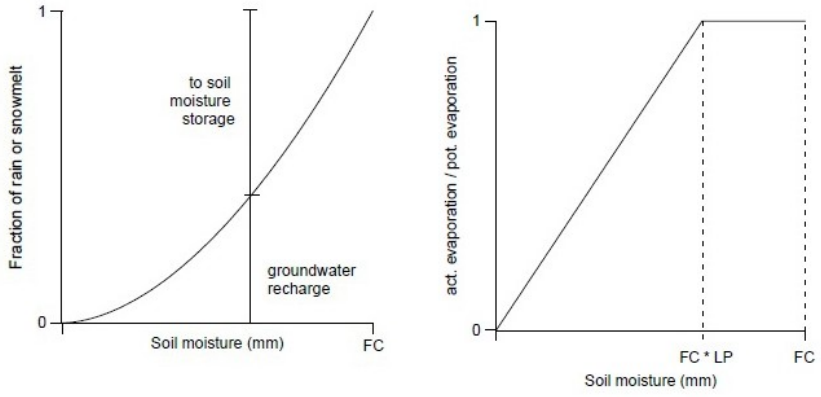

3.2-2 Overview of soil moisture routine (Seibert, 2005). Left-graph represents the portion of rain or snowmelt partitioned to groundwater recharge or soil moisture. Right-graph represents relationship between actual and potential evapotranspiration.

The rainfall and snowmelt contributions allocated to groundwater recharge are added to the upper groundwater box for the response function.

The response function determines runoff contributions and maintains groundwater levels. There are four parameters in the response function listed in Table 3.2-4.

Table 3.2-4. Parameters used by HBV's response function.

Parameter	Description	Unit
PERC	Maximum percolation rate from the upper to the lower groundwater box.	mm $\Delta t^{-1\ Day}$
Alpha	Non-linearity coefficient	N/A
K0	Storage/recession coefficient	$\Delta t^{-1\ Day}$
K1	Storage/recession coefficient	$\Delta t^{-1\ Day}$

The first procedure in the response function is to determine the groundwater that percolates from the upper groundwater box to the lower groundwater box, [*19-20*].

$$Lower\ Gw\ Box = Lower\ Gw\ Box + PERC \quad [19]$$

$$Upper\ Gw\ Box = Upper\ Gw\ Box - PERC \quad [20]$$

Runoff from the groundwater boxes are computed based on equations [*21-23*]. An overview of the response function is depicted in Figure 3.2-3.

$$Q1 = \min(K1 * Upper\ Gw\ Box^{1+Alpha}, Upper\ Gw\ Box) \quad [21]$$

$$Q2 = K2 * Lower\ Gw\ Box \quad [22]$$

$$runoff = Q1 + Q2 \quad [23]$$

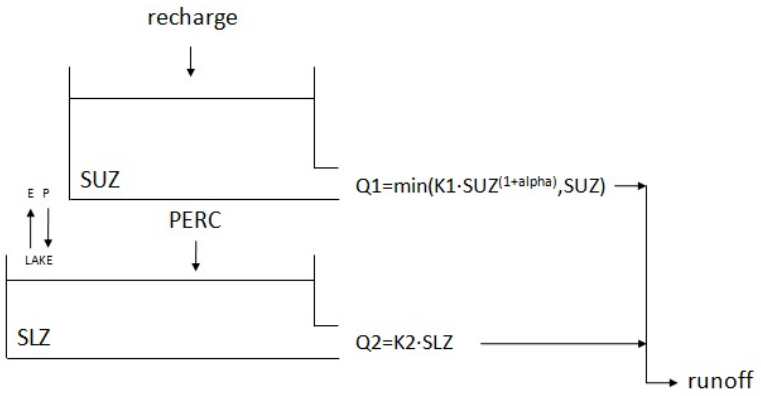

3.2-3 Overview of response function (Seibert, 2005).

The runoff is finally transformed in the routing routine by applying a triangular weighted function. The routing routine has one parameter, MAXBAS (Δt), that determines the length of triangular weighting. The runoff is transformed using equations [*24-25*]. A conceptual overview of HBV-Light's model structure is depicted in Figure 3.2-4.

$$runoff(t) = \sum_{i=1}^{MAXBAS} c(i) * Q_{gw}(t-i+1) \text{ [24]}$$

$$c(i) = \int_{i-1}^{i} \frac{2}{MAXBAS} - \left| u - \frac{MAXBAS}{2} \right| \frac{4}{MAXBAS^2} du \text{ [25]}$$

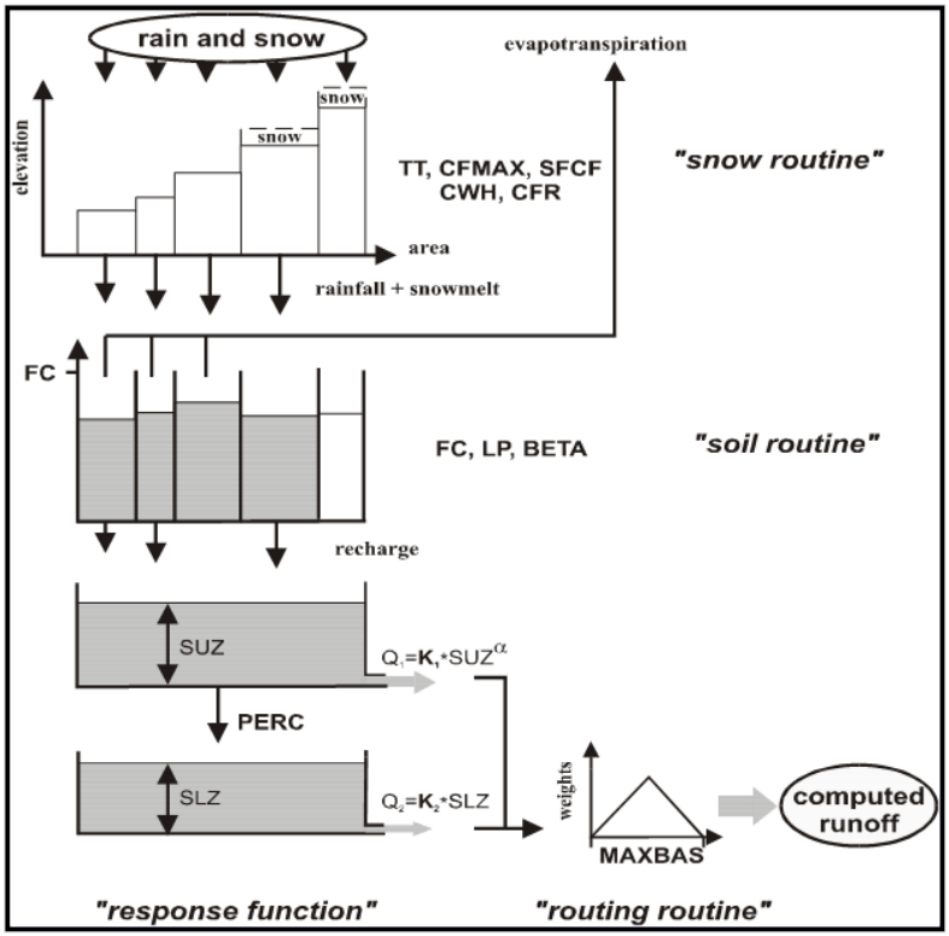

3.2-4. Conceptual overview of HBV-Light model structure (Seibert, 2014).

3.3 Methods 1 – Model Calibration and Uncertainty Analysis

The following chapter describes the methods associated with the first objective of this thesis, which involves a comparison and evaluation of the predictive capability of TOPMODEL and HBV-Light in a James Bay Lowland peatland complex.

3.3.1 Model Calibration

The calibration of the model parameters was performed using the Monte Carlo method. The Monte Carlo method is popular for model calibration. This method uses a large number of randomly generated parameter sets that are applied to generate an equivalent number of model outputs (Metropolis & Ulam, 1949; Eckhardt, 1987). The random parameter sets can be generated using different distributions: uniform, normal,

log, exponential, and many more. The benefit of this method is that its application is not limited to optimizing model performance, as is the case with auto-optimization methods, but can also be applied for other calibration purposes. Those purposes range from assessing model and parameter uncertainty (Kuczera & Parent, 1998; Wagener et al., 2003; Marshall et al., 2004; Lee et al., 2005), performing regionalization (Seibert, 1999; Edward & Bates, 2001; Bastola et al., 2008), and assessing input uncertainty (Vrugt et al., 2008; Renard et al., 2010).

The random samples for Monte Carlo simulations require that an upper and lower limit of a parameter's distribution be defined. The upper and lower limits of the distribution ranges define the prior distribution. The prior distribution is the initial perception of the characteristics of the system under study before data analysis (Beven, 2009). This perception is defined either by the literature, experiences, or assumptions. Using the upper and lower limits the parameter sets were generated using a pseudo-uniform sampling distribution. A uniform sampling distribution was selected due to its simplicity that does not require tail trimming. However, if more time was available an analysis of the optimal distribution for each parameter would have been performed.

From the prior distribution the intent is to establish a refined prior distribution. The refined prior distribution defines the upper and lower limits of the distribution ranges based on initial model calibration and uncertainty analysis. This provides the ability to determine parameter values that are representative of the system under study.

For each catchment 200,000 Monte Carlo simulations were performed. A warm-up period was applied during 2007 and the model was calibrated between 2008 and 2010. Each model output was evaluated using a fuzzy measure that combines Nash-Sutcliffe (NS) [*26*], logged Nash-Sutcliffe (LNS) [*27*] and volumetric error (VE) [*28*] (Seibert, 1997). The benefit of the fuzzy measure is that it combines the unique ability of each objective function to evaluate certain aspects. The NS objective function is sensitive to hydrograph peaks, the LNS objective is sensitive to low flows, and VE quantifies the magnitude of the volumetric error (Krause et al., 2005). The fuzzy measure applies the three objective functions to determine the optimal parameter sets that optimize hydrograph simulations in relation to all three of these flow characteristics rather than

favouring any one aspect, in particular. The optimal parameter set is determined from intersecting the degree of membership of each objective function [*29-32*].

$$NS = 1 - \frac{\sum_{i=1}^{n}(O_i - S_i)^2}{\sum_{i=1}^{n}(O_i - \bar{O})^2} \quad [26]$$

$$\ln(LNS) = 1 - \frac{\sum_{i=1}^{n}(\log(O_i) - \log(S_i)^2}{\sum_{i=1}^{n}(\log(O_i) - \log(\bar{O}))^2} \quad [27]$$

$$VE = \frac{|\sum_{i=1}^{n}(O_i - S_i)|}{\sum_{i=1}^{n}(O_i)} \quad [28]$$

$$X1(NS) = \max\left(0, \frac{NS_i - 0.8NS_{max}}{0.2NS_{max}}\right) \quad [29]$$

$$X2(LNS) = \max\left(0, \frac{LNS_i - 0.8LNS_{max}}{0.2LNS_{max}}\right) \quad [30]$$

$$X3(VE) = \max(0, 1 - 5|VE|) \quad [31]$$

$$F = \mathrm{X1} \cap \mathrm{X2} \cap \mathrm{X3} \quad [32]$$

3.3.2 Uncertainty Analysis

In this study uncertainty analysis was applied for two purposes: (1) to refine the limits of the prior distribution, and (2) for model validation. To refine the prior distribution the Monte Carlo Analysis Toolbox (MCAT) was applied. MCAT provides an array of tools to analyze the results of Monte Carlo simulations. Among those tools are: generalized sensitivity analysis (GSA), regional sensitivity analysis (RSA) (Spear & Hornberger, 1980; Hornberger & Spear, 1981), generalized likelihood uncertainty estimation (Beven & Binley, 1992; Beven, 1993; Beven & Freer, 2001), and *posteriori* parameter plots. A number of those tools were applied to refine the upper and lower limits of the parameter distributions to establish a refined prior distribution.

The application of uncertainty analysis for model validation to evaluate model performance was the generalized likelihood uncertainty estimation (GLUE) framework. The purpose of GLUE in this application was to determine if TOPMODEL or HBV can adequately represent rainfall-runoff response in James Bay Lowland peatland basins. To determine representativeness of the two modelling approaches, uncertainty of the predictive capabilities was expressed as the relationship between the refined prior distributions and the *limits of acceptability*. The limits of acceptability imply that model

predictions should to be within a certain range from the observations. This approach was suggested by Beven (2006) as a method of model falsification to determine whether or not a model is representative. The application of the GLUE framework for model validation is explained in more detail in the next section.

3.3.3 Model Validation

Model validation is important for determining a model's predictive capability and for falsifying or assessing a model's structure (Popper, 1963). Model validation is traditionally performed by evaluating the goodness-of-fit between model predictions and observations from a split sample. This approach is considered the minimum requirement for validating models. However, both Klemes (1986) and Kuczera et al. (1993) scrutinize this approach in its ability to adequately falsify model structures. In addition, validation using only a goodness-of-fit measure could potentially be misleading in a model's predictive capability for a certain environment (Vogel & Sankarasubramanian, 2003; Kirchner, 2006).

A validation procedure was established that combined both goodness-of-fit measures and uncertainty analysis to evaluate model performance. The goodness-of-fit measure is the fuzzy measure previously discussed in subsection 3.3.1. The uncertainty analysis portion was briefly explained in the previous subsection. However, there is a need to expand on the limits of acceptability. The limits of acceptability were defined in two manners: (1) using a threshold for the fuzzy measure that indicates whether a parameter set is representative or not, and (2) using prediction limits. The threshold applied was any parameter set that yielded a fuzzy measure value greater than 0 as this was considered acceptable. In order to obtain a value greater than 0 a minimum value of 0.4 for both NS and LNS was required.

The prediction limits provide a range of the potential model output at a timestep. The prediction limits were applied to determine the percentage of observation data within the range of the prediction limits. This provides a measure of predictive uncertainty and an additional metric for model validation. Prediction limits were generated using the quantiles of the cumulative likelihood distribution of the parameter sets with a fuzzy measure greater than 0.

An evaluation of both models with respect to suitability for the peatland catchments in the James Bay lowlands was performed using the validation procedure described above in order to critically appraise model performance.

3.4 Methods 2 - Model Regionalization

PUB efforts to maximize the predictive value of information have aimed at improving understanding of the underlying hydrological processes to subsequently overcome data scarcity issues (Hrachowitz et al., 2013). To improve understanding of the underlying hydrological processes, the focus has been on linking physical catchment properties like topography, climate, geology, soil type, and land use to hydrological function. In this research, linking physical catchment properties to hydrological function to overcome data scarcity was performed by applying regionalization methods. The regionalization methods incorporated information acquired from topographical analyses and image processing to calibrate the HBV model.

The following chapter describes the methods related to the second main objective of this thesis: the evaluation of model regionalization methods in a James Bay Lowland peatland complex.

3.4.1 Topographical Analysis

Topography is an important element of the landscape that drives hydrology. Topography dictates the gross drainage area (Wagener et al., 2007), hydrological connectivity (Lane et al., 2009), distribution of soil moisture (Yeh & Eltahir, 1998), soil hydraulic characteristics (Raghavendra & Mohanty, 2012), landscape organization (McGuire et al., 2005), spatial distribution of snow depth (Trujillo et al., 2007), and many more. In peatlands, topography is especially important for flow routing and moisture distribution (Holden, 2005). Topographical characteristics are invaluable in hydrological studies and subsequently have become central towards PUB.

Topography was incorporated using metrics derived from various algorithms. The topographical metrics were obtained from terrain analysis algorithms available in SAGA using hydrologically pre-processed DEMs and the raw DEM, as described in section 2.4.

For each terrain analysis algorithm applied, metrics were computed for the arithmetic mean, standard deviation (STDEV), coefficient of variation (CV), minimum value (MIN), and maximum value (MAX). The topographical metrics generated for the regionalization analysis are listed and described in Table 3.4-1.

The accuracy of topographical metrics especially first-order derivatives decrease with increasing DEM resolution (Chang & Tsai, 1991). The accuracy of the topographical metrics derived from the DEMs is unknown. However, the MNR DEMs have been prepared specifically for hydrological applications in the James Bay Lowland (MNR, 2012).

Table 3.4-1. Topographical metrics derived to assist in the regionalization process.

Derivative	Description	Source
Drainage Area	Indicates the volume of water that can be generated during rainfall events.	McCuen, 2005
Catchment Length	Representative of the potential time of concentration.	McCuen, 2005
Catchment Slope	Describes the rate of change of elevation along the main flow path that is representative of the potential momentum of runoff.	McCuen, 2005
Slope	Describes the rate of change of elevation within the catchment.	McCuen, 2005
Perimeter	Perimeter of the drainage area.	McCuen, 2005
Elevation	Elevation of the drainage area.	
Aspect	Average catchment orientation. Orientation can influence snowmelt rates.	McCuen, 2005
Terrain Ruggedness Index	Reflects average topographical heterogeneity.	Riley et al., 1999
Saga Wetness Index	Reflects average lateral dispersion of moisture.	
Flow Path Gradient	The ratio of the overland flow distance and the elevation difference towards the nearest channel.	McGuire et al., 2005
Flow Path Length Over Gradient	The ratio of the flow path gradient and the overland flow distance towards the nearest channel.	McGuire et al., 2005
Total Stream Length	The combined length of all stream segments within a catchment.	McCuen, 2005
Drainage Density	Drainage Density is the ratio of the total length of streams within the drainage area.	McCuen, 2005
Gravelius Shape Index	Shape determined based on the drainage area and perimeter of the drainage area.	Bendjoudi & Hubert, 2002
Gravelius Circularity Ratio	Circularity ratio determined based on the drainage area and perimeter of the drainage area.	Bendjoudi & Hubert, 2002
Shape Index	Shape determined based on the length of the center of the catchment along the main flow path.	McCuen, 2005

3.4.2 Land Cover Classification

Regionalization depends on extrapolating information from gauged catchments for ungauged catchments that are similar. An important consideration when comparing the similarity of catchments is *hydrologic function*. A catchment's hydrologic function is defined both by its response behaviour and storage characteristics: (1) response behaviour entails the release of water through streamflow, groundwater and soil moisture release mechanisms: and (2) storage behaviour is the retention of water by various means such as

channel networks, water entities (lakes, wetlands, etc.), vegetation, soil, and groundwater aquifers (Wagener et al., 2007). Furthermore, both response behaviour and storage characteristics are unique to land covers that define a catchment's function.

In northern peatlands, Quinton et al. (2003) demonstrated that channel fens and bogs have contrasting hydrological functions. Channel fens have a greater runoff response as conveyors of runoff, and bogs are an effective storage medium. Quantifying these contrasting functions is important towards regionalization efforts. An approach to quantify both contrasting functions is a land cover classification.

Channel fens and bogs were quantified by performing a series of land cover classifications. Land cover classification is the practice of quantifying the surface of the earth. The quantification of land cover is achieved by using the spectral information available in optical imagery to group similar land cover. The land cover groups are defined in a classification scheme prior to classification. The classification scheme applied in this study partitioned the landscape into three land cover groups: fen, bog, and open water.

Many approaches to land cover classification are available (Lu & Weng, 2007). Establishing an optimal classification procedure is critical towards successfully partitioning land cover. The classification of northern peatlands requires certain considerations that result from two main issues: (1) fens and bogs exhibit similar spectral signatures (Ozesmi & Bauer, 2002), and (2) transitional zones between fens and bogs are difficult to assign a land cover (Dissanska et al., 2009). To address these issues, an object-based image analysis (OBIA) classification approach was applied, because this technique makes use of spatial and contextual information in addition to spectral information.

OBIA is a classification approach that partitions land cover in two steps. In the first step, image pixels are grouped into objects using image segmentation algorithms that evaluate the homogeneity between pixels (Dey et al., 2010). In the second step, the objects are classified instead of the individual image pixels. This approach was selected based on previous successful applications to classify peatlands (Mahoney et al., 2007; Grenier et al., 2008). An element of OBIA that contributes to its successful application is the large number of properties that improve the classification procedure (Lang et al.,

2006). The properties (see Table 3.4-2) available for each object are derived from the spectral, spatial, and textural information.

Table 3.4-2. List of properties available to each object following segmentation.

Property	Description
Custom Features	Properties that are user generated. (ex:Vegetation indices)
Type Features	An object's position in space.
Layer Values	Information derived from the spectral properties of each band.
Geometry Features	Information based on an object's geometry.
Position Features	The position of an object in relation to the scene.
Texture	Information on the texture of an object. (ex: Texture after Haralick)
Object Variables	User defined variables.
Hierarchy Features	Information based on object's relation to position in hierarchical structure of layers.
Thematic Attributes	Information provided by thematic layers.

To improve the classification procedure topographical derivatives and statistics were added to the delineated objects. Anderson et al. (2010) demonstrated that topographical derivatives and statistics are beneficial in the classification of northern peatlands. Various topographical derivatives and statistics were chosen because their potential was demonstrated by Di Febo (2011), and they are listed in Table 3.4-3.

Table 3.4-3. Topographical derivatives and statistics applied to improve land cover mapping.

Topographical Derivative / Statistic	Description	Method
Slope	Maximum triangle slope method that delineates slope to be representative of flow direction.	Tarboton (1997)
Difference from mean elevation (DiME5)	The difference between a cell's elevation to the mean elevation within a 5x5 moving window.	Wilson & Gallant (2000)
Deviation from mean elevation (DeME5)	The standard deviation from the mean elevation in a 5x5 moving window.	Wilson & Gallant (2000)
Elevation percentile (Perc5)	Relative position of a cell within a 5x5 moving window.	Wilson & Gallant (2000)

The classification procedure was performed using eCognition software, and the outline of the procedure follows. In the first portion, image pre-processing techniques were applied to the GeoEye imagery to reduce processing time. This was accomplished in two procedures: (1) the imagery was resampled from 0.5 m to 1m using a cubic convolution method (Parker et al., 1983; GeoEye, 2010), and (2) the imagery was clipped to the boundary of each catchment. The cubic convolution algorithm was selected because it was suggested by GeoEye (GeoEye, 2010). However, the cubic convolution method is likely to decrease radiometric accuracy as it can result in the output values being outside of the range of the input values (Baboo & Devi, 2010).

In the second step, the topographical derivatives and statistics were generated using the raw DEM. The raw DEM was used in SAGA to perform a number of residual analyses.

In the third step, both the imagery and topographical derivatives were imported into eCognition. Image segmentation was performed using the multi-resolution segmentation algorithm (Baatz & Schape, 2000). Following image segmentation, objects were selected manually for training data. The training data were applied to train a neural network classifier and classify the objects.

In the fourth step, an accuracy assessment was performed on the classified imagery. Validation data were manually selected for each class. Error matrices were generated to provide users, producers, and overall accuracy. User's accuracy is the probability that an object classified is truly representative of that class. Producer's accuracy represents the classification accuracy of the validation data. Overall accuracy is a summary of the producer's accuracy (Congalton, 1991).

3.4.3 Model Calibration & Regionalization

The model calibration approach applied was the same as in objective 1. However, the number of parameter sets was increased to 300,000 and only HBV was calibrated. TOPMODEL was excluded since it was deemed unsuitable for this landscape. In addition, HBV's upper and lower distribution limits were slightly modified, notably FC and PERC (Table 3.4-4). The model outputs from the calibration were evaluated using the fuzzy measure and only parameter sets attaining the threshold requirement were applied for regionalization.

Table 3.4-4. Upper and lower limits of HBV's refined priori parameter distributions.

Parameter	Description	Unit	Lower Limit	Upper Limit
TT	Threshold temperature	°C	-1.5	1
CFMAX	Degree-Δt factor	mm °C^{-1} Δt$^{-1\ day}$	1	4
SFCF	Snowfall correction factor	N/A	0.5	1.3
CFR	Refreezing coefficient	N/A	0	0.1
CWH	Water holding capacity	N/A	0	0.1
FC	Maximum soil moisture storage (field capacity)	mm	150	650
LP	Soil moisture value above which AET reaches PET	mm	0.3	1
BETA	Determines the relative contribution to runoff from rain or snowmelt	N/A	1	10
PERC	Maximum percolation rate from the upper to the lower groundwater box	mm Δt$^{-1\ day}$	0.01	2
Alpha	Non-linearity coefficient	N/A	0.005	1.5
K1	Storage/recession coefficient	Δt$^{-1\ day}$	0.0001	0.3
K2	Storage/recession coefficient	Δt$^{-1\ day}$	0.00001	0.1
MAXBAS	Length of triangular weighting function	Δt$^{-1\ day}$	1	8

Regionalization, as previously described, is the process of transferring information, such as model parameters, from gauged to ungauged catchments (Kleeberg, 1992; Bloschl & Sivapalan, 1995; Parajka et al., 2005). The applied regionalization techniques transferred or estimated model parameters using information from gauged catchments. Three approaches to regionalization were tested.

The first approach of regionalization methods constructs regional parameter sets from simple descriptive statistics such as means or medians. The successful application of regional parameter sets has been demonstrated to be dependent on the degree of homogeneity in the hydrology of a region (Merz & Bloschl, 2004; Jin et al., 2009). Four regional parameter sets were constructed using the gauged model parameters. The first

regional parameter set (A1) was constructed using the median values of all parameter sets that attained the fuzzy measure threshold. The second regional parameter set (A2) was constructed from the arithmetic mean of all parameter sets. The third regional parameter set (A3) was constructed from the arithmetic weighted mean using the percentage of bog land cover. The fourth regional parameter set (A4) was constructed from the arithmetic weighted mean using the percentage of fen land cover.

The second approach of regionalization methods directly transfers model parameters from observable catchment properties and spatial proximity. The first method *spatial proximity* (A5), transfers model parameters from the spatially nearest catchment. This method is applied on the basis that catchments in proximity to the ungauged site have hydrologically and climatically homogeneous regimes (Jin et al., 2009). The second method *physical similarity* (A6), transfers model parameters based on the similarity of observable catchment properties. This method is applied on the basis that hydrologically similar catchments can be identified from physical catchment attributes (Oudin et al., 2010). The physical similarity between catchments was determined by computing the Euclidean distance between catchments using the topographical and classified land cover metrics. The third method *spatial proximity and physical similarity* (A7), combines both A5 and A6. The donor catchment was determined by first performing hierarchical clustering using Ward's method. Then spatial proximity was applied, considering only the catchments within the cluster of the ungauged catchment.

The third approach of regionalization methods involves estimating model parameters from trained statistical models. The first method is based on regression models (A8) and the second method is based on artificial neural network models (A9). For both A8 and A9 training the models followed the procedure outlined in Seibert (1999). The procedure trains a model for each individual model parameter in two steps. The first step applied a non-parametric Spearman correlation analysis. Each physical catchment attribute was compared to each model parameter to determine the combination that had the highest coefficient of correlation (r). The second step applied regression to determine if that combination had a coefficient of determination (r^2) value greater or equal than 0.25. Under the circumstance that r^2 was below 0.25 or the correlation analysis

was not statistically significant the median model parameter value from A1 was applied. The application of each method is described in details in the following subsection.

3.4.4 Model & Regionalization Validation

Model validation of the performance of the regionalization methods were implemented with two specific details. The first detail was that validation was performed using a *jackknife cross-validation* approach (Miller, 1974). Jackknife cross-validation is an iterative process that successively removed one catchment from the sample. The removed catchment then had its model parameters transferred or estimated using the remaining catchments in the sample. The benefit of this approach is that it treats the gauged catchment as ungauged. Furthermore, this approach reduces or can eliminate the bias of linear functions and diminishes the chance of over-fitting (Abdi & Williams, 2010).

The second detail was the objective functions applied. The NS, and LNS, and the difference between the calibrated NS and LNS and the regionalized NS and LNS were applied to evaluate model performance and performance of the regionalization method.

This completes the outline of the methods applied in this study. Figure 3.4-1 summarizes the entire procedure from preparing the data to model regionalization.

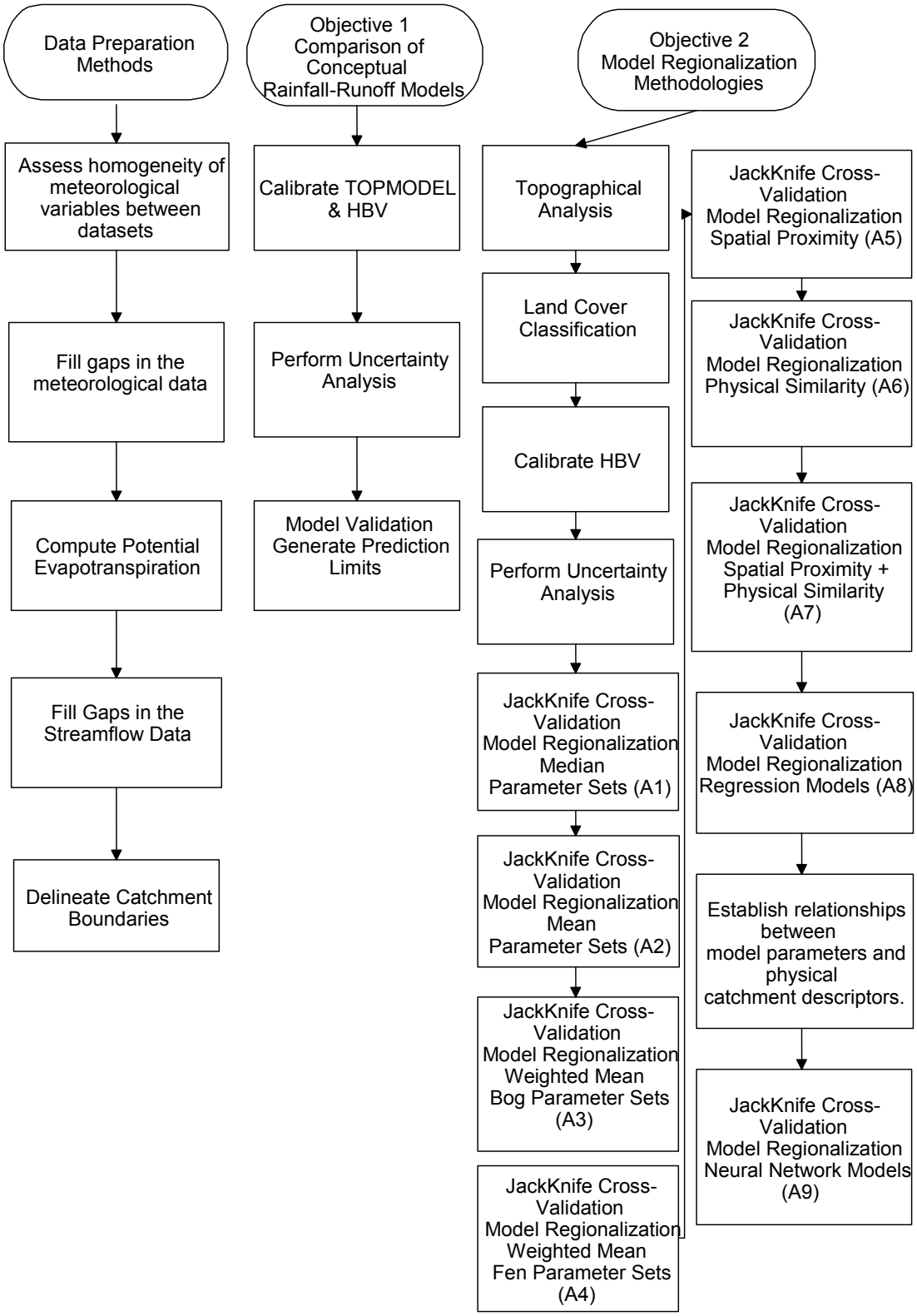

Figure 3.4-1. Entire workflow of methods.

Chapter 4: Results

The thesis results are presented here in three sections. The first section reports on the preparation of the meteorological data, streamflow data, and the delineation of catchment boundaries. The second section reports on the results of the first objective, which is the assessment and comparison of the predictive capability of TOPMODEL and HBV in a James Bay Lowland peatland complex. The third section reports the results of the second objective, including the land cover classification and the application of the regionalization methods.

4.1 Data Preparation Results

4.1.1 Meteorological Data

The preparation of the meteorological data began with an assessment of the homogeneity between the four meteorological stations. This assessment was necessary to ensure the development of a reliable master dataset based on the MC station. The methods in section 3.1.1 were applied to determine homogeneous meteorological station data as a surrogate to fill gaps in the MC dataset. The homogeneous meteorological station data applied as a surrogate is listed in Table 4.1-1.

Table 4.1-1. Meteorological data determined to be a reliable surrogate to resolve gaps in the Muskeg Crew dataset.

	Surrogate Dataset(s)	Period covered by surrogate	Period requiring interpolation	Additional information
Temperature	Lansdowne House, Victor	2007 - 2010	2011-2012	
Net Radiation	Victor	2007-2010	2011-2012	Gaps in Victor dataset also needed to be estimated
Precipitation	Lansdowne House, Victor, MOE	2007-2012		

The LH and Victor datasets were applicable to temperature and precipitation. Both datasets were able to cover a period from 2007 to 2010. However, the MOE stations were not determined to be homogeneous. The MOE stations covered a period from 2011 to 2012. This resulted in having to apply methods to estimate missing values for net radiation and temperature during that period. In addition, the Victor dataset had gaps in the net radiation measurements prior to 2011 that required gap filling measures.

The estimation of the missing measurements applied M5 regression tree models. The performances of the trained models were validated against 20% of the observational data and the results are listed in Table 4.1-2. Both trained models were capable of reliably estimating known values. Validation of the temperature model demonstrated an r of 0.97, r^2 of 0.94, and a root mean square error (RMSE) value of 3.19. Net radiation demonstrated an r of 0.87, r^2 of 0.77, and a RMSE of 30.72.

Table 4.1-2. Validation results of estimated temperature and net radiation data.

	r^2	RMSE
Temperature	0.94	3.19
Net Radiation	0.77	30.72

4.1.2 Streamflow Data

The streamflow data was corrected using an SKNN multiple imputation technique as described in section 3.1.2 (Kim et al., 2004). The technique's performance was validated against 20% of the observational data. The results are listed in Table 4.1-3. The performance of the SKNN imputation technique was generally excellent with the exception of the SG.001 and Trib 5A catchments.

Table 4.1-3. Performance of SKNN streamflow imputation per catchment.

Catchment	RMSE	R^2	NS
NNGC	0.02	0.88	0.88
SNGC	0.07	0.84	0.83
Trib 3	0.35	0.97	0.97
Trib 5	0.39	0.98	0.97
Trib 5A	0.17	0.68	0.63
Trib 7	0.33	0.89	0.88
NG.001	0.09	0.90	0.90
SG.001	0.35	0.54	0.49

4.2 Comparison of Catchment Boundaries Delineated using SRTM and LiDAR

A visual comparison of the boundaries of NNGC and SNGC generated from SRTM data and LiDAR data is illustrated in Figures 4.2-1 and 4.2-2. There are notable differences in the delineated boundaries. The NNGC catchments differ slightly with a difference in area of 1.50 km^2 or 13%. The LiDAR NNGC boundary is longer and the SRTM boundary is wider. Tracing the channel fens across the NNGC catchment reveals that the SRTM boundary includes area that is unlikely to be part of the NNGC catchment, notably along the north-east portion of the catchment. The LiDAR boundary encounters the same issue along the western portion of the boundary, but to a much lesser extent. The SNGC boundaries differ a little more with a difference in area of 4.35 km^2 or 21%. The southern portion of the catchments differs considerably within a bog complex. Tracing the channel fen network suggests the LiDAR boundary is likely more accurate than the SRTM boundary.

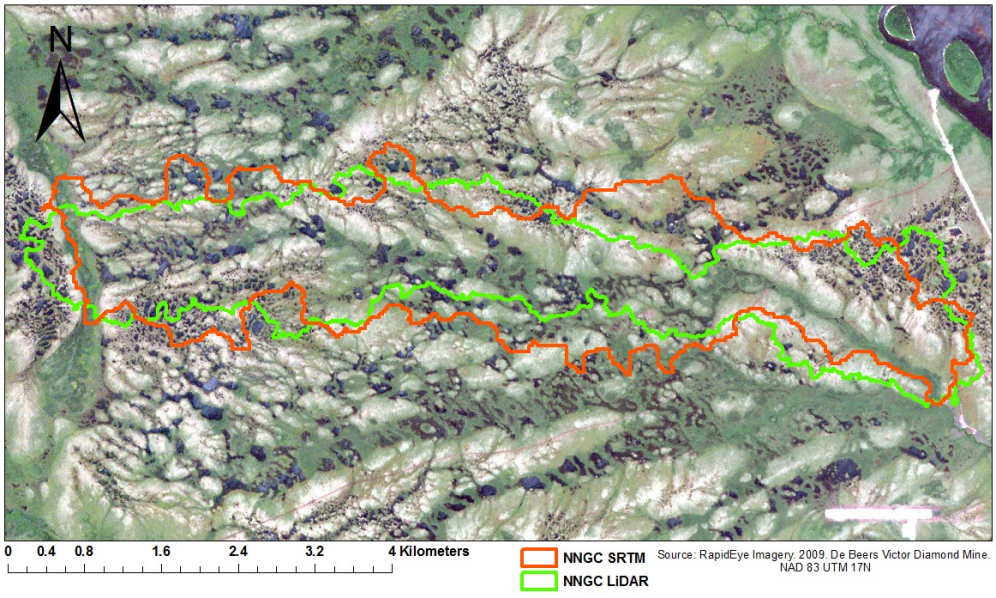

Figure 4.2-1. Boundaries of NNGC SRTM (12.40 km^2) and NNGC LiDAR (10.81 km^2).

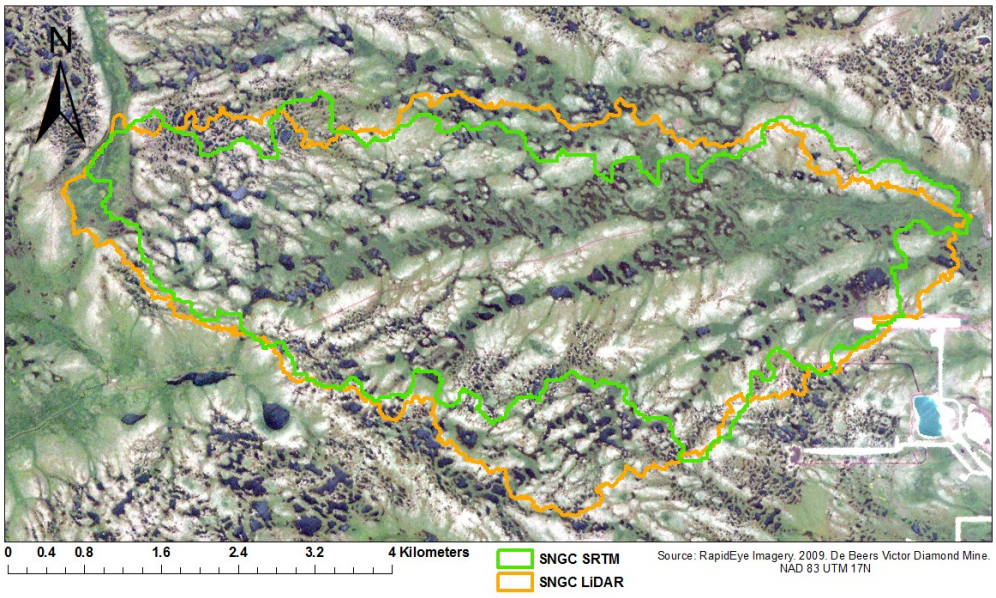

Figure 4.2-2. Boundaries of SNGC (19.80 km^2) and SNGC (24.15 km^2).

Despite these variations, the coarser SRTM DEM should not be dismissed as inaccurate. Charrier & Li (2012), demonstrated that coarser DEMs (10 m) are often more appropriate for boundary delineation than finer DEMs, because finer DEMs are sensitive to minor topographic changes including artefacts which could cause boundary delineation errors. However, in peatlands finer DEMs are necessary for those minor topographic changes (Holden, 2005). The LiDAR DEM results are likely more accurate than the SRTM DEM, but the SRTM results are presumably acceptable. If a similar discrepancy were to exist along the boundaries of the larger catchments, it would represent a smaller fraction of the total area and the relative error would not be an issue.

4.3 Comparison of Conceptual Rainfall-Runoff Models Results

The first objective involved assessing and comparing the predictive capability of TOPMODEL and HBV. The first objective applied the methods in 3.3. The results are presented in three parts. The first part reports on the refined prior parameter distribution limits derived from Monte Carlo simulations and uncertainty analysis. The second part reports on the evaluation metrics for both models and each catchment. The third part provides hydrographs of the best simulations for both models and each catchment.

4.3.1 Refined Prior Parameter Distribution Limits

The first step was to refine the *a priori* parameter distributions of both models to optimize model performance. Monte Carlo simulations were performed and the model outputs were analyzed using MCAT. The refined prior parameter distribution limits are listed in Table 4.3-1 and 4.3-2.

Table 4.3-1. TOPMODEL refined prior parameter distribution limits.

Parameter	Description	Unit	Lower Limit	Upper Limit
TT	Threshold temperature	°C	-1.5	1
CFMAX	Degree-Δt factor	mm °C^{-1} Δt$^{-1\ day}$	1	4
SFCF	Snowfall correction factor	N/A	0.5	1.3
CFR	Refreezing coefficient	N/A	0	0.1
CWH	Water holding capacity	N/A	0	0.1
QS0	Initial subsurface flow per unit area	m	0.00001	0.001
lnTe	Log of the areal average of transmissivity (T0)	m² h	9	15
M	Model parameter	m	0.01	0.08
Sr0	Initial root zone storage deficit	m	0.00003	0.9
Srmax	Maximum root zone storage deficit	m	0.005	0.15
TD	Unsaturated zone time delay per unit storage deficit	h/m	0.001	15
VR	Channel velocity	m/h	50	2000
K0	Surface hydraulic conductivity	m/h	1	10
CD	Capillary drive	N/A	10	20

Table 4.3-2. HBV refined prior parameter distribution limits.

Parameter	Description	Unit	Lower Limit	Upper Limit
TT	Threshold temperature	°C	-1.5	1
CFMAX	Degree-Δt factor	mm °C^{-1} Δt$^{-1\ day}$	1	4
SFCF	Snowfall correction factor	N/A	0.5	1.3
CFR	Refreezing coefficient	N/A	0	0.1
CWH	Water holding capacity	N/A	0	0.1
FC	Maximum soil moisture storage (field capacity)	mm	150	500
LP	Soil moisture value above which AET reaches PET	mm	0.3	1
BETA	Determines the relative contribution to runoff from rain or snowmelt	N/A	1	10
PERC	Maximum percolation rate from the upper to the lower groundwater box	mm Δt$^{-1\ day}$	0.1	4
Alpha	Non-linearity coefficient	N/A	0.005	1.5
K1	Storage/recession coefficient	Δt$^{-1\ day}$	0.0001	0.3
K2	Storage/recession coefficient	Δt$^{-1\ day}$	0.00001	0.1
MAXBAS	Length of triangular weighting function	Δt$^{-1\ day}$	1	8

4.3.2 Performance Evaluation Metrics

The second part was the evaluation of the newly calibrated models using the refined prior parameter distributions. For each catchment and both models the optimal parameter set was determined using the fuzzy measure. Under the circumstance in which a catchment had a fuzzy measure of 0 the optimal parameter set was determined from the sum of NS and LNS. The results for TOPMODEL are listed in Table 4.3-3 and HBV in Table 4.3-4.

Table 4.3-3. TOPMODEL performance results of optimal parameter sets.

	Calibration Period					Validation Period		
	NS	LNS	Verr	Fuzzy	% within prediction limits	NS	LNS	% within prediction limits
NNGC	0.00	0.43	1.08	0.00	0.00	0.00	0.61	0.00
NG.001	0.44	0.62	0.07	0.35	0.05	0.03	0.65	0.15
SNGC	0.56	0.67	0.04	0.58	0.32	0.17	0.45	0.27
SG.001	0.52	0.42	0.02	0.00	0.00	0.02	0.44	0.00
Trib 3	0.43	0.73	0.08	0.51	0.38	0.27	0.40	0.52
Trib 5	0.55	0.68	0.11	0.38	0.25	0.12	0.55	0.18
Trib 5A	0.55	0.00	0.14	0.00	0.00	0.07	0.00	0.00
Trib 7	0.54	0.00	0.15	0.00	0.00	0.19	0.39	0.00
Overall	**0.45**	**0.44**	**0.21**	**0.23**	**0.13**	**0.11**	**0.44**	**0.14**

Table 4.3-4. HBV performance results of optimal parameter sets.

	Calibration Period					Validation Period		
	NS	LNS	Verr	Fuzzy	% within prediction limits	NS	LNS	% within prediction limits
NNGC	0.40	0.50	0.04	0.52	0.00	0.58	0.72	0.00
NG.001	0.62	0.82	0.03	0.65	0.73	0.45	0.44	0.67
SNGC	0.69	0.72	0.01	0.65	0.62	0.68	0.40	0.44
SG.001	0.61	0.70	0.05	0.63	0.52	0.38	0.57	0.53
Trib 3	0.49	0.75	0.13	0.31	0.51	0.57	0.18	0.30
Trib 5	0.72	0.79	0.06	0.67	0.60	0.50	0.49	0.53
Trib 5A	0.60	0.75	0.10	0.45	0.46	0.39	0.25	0.37
Trib 7	0.53	0.64	0.04	0.43	0.65	0.39	0.38	0.56
Overall	**0.58**	**0.71**	**0.06**	**0.54**	**0.51**	**0.49**	**0.43**	**0.43**

TOPMODEL on average had an NS of 0.45, LNS of 0.44, and fuzzy of 0.23. During the calibration period TOPMODEL was only able to capture on average 13% of the catchments' rainfall-runoff behaviour. In the validation period, the average NS dropped to 0.11, but the LNS remained at 0.44. On average 14% of the catchments' rainfall-runoff behaviour was captured during the validation period. These results do not promote the application of TOPMODEL in this environment.

HBV on average had an NS of 0.58, LNS of 0.71, and a fuzzy of 0.54. During the calibration period HBV was able to capture on average 51% of the catchments' rainfall-runoff behaviour. In the validation period, the average NS dropped to 0.49, and the LNS dropped to 0.43. On average 43% of the catchments' rainfall-runoff behaviour was

captured during the validation period. These results suggest that the application of the HBV model structure in this environment is sensible.

4.3.3 Hydrographs

The following section provides the hydrographs illustrating the optimal model output for each catchment for both TOPMODEL and HBV-Light.

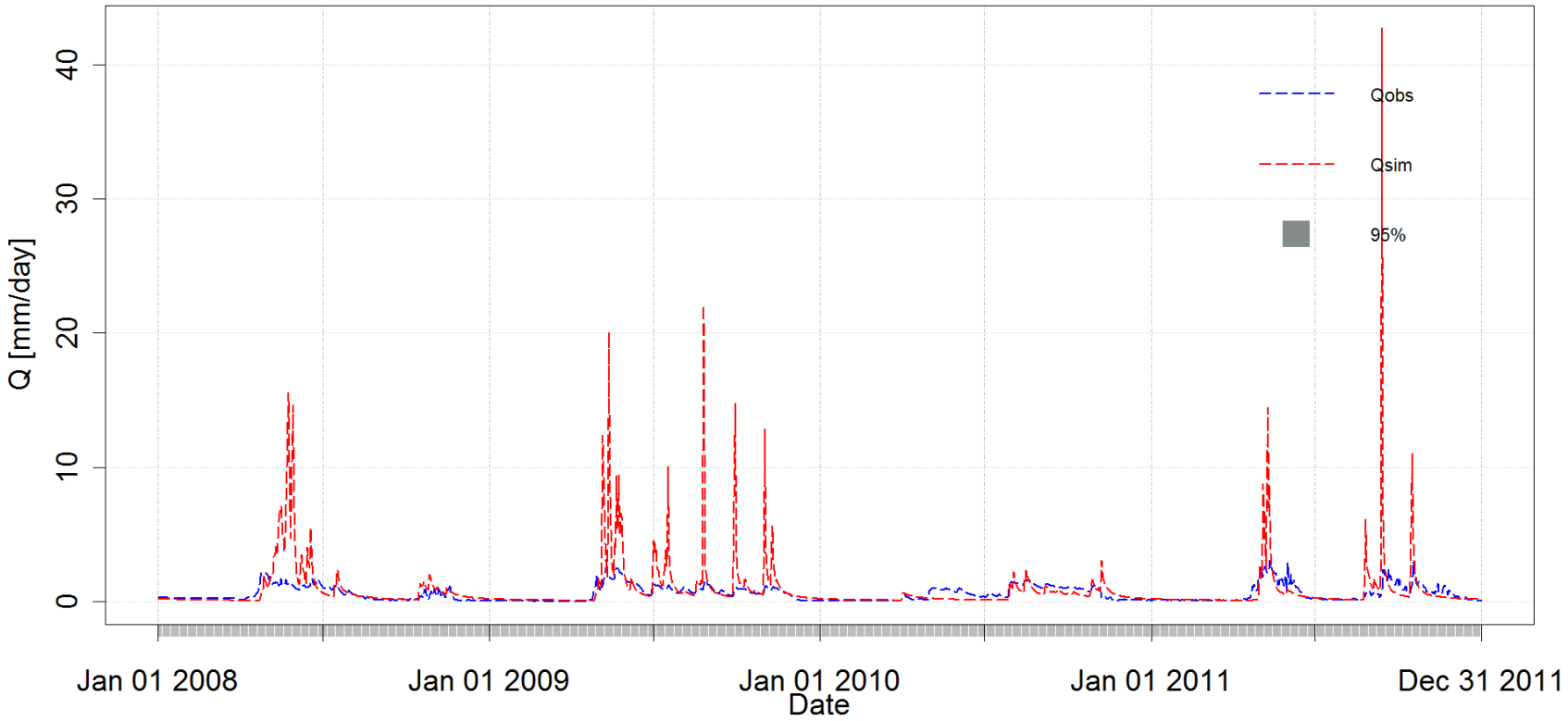

Figure 4.3-1. TOPMODEL - NNGC best model output. Qobs: Observed runoff, Qsim: Simulated runoff, 95%: Prediction limit 5% - 95% quantile interval.

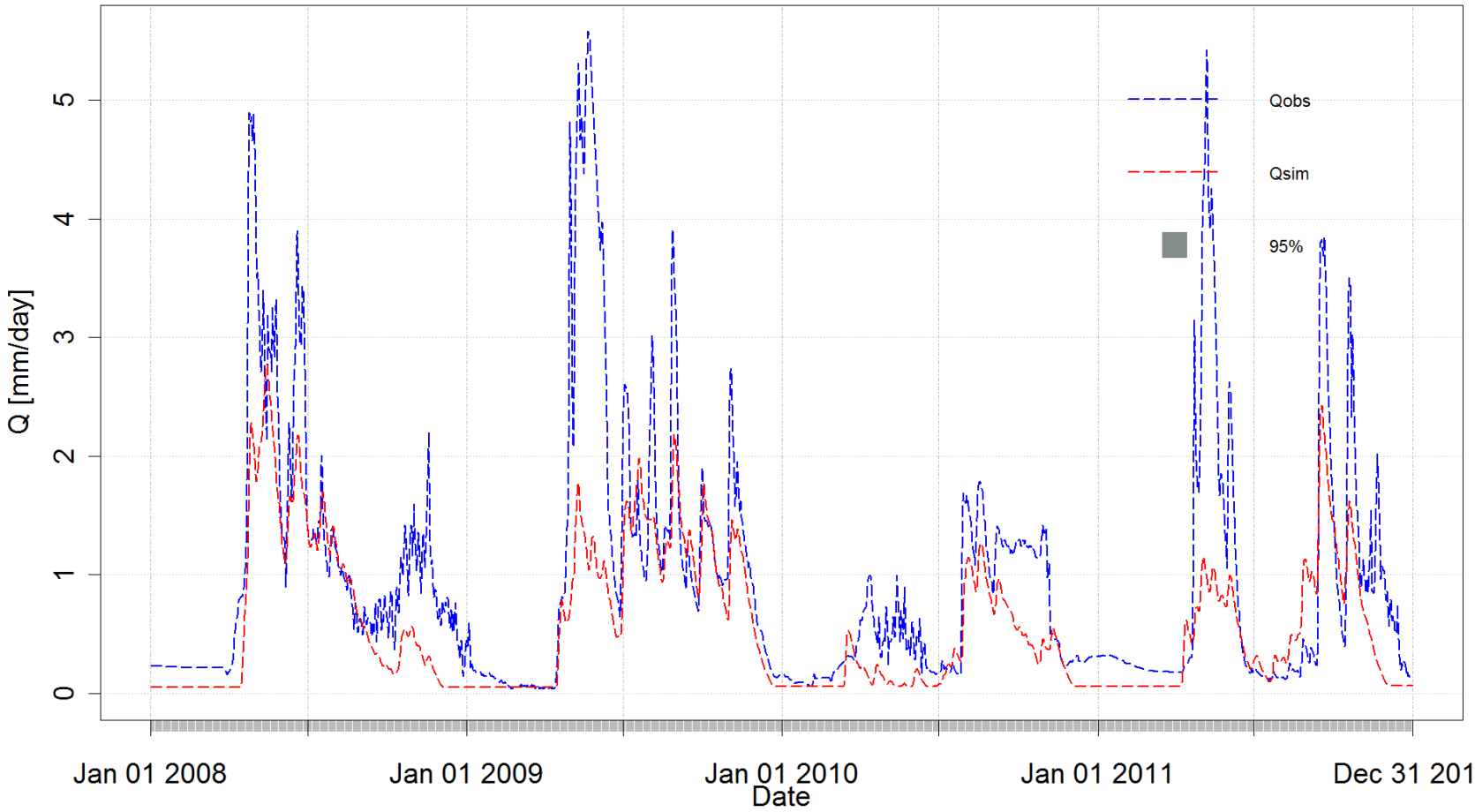

Figure 4.3-2. HBV - NNGC best model output. Qobs: Observed runoff, Qsim: Simulated runoff, 95%: Prediction limit 5% - 95% quantile interval.

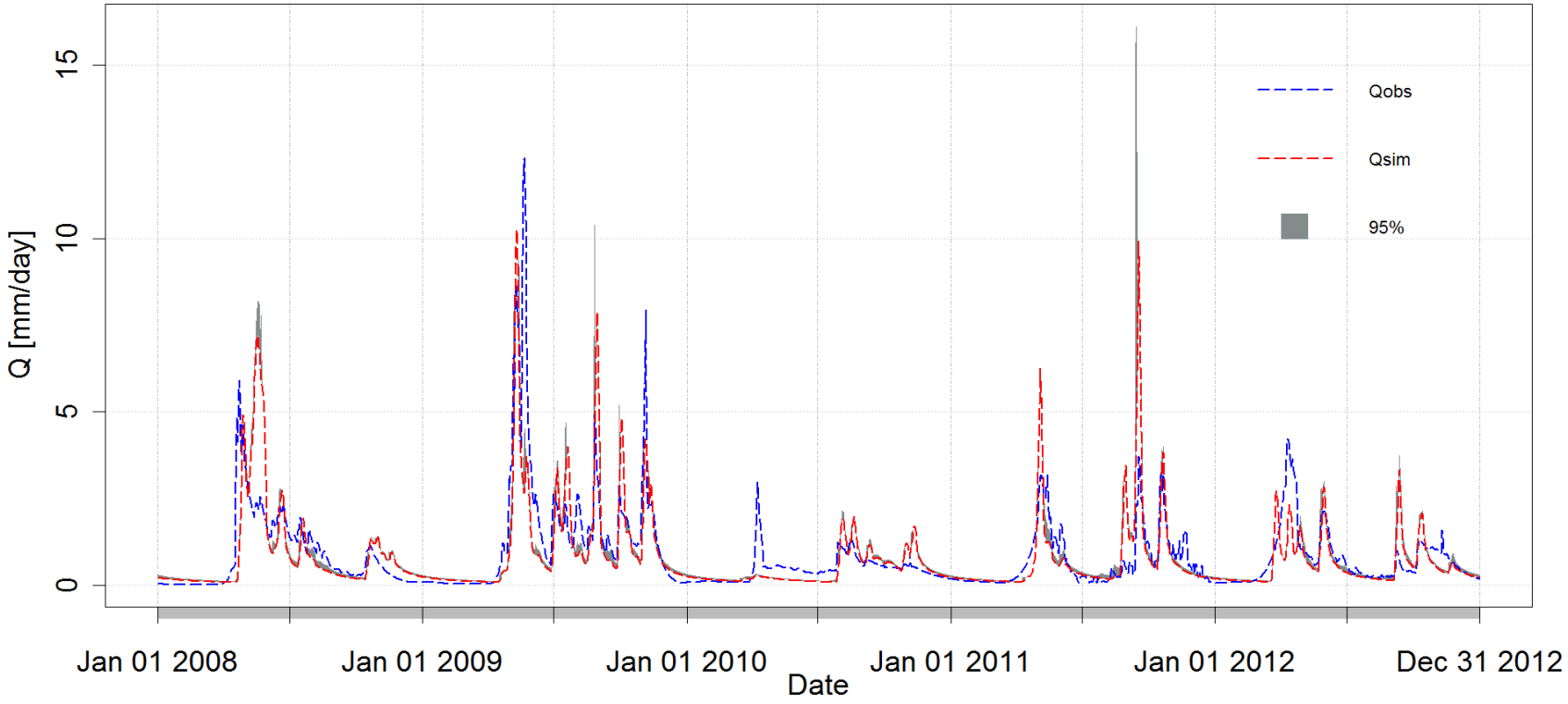

Figure 4.3-3. TOPMODEL - NG.001 best model output. Qobs: Observed runoff, Qsim: Simulated runoff, 95%: Prediction limit 5% - 95% quantile interval.

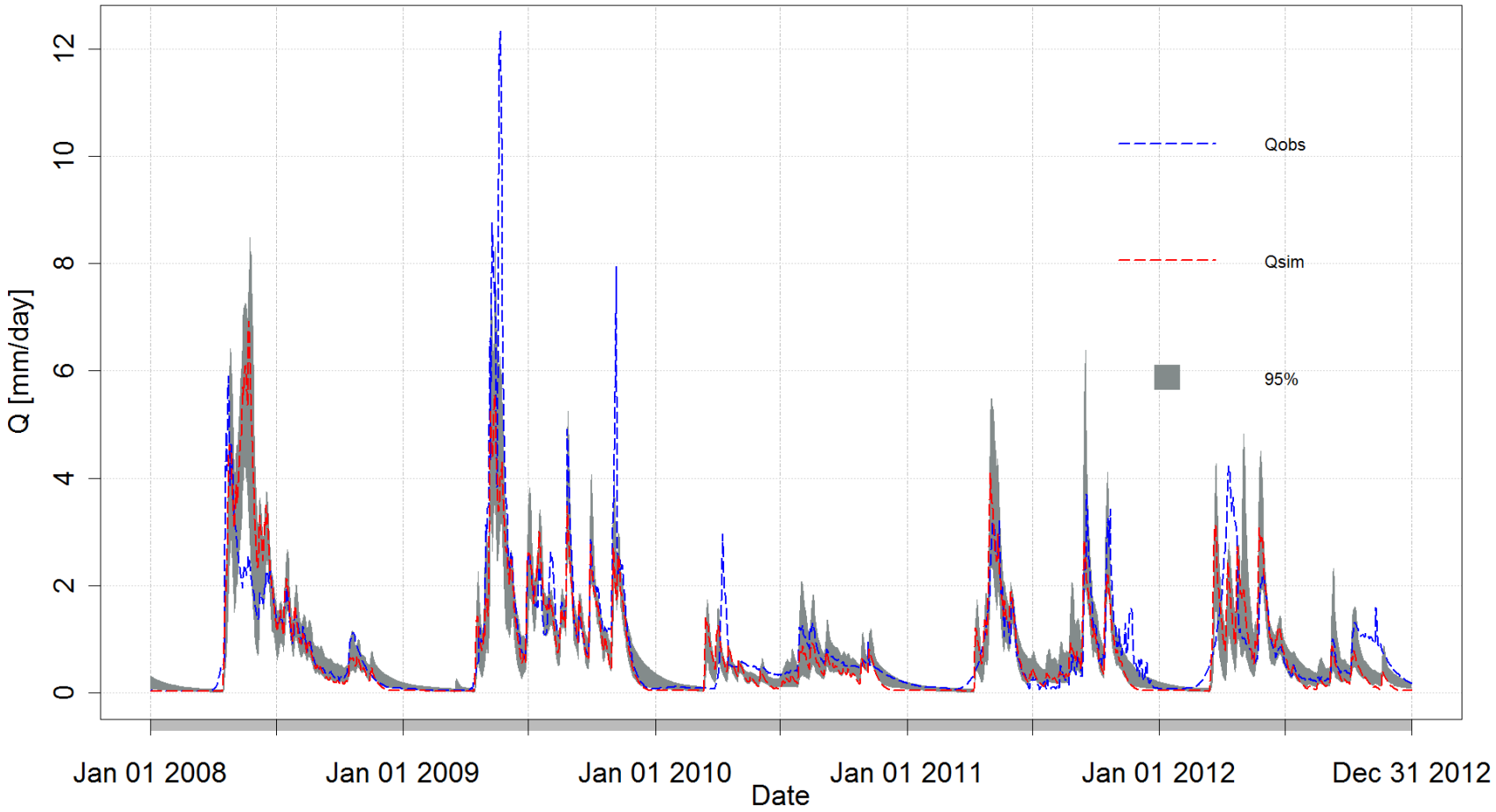

Figure 4.3-4. HBV - NG.001 best model output. Qobs: Observed runoff, Qsim: Simulated runoff, 95%: Prediction limit 5% - 95% quantile interval.

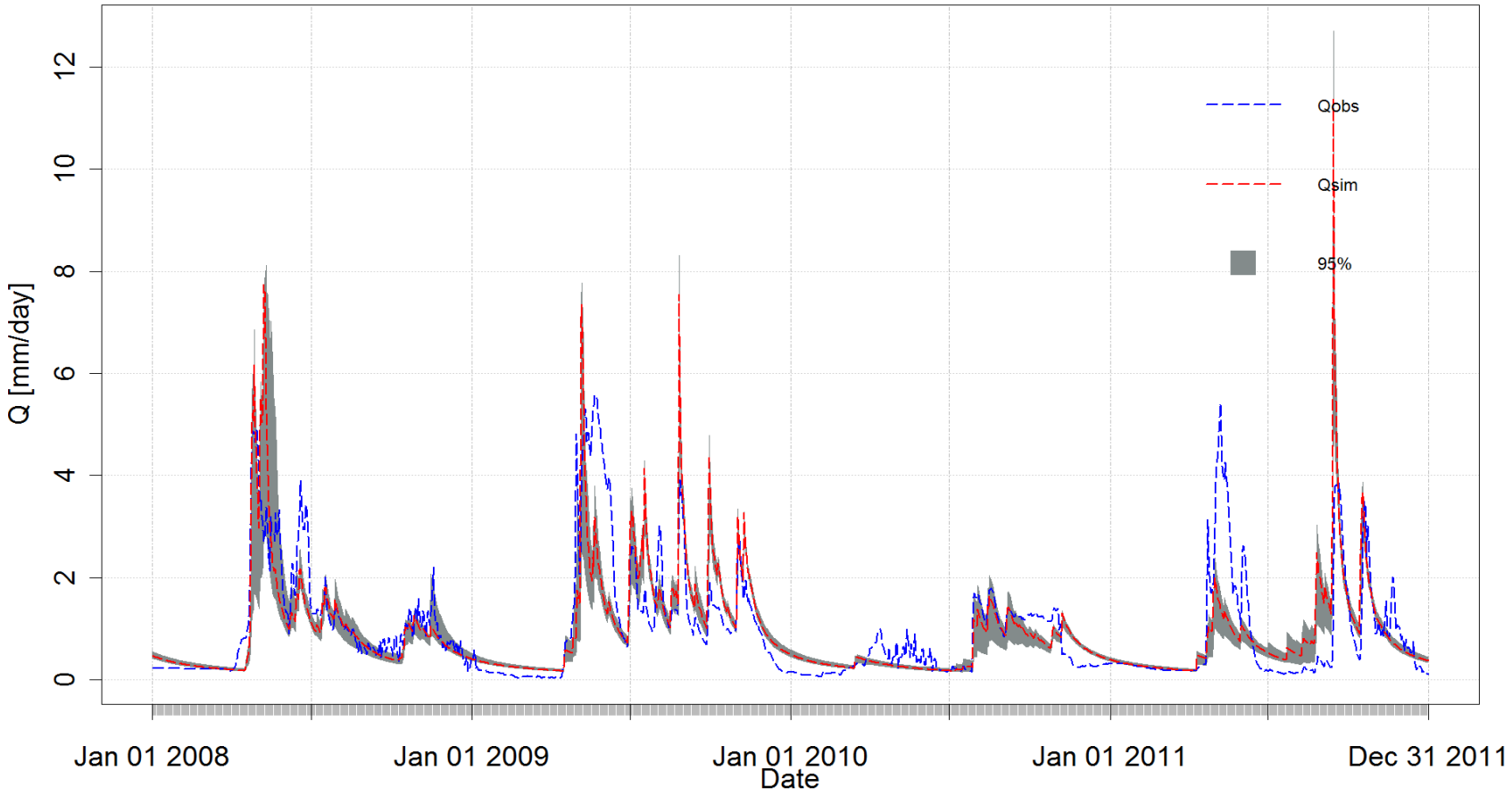

Figure 4.3-5. TOPMODEL - SNGC best model output. Qobs: Observed runoff, Qsim: Simulated runoff, 95%: Prediction limit 5% - 95% quantile interval.

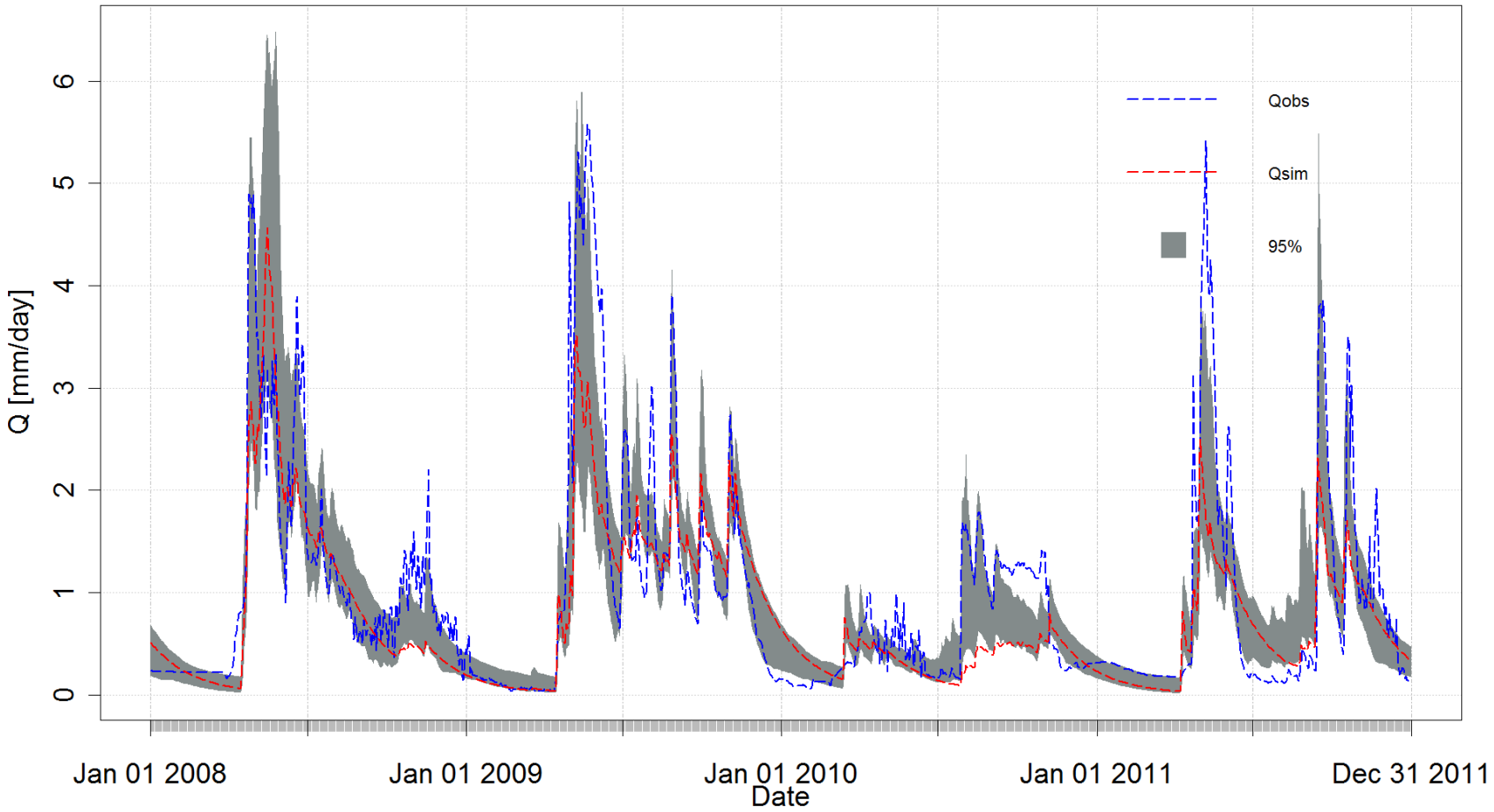

Figure 4.3-6. HBV - SNGC best model output. Qobs: Observed runoff, Qsim: Simulated runoff, 95%: Prediction limit 5% - 95% quantile interval.

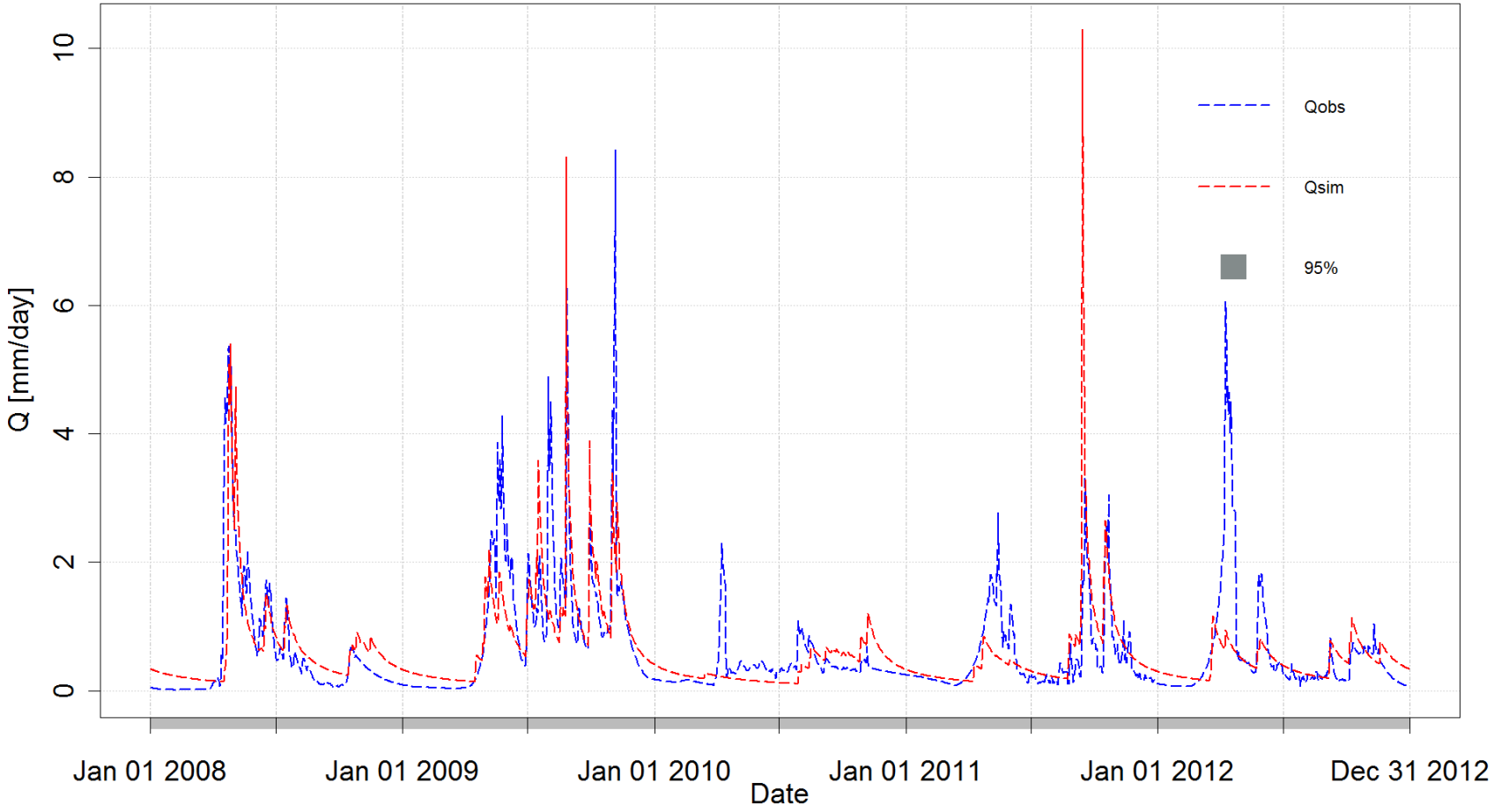

Figure 4.3-7. TOPMODEL - SG.001 best model output. Qobs: Observed runoff, Qsim: Simulated runoff, 95%: Prediction limit 5% - 95% quantile interval.

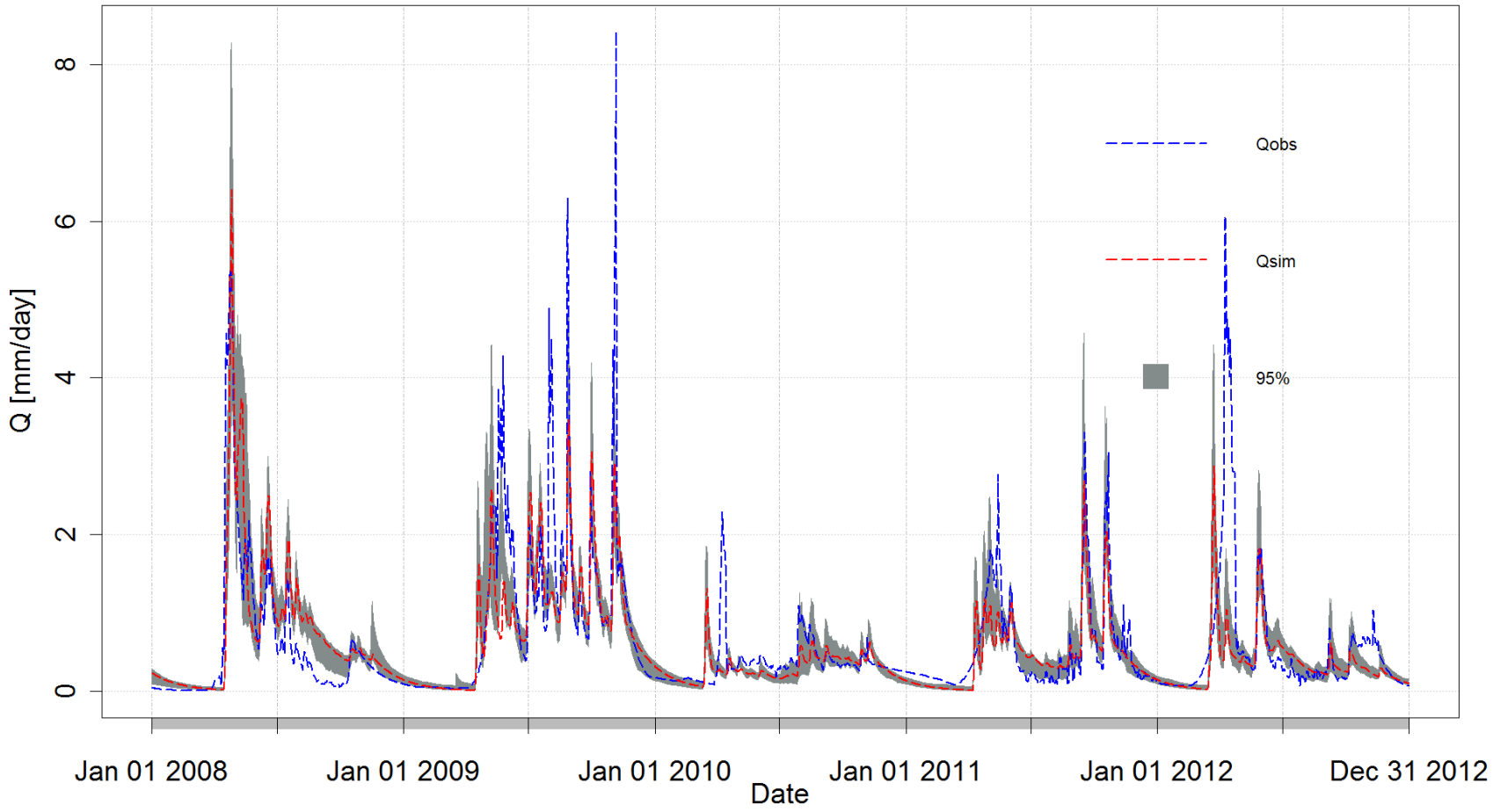

Figure 4.3-8. HBV - SG.001 best model output. Qobs: Observed runoff, Qsim: Simulated runoff, 95%: Prediction limit 5% - 95% quantile interval.

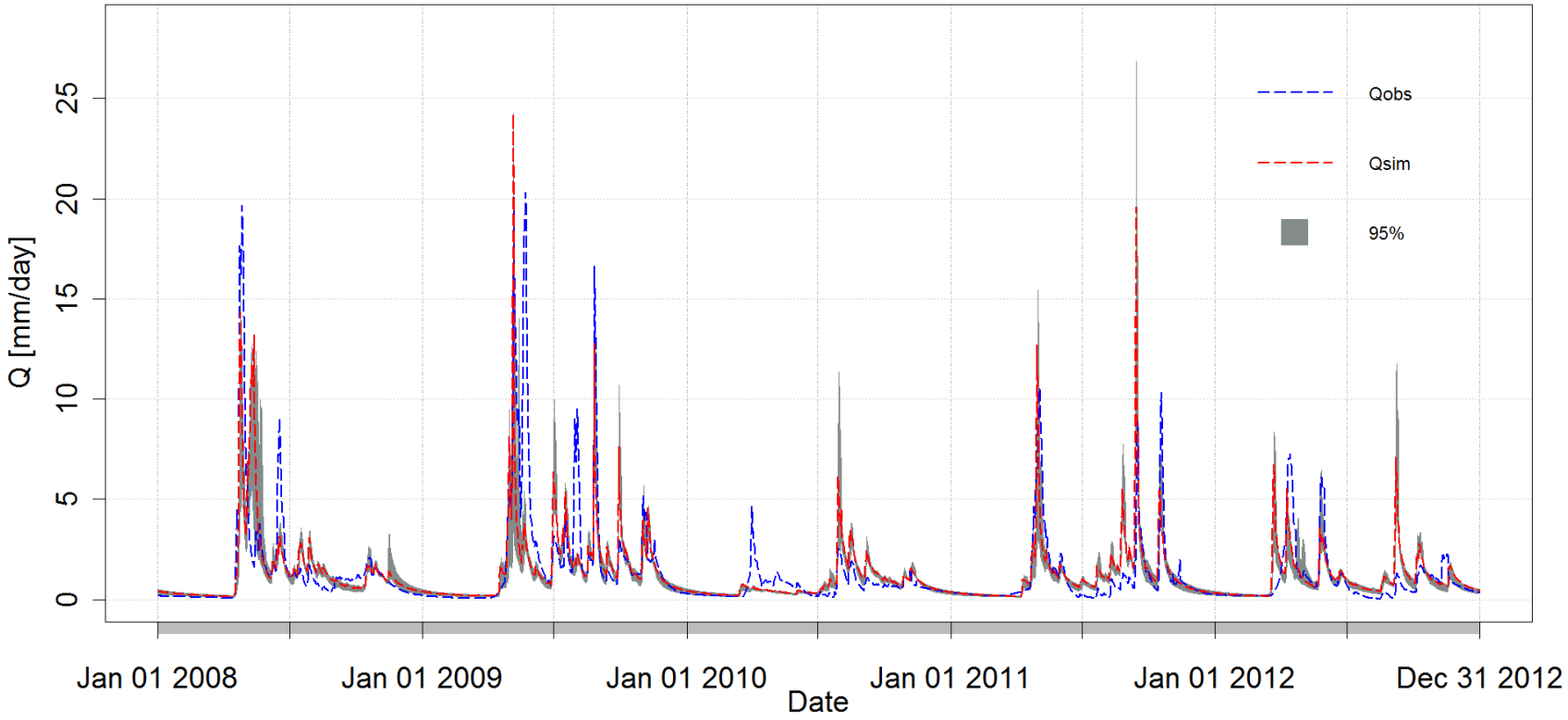

Figure 4.3-9. TOPMODEL - Trib 3 best model output. Qobs: Observed runoff, Qsim: Simulated runoff, 95%: Prediction limit 5% - 95% quantile interval.

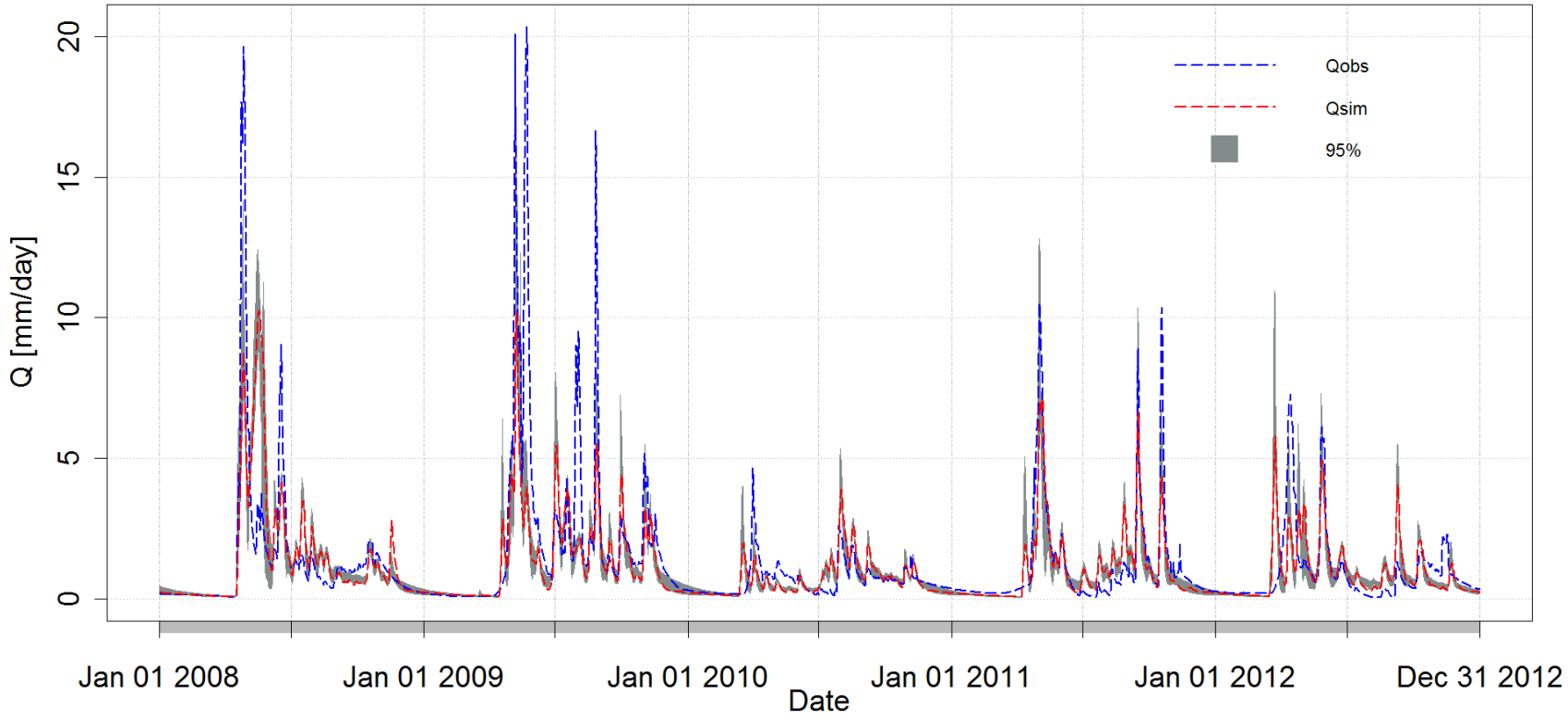

Figure 4.3-10. HBV - Trib 3 best model output. Qobs: Observed runoff, Qsim: Simulated runoff, 95%: Prediction limit 5% - 95% quantile interval.

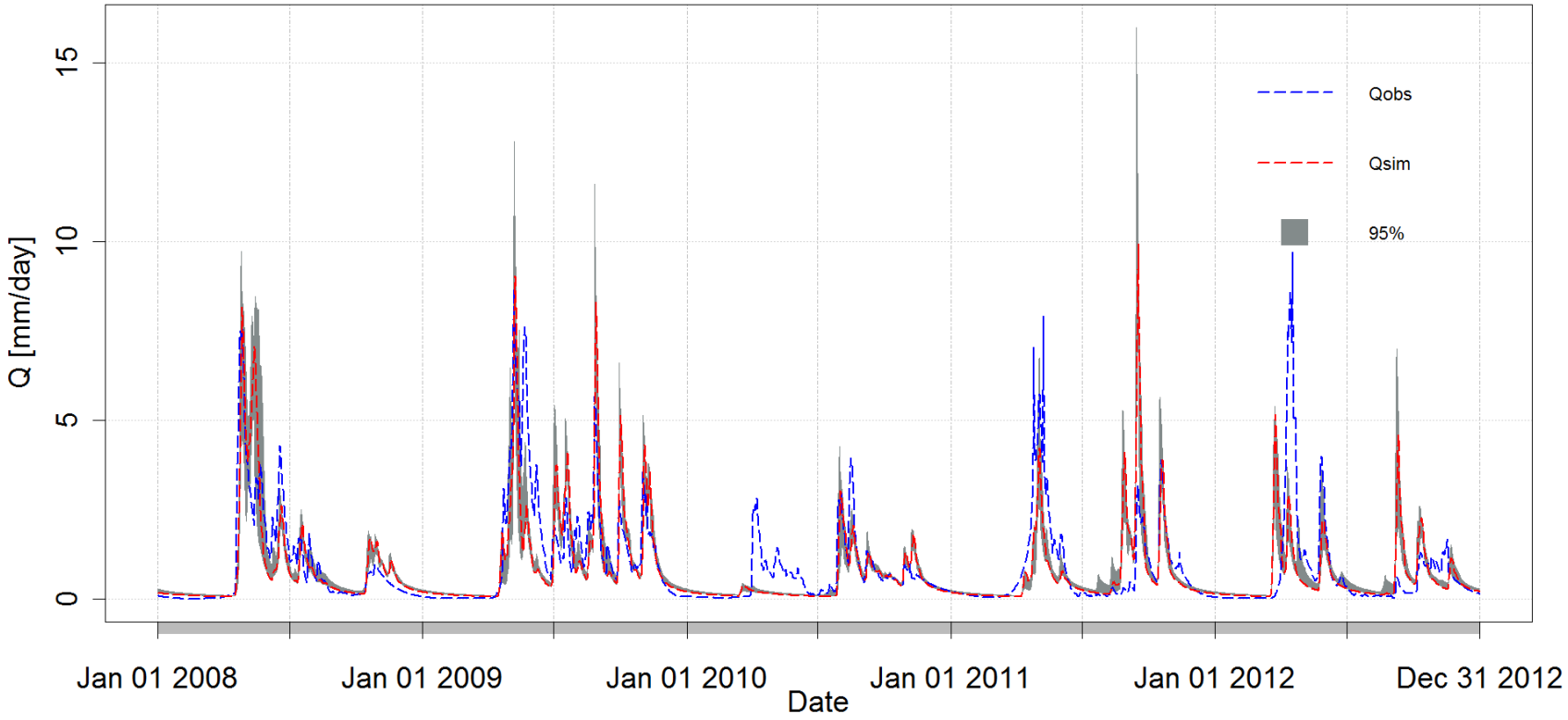

Figure 4.3-11. TOPMODEL - Trib 5 best model output. Qobs: Observed runoff, Qsim: Simulated runoff, 95%: Prediction limit 5% - 95% quantile interval.

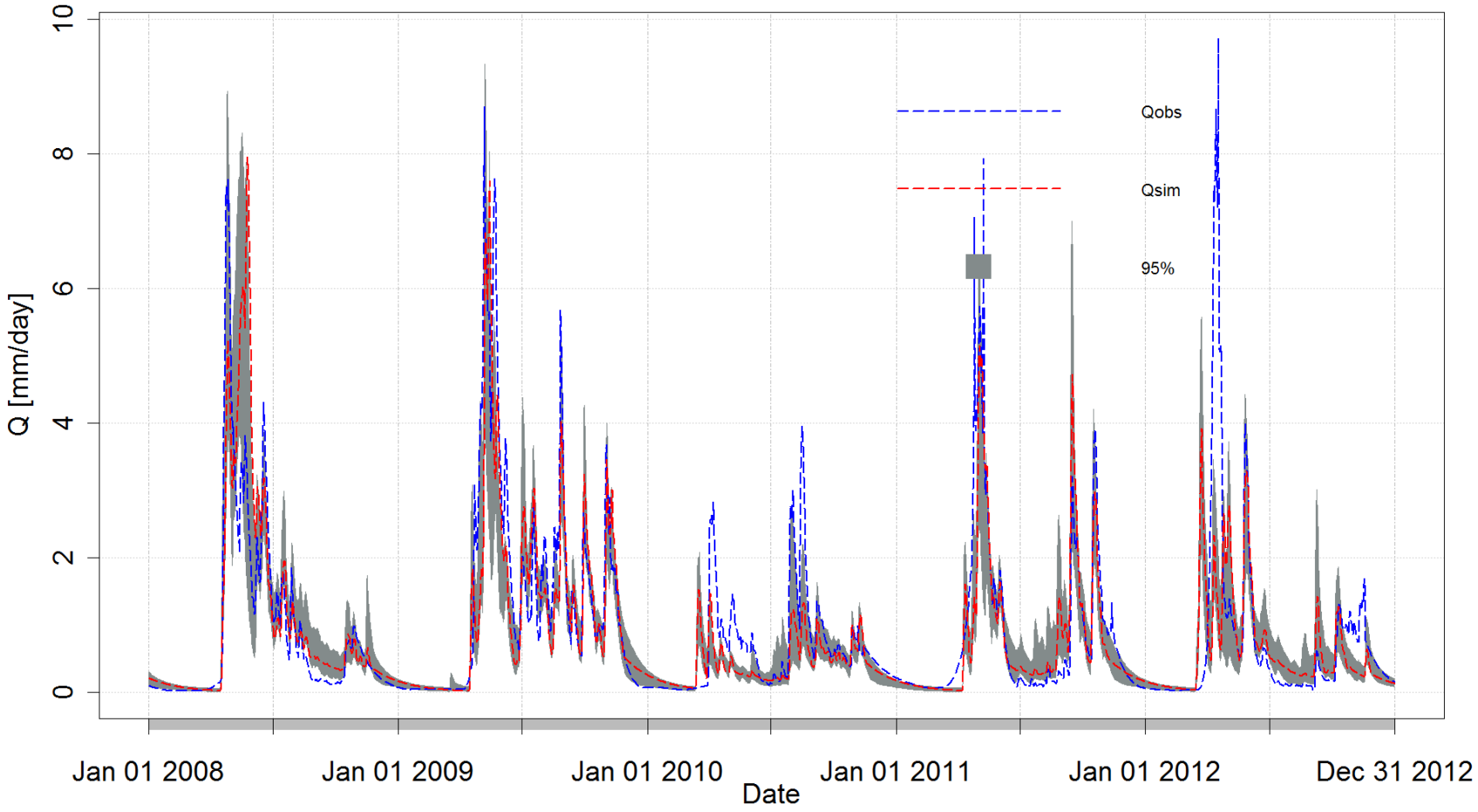

Figure 4.3-12. HBV - Trib 5 best model output. Qobs: Observed runoff, Qsim: Simulated runoff, 95%: Prediction limit 5% - 95% quantile interval.

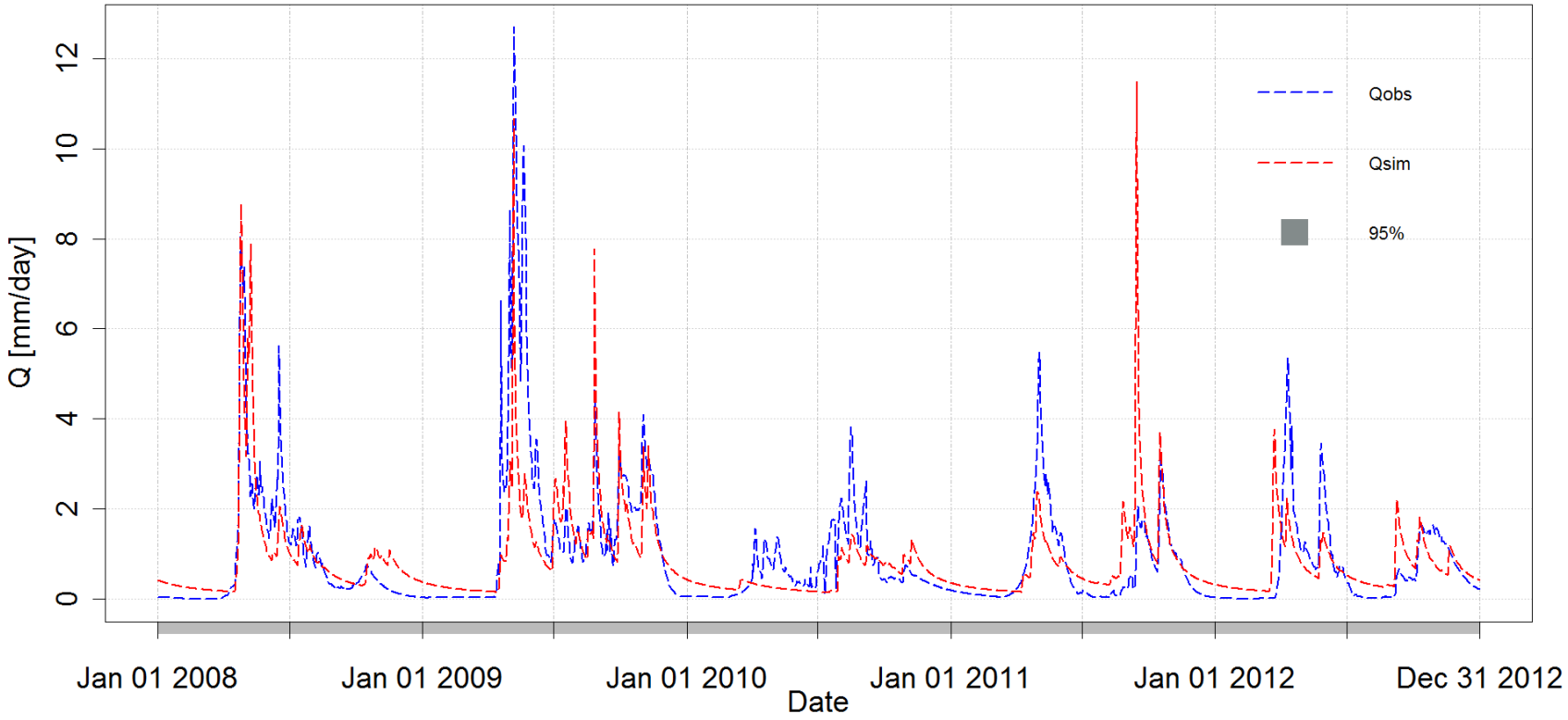

Figure 4.3-13. TOPMODEL - Trib 5A best model output. Qobs: Observed runoff, Qsim: Simulated runoff, 95%: Prediction limit 5% - 95% quantile interval.

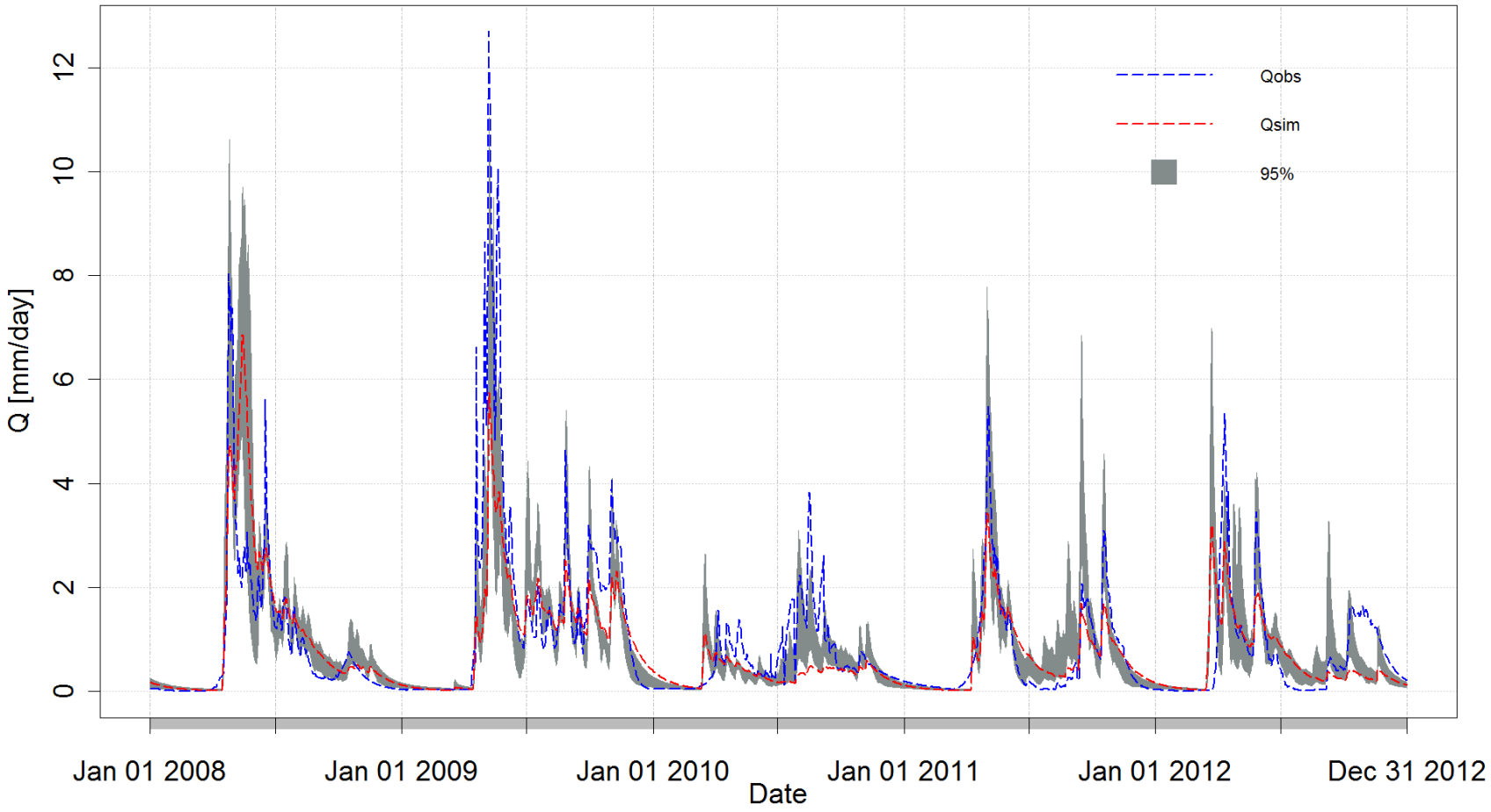

Figure 4.3-14. HBV - Trib 5A best model output. Qobs: Observed runoff, Qsim: Simulated runoff, 95%: Prediction limit 5% - 95% quantile interval.

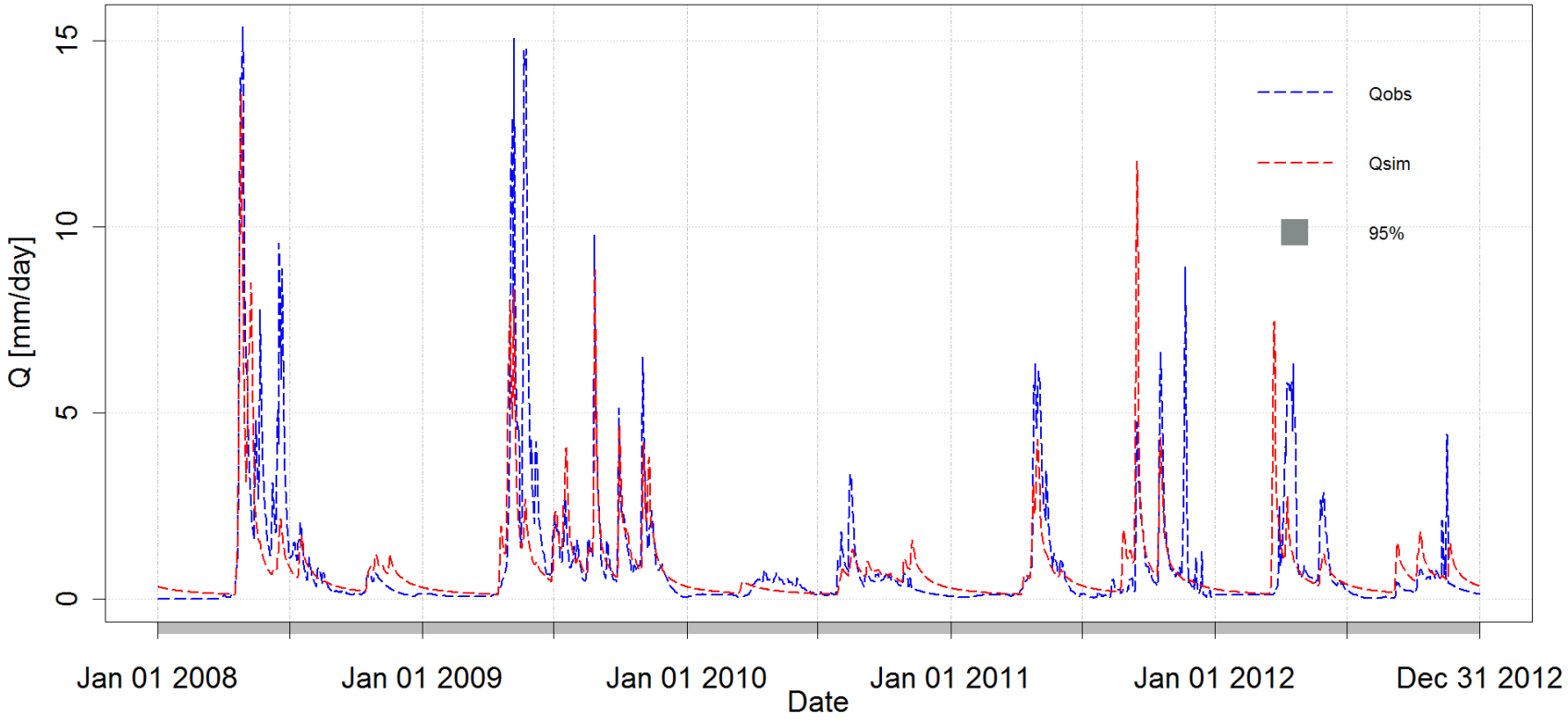

Figure 4.3-15. TOPMODEL - Trib 7 best model output. Qobs: Observed runoff, Qsim: Simulated runoff, 95%: Prediction limit 5% - 95% quantile interval.

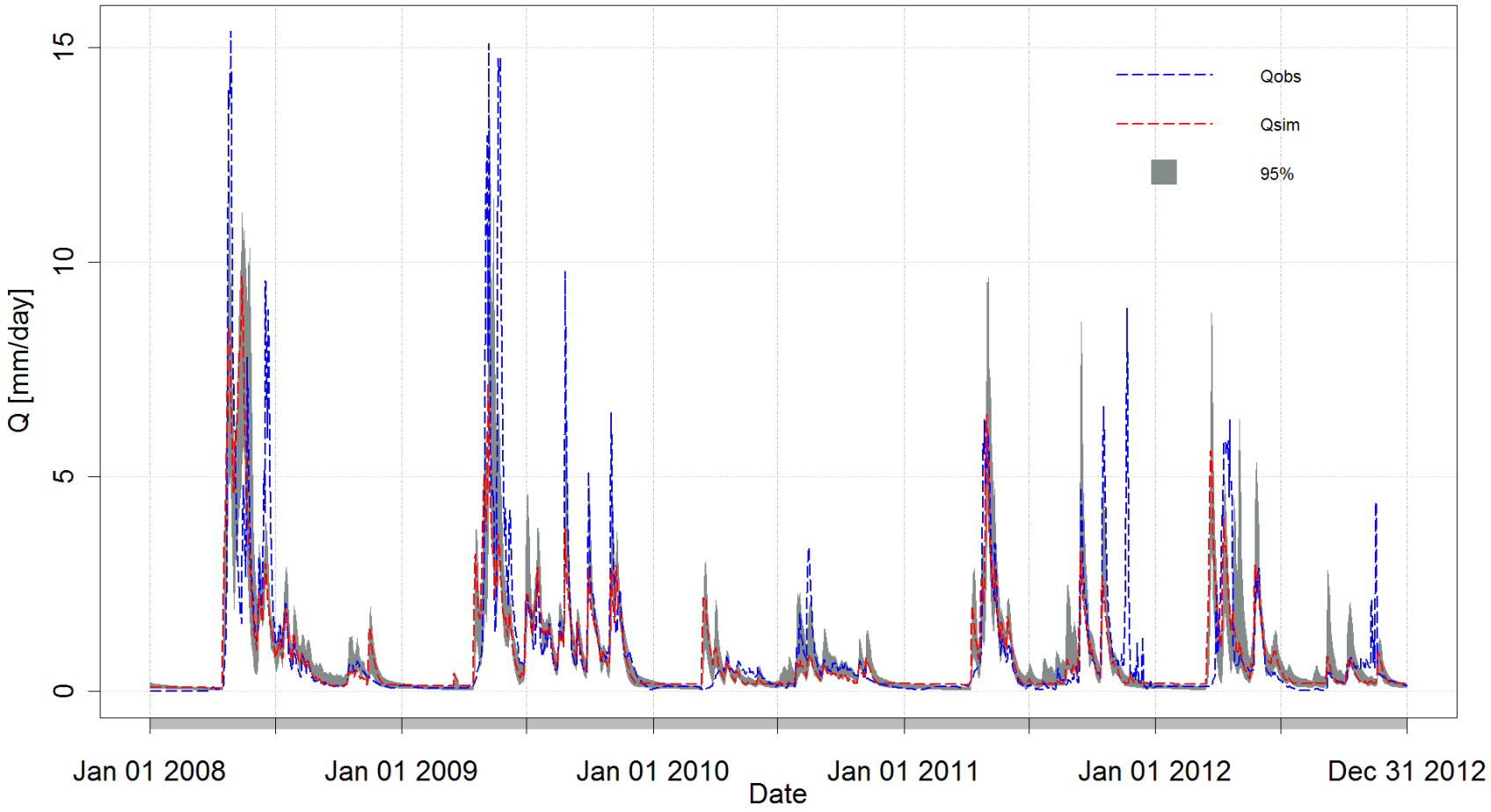

Figure 4.3-16. HBV - Trib 7 best model output. Qobs: Observed runoff, Qsim: Simulated runoff, 95%: Prediction limit 5% - 95% quantile interval.

4.4 Model Regionalization Results

The second objective was the application and evaluation to determine an optimal and suitable regionalization methods to transfer or estimate model parameters for HBV. The intent was to determine a suitable regionalization method to reduce operational cost and calibrate models in ungauged northern peatland catchments. The objective included three main procedures: topographical analyses, land cover classification, and model regionalization.

4.4.1 Topographical Analysis

The topographical metrics generated following the methods outlined in section 3.4.1 are summarized in Table 4.4-1.

Table 4.4-1. Topographical metrics generated.

Descriptors / Catchments	NNGC	NG.001	SNGC	SG.001	Trib 3	Trib 5	Trib 5A	Trib7
Area (Km²)	12.40	42.90	19.80	34.80	105.60	215.70	27.70	88.00
Average Elevation (m)	88.40	86.94	88.44	86.42	94.00	104.40	93.65	82.21
Average Catchment Slope (°)	1.24	1.21	1.21	1.21	1.26	1.19	1.14	1.13
Average SWI (-)	17.96	18.51	18.12	18.39	18.37	18.99	18.40	18.32
Average Flow Path Gradient (-)	0.0138	0.0072	0.0109	0.0069	0.0109	0.0107	0.0100	0.0099
Average L/G (-)	139620.68	446665.08	292029.90	481244.05	265557.49	239161.65	332269.52	384877.95
Total Stream Length (m)	18896.90	53728.30	33819.75	46378.77	137933.93	335667.73	41022.10	121661.59
Drainage Density (m)	0.0015	0.0013	0.0017	0.0013	0.0013	0.0016	0.0015	0.0014
Basin Slope (°)	0.0007	0.0010	0.0006	0.0009	0.0006	0.0009	0.0010	0.0007
Gravelius Shape Index (-)	3.05	2.62	2.35	3.06	2.57	2.76	2.33	2.44
Gravelius Circularity Ratio (-)	0.11	0.14	0.18	0.11	0.15	0.13	0.18	0.17
Shape Index (-)	10.96	6.84	7.79	6.69	1.88	10.39	6.03	5.60
Basin Length (m)	13172.64	19322.91	14029.92	17219.16	15894.84	53414.39	14578.89	25041.99
Bog (%)	0.75	0.70	0.70	0.63	0.68	0.60	0.50	0.54
Fen (%)	0.20	0.25	0.24	0.30	0.26	0.35	0.46	0.39
Water (%)	0.05	0.05	0.06	0.07	0.06	0.05	0.04	0.07

4.4.2 Land Cover Classification

The second procedure following the methods outlined in section 3.4.2 was the land cover classification. The classification scheme was partitioned between fen, bog, and open water. The validation of the classification procedure is provided in Table 4.4-2, and the classifications are illustrated in Figure 4.4-1 to 4.4-4.

Table 4.4-2. Accuracy assessment of classification procedure.

	Fen User Accuracy	Bog User Accuracy	Fen Producer Accuracy	Bog Producer Accuracy	Overall Accuracy
NNGC, SNGC, SG.001, NG.001	0.99	0.98	0.99	0.96	0.98
Trib 3	0.72	0.96	0.81	0.93	0.91
Trib 5, Trib 5A	0.96	0.81	0.87	0.92	0.91
Trib 7	0.94	0.97	0.93	0.97	0.96

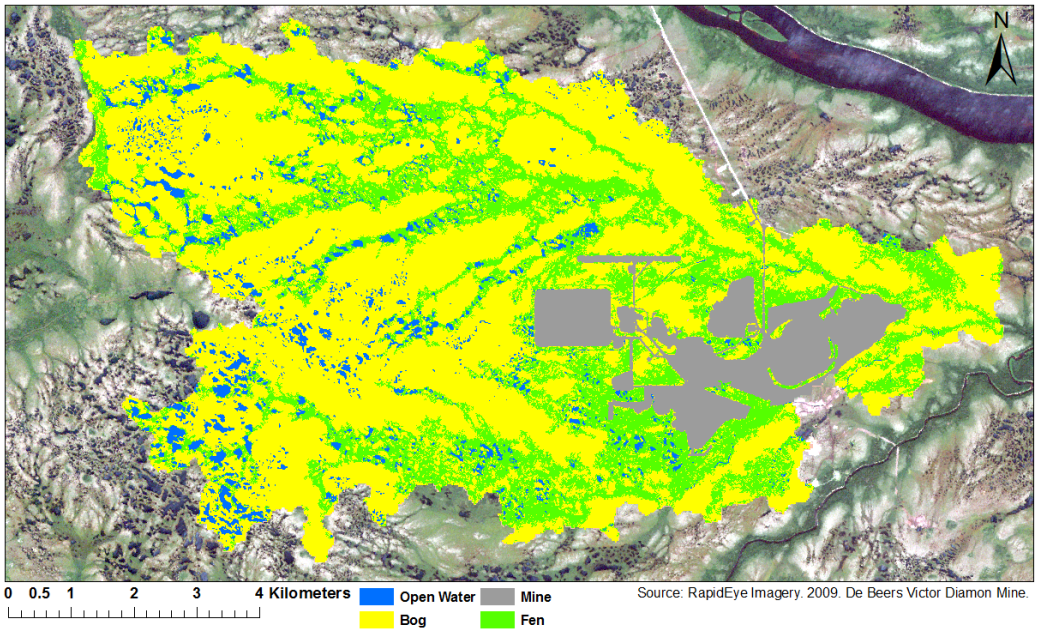

Figure 4.4-1. Classification of NNGC, SNGC, NG.001, and SG.001. Yellow represents bog, green represents fen, grey represents mine, and blue represents open water.

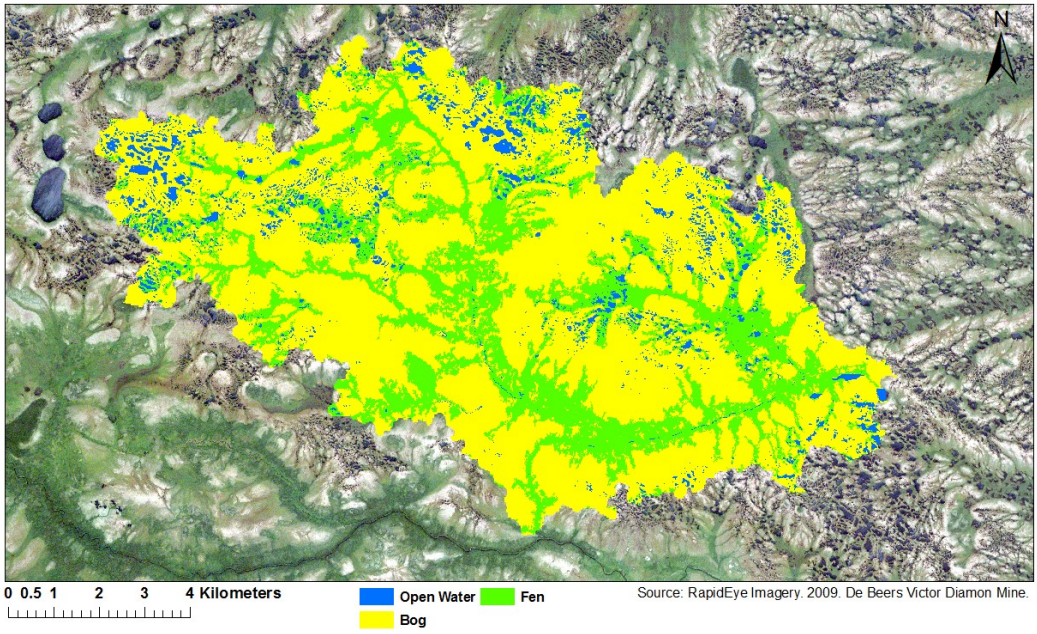

Figure 4.4-2. Classification of Trib 3. Yellow represents bog, green represents fen, and blue represents open water.

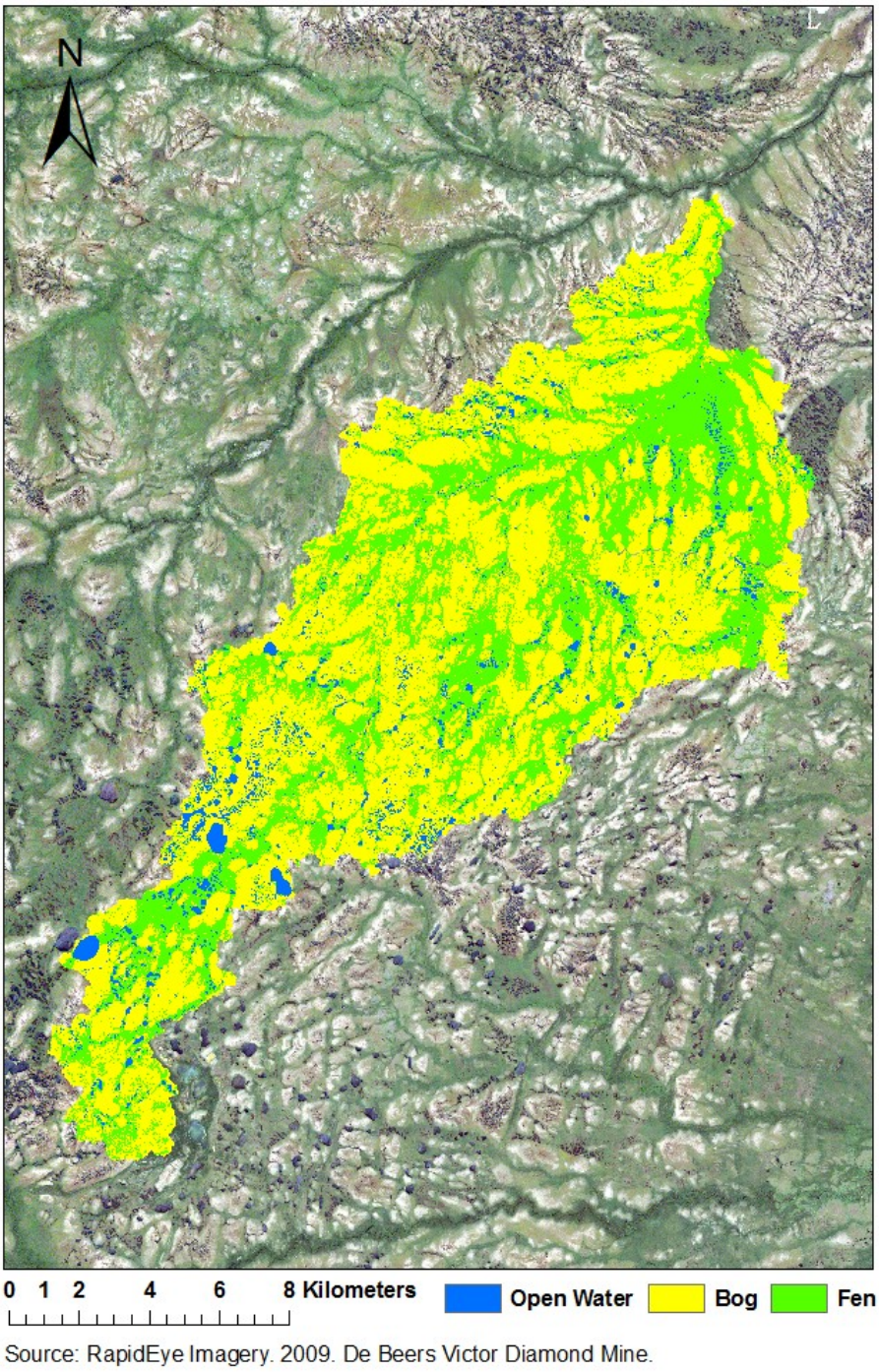

Figure 4.4-3. Classification of Trib 5 and Trib 5A. Yellow represents bog, green represents fen, and blue represents open water.

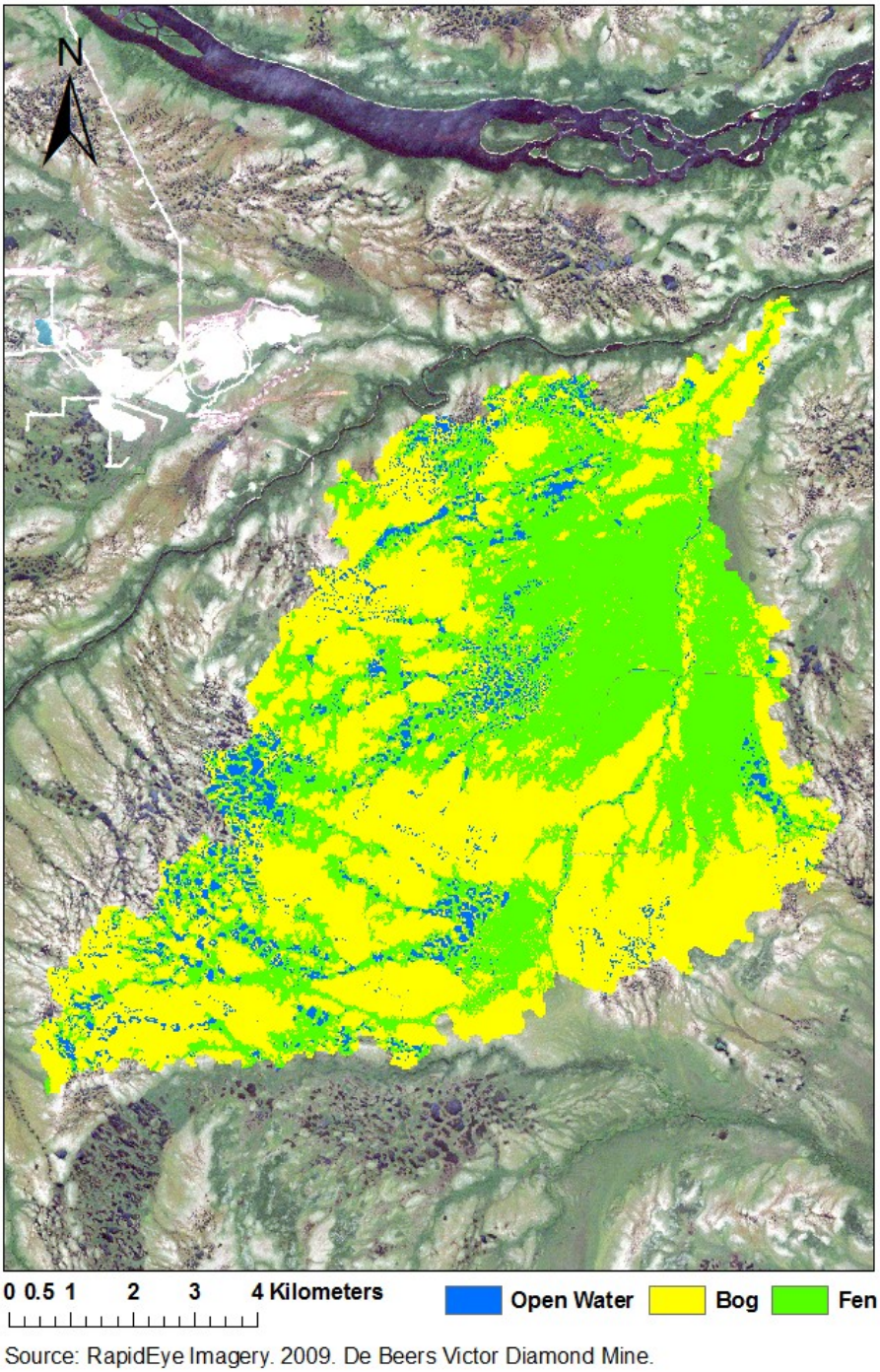

Figure 4.4-4. Classification of Trib 7. Yellow represents bog, green represents fen, and blue represents open water.

4.4.3 Model Regionalization

The third procedure was the regionalization of model parameters. Nine methods were applied from the methods outlined in section 3.4.3 and 3.4.4. The first item to report is the empirically determined relationships between model parameters and physical catchment attributes (Table 4.4-3).

Table 4.4-3. Relationships empirically determined between model parameters and physical catchment attributes.

Catchment Descriptors	Parameter	r
CV Gradient	**CWH**	0.73
Drainage Density	**BETA**	0.90
Gravelius Circularity Ratio	**Alpha**	0.90
Gravelius Circularity Ratio	**K0**	-0.73
Gravelius Shape Index	**LP**	-0.80
Gravelius Shape Index	**MAXBAS**	-0.71
Max Gradient	**CFR**	-0.75
Max Slope	**TT**	-0.90
Min Elev	**K1**	0.88
Min Elev	PERC*	0.57
Min L/G	FC*	0.61
Min L/G	**SFCF**	-0.95
Median	CFMAX	

Asterisk denotes significant at 0.1 level
Bold denoted significant at 0.05 level
Underline denotes ANN only

In the snow routine, parameters TT, CWH, SFCF, and CFR were estimated using catchment descriptors derived from slope or metrics computed with slope, except for CFMAX that applied the median value. In the soil moisture routine, FC was estimated using the minimum value of flow path length over flow path gradient. The LP parameter was estimated using the Gravelius shape index, and BETA was estimated using drainage density. In the response routine, PERC and K1 were estimated using a catchments lowest elevation point. Alpha and K0 were estimated using the Gravelius circularity ratio. Finally in the routing routine, MAXBAS was estimated using the Gravelius shape index. The second item to report is the performance of each regionalization method listed in Table 4.4-4.

Table 4.4-4. Performance of regionalization methods. The Monte Carlo best parameter set is the optimal model outputs and provides a benchmark to evaluate the performance of the regionalization methods. The difference NS and LNS are the difference in performance between the benchmark and the regionalization method.

	NNGC	NG.001	SNGC	SG.001	Trib3	Trib5	Trib5A	Trib7	Average
Monte Carlo Best Parameter Set									
NS	0.42	0.61	0.72	0.65	0.47	0.60	0.59	0.49	0.57
Log NS	0.52	0.76	0.73	0.67	0.64	0.70	0.63	0.63	0.66
Median (A1)									
NS	0.00	0.60	0.59	0.07	0.41	0.60	0.59	0.50	0.42
Log NS (LNS)	0.50	0.73	0.47	0.61	0.57	0.69	0.54	0.53	0.58
Difference NS	-0.42	-0.01	-0.13	-0.58	-0.06	0.00	0.00	0.01	-0.15
Difference LNS	-0.02	-0.03	-0.26	-0.06	-0.07	-0.01	-0.09	-0.10	-0.08
Mean (A2)									
NS	0.00	0.54	0.50	0.00	0.43	0.57	0.58	0.51	0.39
Log NS (LNS)	0.48	0.70	0.49	0.59	0.55	0.66	0.50	0.51	0.56
Difference NS	-0.42	-0.07	-0.22	-0.65	-0.04	-0.03	-0.01	0.02	-0.18
Difference LNS	-0.04	-0.06	-0.24	-0.08	-0.09	-0.04	-0.13	-0.12	-0.10
Weighted Mean Bog (A3)									
NS	0.00	0.54	0.50	0.01	0.43	0.57	0.57	0.51	0.39
Log NS (LNS)	0.47	0.70	0.51	0.59	0.57	0.65	0.50	0.51	0.56
Difference NS	-0.42	-0.07	-0.22	-0.64	-0.04	-0.03	-0.02	0.02	-0.18
Difference LNS	-0.05	-0.06	-0.22	-0.08	-0.07	-0.05	-0.13	-0.12	-0.10
Weighted Mean Fen (A4)									
NS	0.00	0.53	0.48	0.00	0.44	0.57	0.58	0.51	0.39
Log NS (LNS)	0.48	0.70	0.46	0.59	0.52	0.67	0.51	0.51	0.56
Difference NS	-0.42	-0.08	-0.24	-0.65	-0.03	-0.03	-0.01	0.02	-0.18
Difference LNS	-0.04	-0.06	-0.27	-0.08	-0.12	-0.03	-0.12	-0.12	-0.11
Spatial Proximity (A5)									
NS	0.00	0.62	0.46	0.00	0.15	0.62	0.59	0.34	0.35
Log NS (LNS)	0.25	0.58	0.43	0.61	0.36	0.60	0.63	0.54	0.50
Difference NS	-0.42	0.01	-0.26	-0.65	-0.32	0.02	0.00	-0.15	-0.22
Difference LNS	-0.27	-0.18	-0.30	-0.06	-0.28	-0.10	0.00	-0.09	-0.16
Physical Similarity (A6)									
NS	0.00	0.43	0.60	0.00	0.48	0.62	0.53	0.50	0.40
Log NS (LNS)	0.25	0.65	0.05	0.61	0.50	0.60	0.60	0.47	0.47
Difference NS	-0.42	-0.18	-0.12	-0.65	0.01	0.02	-0.06	0.01	-0.17
Difference LNS	-0.27	-0.11	-0.68	-0.06	-0.14	-0.10	-0.03	-0.16	-0.19
Spatial Proximity + Physical Similarity (A7)									
NS	0.00	0.43	0.60	0.00	0.46	0.39	0.38	0.34	0.33
Log NS (LNS)	0.25	0.65	0.05	0.61	0.16	0.60	0.46	0.54	0.42
Difference NS	-0.42	-0.18	-0.12	-0.65	-0.01	-0.21	-0.21	-0.15	-0.24
Difference LNS	-0.27	-0.11	-0.68	-0.06	-0.48	-0.10	-0.17	-0.09	-0.25
Regression (A8)									
NS	0.00	0.61	0.59	0.42	0.45	0.57	0.53	0.52	0.46
Log NS (LNS)	0.41	0.74	0.58	0.61	0.56	0.62	0.56	0.59	0.58
Difference NS	-0.42	0.00	-0.13	-0.23	-0.02	-0.03	-0.06	0.03	-0.11
Difference LNS	-0.11	-0.02	-0.15	-0.06	-0.08	-0.08	-0.07	-0.04	-0.08
ANN (A9)									
NS	0.00	0.53	0.59	0.55	0.45	0.57	0.61	0.50	0.48
Log NS (LNS)	0.46	0.66	0.61	0.64	0.56	0.60	0.49	0.61	0.58
Difference NS	-0.42	-0.08	-0.13	-0.10	-0.02	-0.03	0.02	0.01	-0.09
Difference LNS	-0.06	-0.10	-0.12	-0.03	-0.08	-0.10	-0.14	-0.02	-0.08

The first approach applied regional descriptive statistics to construct model parameters. The first method A1 established model parameters using the median values of all gauged catchments. The results ranged between 0.07 and 0.60 for NS, 0.47 and 0.73 for LNS. On average model performance was lower than the benchmark by -0.11 for NS and -0.09 for LNS. The second method A2 estimated model parameters using the arithmetic mean values of all gauged catchments. The results ranged from 0.00 to 0.58 for NS and 0.49 to 0.70 for LNS. On average model performance was lower than the benchmark by -0.14 for NS and -0.11 for LNS. The third and fourth methods determined model parameter using the weighted arithmetic mean based on bogs (A3) or fens (A4). For A3 the results ranged between 0.01 and 0.57 for NS and 0.50 to 0.70 for LNS. On average model performance was lower than the benchmark by -0.14 for NS and -0.10 for LNS. For A4 the results ranged between 0.00 and 0.58 for NS and 0.46 to 0.70 for LNS. On average model performance was lower than the benchmark by -0.15 for NS and -0.11 for LNS.

The second approach of regionalization methods directly transferred model parameters based on either spatial proximity and/or physical similarity. The fifth method A5 transferred model parameters to recipient catchments from their closest donor catchment in regards to spatial proximity. The results ranged between 0.00 and 0.62 for NS and 0.36 to 0.63 for LNS. On average model performance was lower than the benchmark by -0.19 for NS and -0.14 for LNS. The sixth method A6 transferred model parameters from the catchment determined to be the most physically similar. The results ranged between 0.00 and 0.62 for NS and 0.05 to 0.65 for LNS. On average model performance was lower than the benchmark by -0.14 for NS and -0.18 for LNS. The seventh method A7 transferred model parameters using both physical similarity and spatial proximity. The results ranged between 0.00 and 0.60 for NS and 0.05 to 0.65 for LNS. On average model performance was lower than the benchmark by -0.22 for NS and -0.24 for LNS.

The third approach of regionalization methods estimated model parameters using trained statistical models. The eighth method A8 estimated model parameters using regression analysis. The results ranged between 0.42 and 0.61 for NS and 0.56 to 0.74 for LNS. On average model performance was lower than the benchmark by -0.06 for NS

and -0.07 for LNS. The ninth method A9 estimated model parameters using an artificial neural network. The results range between 0.45 and 0.61 for NS and 0.49 to 0.66 for LNS. On average model performance was lower than the benchmark by -0.05 for NS and -0.08 for LNS.

Chapter 5: Discussion

5.1 Predictive Capabilities of TOPMODEL and HBV

A clear distinction was observed between the predictive capabilities of both models. On average during the calibration period, HBV had a NS or LNS value 10% - 20% higher than TOPMODEL with an average NS of 0.58, LNS of 0.71, and a fuzzy measure value of 0.51. TOPMODEL had an average NS of 0.45, LNS of 0.44, and a fuzzy measure of 0.13. On average during the validation period, HBV had an NS of 0.49, and LNS of 0.43. TOPMODEL had an NS of 0.11 and LNS of 0.44. Thus, there was a significant drop in the performance of TOPMODEL outside of the calibration period.

For the prediction limits, HBV on average was able to capture 51% of the observed streamflow during calibration and 43% during validation. TOPMODEL only had four out of the eight catchments with a fuzzy measure greater than zero. As a result, only four catchments had prediction limits. TOPMODEL on average only captured 11% of the observed streamflow during calibration and 14% during validation. The contrast in the results clearly indicates two things: (1) HBV outperforms TOPMODEL in this James Bay Lowland peatland complex: and (2) TOPMODEL was altogether unsuitable for runoff simulation in this landscape.

The simulation results suggest that TOPMODEL's inability to simulate streamflow in this environment likely has to do with the fact that it cannot simulate both high and low flow conditions with a single parameter set. This parametric failure to capture both flow conditions was observed in dotty plots and the hydrograph. The dotty plots generated during uncertainty analysis revealed a conflict between the NS and LNS objective function and the distribution of TOPMODEL's M parameter (Figure 5.1-1). The conflict is the differences in where the optimal parameter values peak in the distributions of the M parameter.

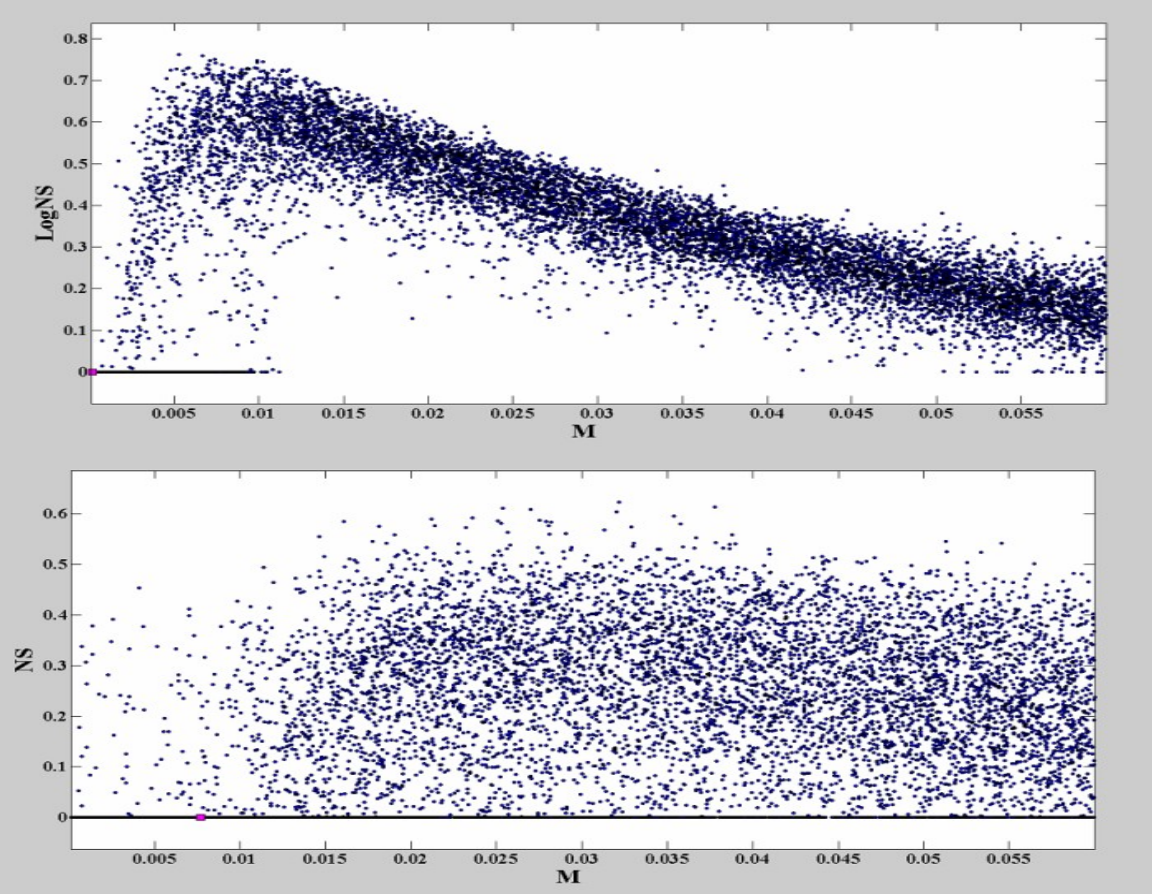

Figure 5.1-1. Dotty plot of M parameter and LNS (top), M parameter and NS (bottom). The LNS objective function peaks with M values between 0.005 and 0.015, and the NS objective function is uniformly distributed with M values between 0.015 and >0.055. The optimal M values of each objective function do not overlap.

TOPMODEL's M parameter is the most important model parameter. A small M parameter value decreases the contribution of subsurface flow and the time required to reach the outlet, and a large M parameter value increases the contribution of subsurface flow and the time required to reach the outlet (Nourani et al., 2011). In addition, the performance of NS is sensitive to peaks in the hydrograph, and LNS is sensitive to low flows (Krause et al., 2005). Considering the importance of the M parameter and both objective functions this suggests that TOPMODEL cannot be calibrated to represent high and low flow conditions.

The issue of calibrating TOPMODEL to simulate both high and low flow conditions results from the uniform subsurface flow assumption. This assumption has

been identified as an issue in previous studies (Seibert et al., 1997; Guntner et al., 1999; Beven & Freer, 2001). This assumption is represented in TOPMODEL by the M parameter. Issues with this assumption can be observed in the hydrographs.

In the hydrographs TOPMODEL severely overestimates peak flows and fails to represent low flows. In Figure 4.3-1, peak flow events were extremely overestimated for NNGC, and the remainders of the catchments overestimate peak flow events by ~4 mm. Difficulties in representing different flow conditions have often required modifications of TOPMODEL's structure (Scanlon et al., 2000; Beven & Freer, 2001; Walter et al., 2002). This issue is not unique to James Bay Lowland peatlands. However, any attempt to increase the predictive capability of TOPMODEL in James Bay Lowland peatlands would require modifying the model's structure to allow non-uniform subsurface flow and revisit the assumption of uniform subsurface flow.

The predictive capabilities of HBV were considerably better than TOPMODEL. However, HBV did not demonstrate perfect performance and simulation efficiencies varied across catchments. Unlike TOPMODEL, HBV could adequately represent both high and low flow conditions. The main issue with HBV was its inability to fully represent the storage-discharge relationship. This issue was observed in the simulated hydrographs in three manners: (1) in a series of peak flow events the initial peak flow event was overestimated and the subsequent peak flow events were underestimated: (2) in a series of peak flow events the model output was generalized between peak and baseflow: and (3) the relationship between high-frequency low-magnitude rainfall events and runoff was problematic.

The discrepancies in the formulation of the storage-discharge relationship may be the result of differences between bog and fen land cover types. In Quinton et al. (2003), they demonstrated that bogs are not consistently connected to the drainage network suggesting *fill-and-spill*. The fill-and-spill concept is that spatially variable storage throughout the landscape must attain a storage threshold before generating surface or subsurface flow and connecting to the drainage network (Spence & Woo, 2003). The fill-and-spill concept can explain issues (1) and (3) listed above. For example: the overestimated portion of the peak flow (issue 1) could have resulted if storage deficits in bogs were not exceeded, effectively disconnecting these parts of the landscape from the

drainage network. This highlights a potential issue of the applicability of the HBV model structure in this environment.

The structure of the HBV model is conceptually well-aligned with the contrasting hydrologic roles of bogs versus fens in this landscape. In the response function (section 3.2.2, Figure 3.2-3) there are two reservoirs. The first reservoir receives water from the soil moisture routine and either transfers water through percolation to the second reservoir or directly generates runoff. Therefore, the first reservoir may capture the hydrologic function of bogs. The water that is discharged from the reservoir is represented by equation [21] in section 3.2.2 that possesses a non-linear coefficient, the alpha parameter. This non-linear equation is similar to the fill-and-spill (Spence & Woo, 2003) concept that may characterize the transient hydrological connectivity of bogs (Quinton et al., 2003).

The second reservoir receives water from the first reservoir and directly generates runoff. The water received from the upper reservoir generalizes the groundwater recharge from bogs that is discharged in fens. The water that is directly discharged is represented by a linear runoff function, equation [21] in section 3.2.2 that maintains constant connectivity to the drainage network. The second reservoir may capture the hydrologic function of fens (Quinton et al., 2003). The relation of the hydrological characteristics of bogs and fens to components of the HBV model suggests that the model structure may not entirely be the source of error in the runoff simulation results. Potential sources of error are later discussed in section 5.4.

Hydrograph issues as described above are not uncommon. Previous applications with other models have reported similar issues (Kouwan et al., 1993; Pietroniro et al., 1996; Quinton et al., 2003; Jing & Chen, 2011; Chen et al., 2012). Chen et al. (2012), compared the WATFLOOD and semi-distributed land use-based runoff processes (SLURP) models in a northern peatland complex located in the Hudson Bay Lowland. In comparison to the HBV LNS results in this study, WATFLOOD had a lower performance with an average LNS of 0.38 that ranged annually between 0.07 to 0.66 over twenty years, and SLURP had similar performance with an average LNS 0.49 that ranged annually between 0.13 to 0.72 over twenty years. A detailed comparison of all four models is provided in Table 5.1-1. However, both models required the calibration of over

20 parameters. Bloschl and Sivapalan (1995) stated that the greater the number of parameters the more difficult model calibration and validation becomes. This highlights the applicability of HBV that provided similar results with only half the number of model parameters to calibrate. However, Chen et al.'s (2012) study site has continuous permafrost that may result in lower model performance.

Table 5.1-1. Comparison of model performance between WATFLOOD (Chen et al., 2012), SLURP (Chen et al., 2012), TOPMODEL (this study), and HBV-Light (this study).

Model	Location	Source	# catchments	# years	Lowest LNS	Highest LNS	Average LNS
WATFLOOD	Deer River Watershed. ~150km from Churchill, Manitoba.	Chen et al. (2012)	1				
			Model Calibration	10	0.08	0.66	0.33
			Model Validation	10	0.07	0.68	0.42
SLURP	Deer River Watershed. ~150km from Churchill, Manitoba.	Chen et al. (2012)	1				
			Model Calibration	10	0.38	0.71	0.54
			Model Validation	10	0.13	0.72	0.43
TOPMODEL	Victor De Beers, ~90km from Attawapiskat, Ontario.	This study	8				
			Model Calibration	3	0.00	0.73	0.44
			Model Validation	1 to 2	0.00	0.65	0.44
HBV-Light	Victor De Beers, ~90km from Attawapiskat, Ontario.	This study	8				
			Model Calibration	3	0.50	0.82	0.71
			Model Validation	1 to 2	0.18	0.72	0.43

In summary, TOPMODEL could not adequately represent high and low flow conditions, whereas HBV could adequately simulate a range of flow conditions. The applicability of HBV in this environment has many potential benefits.

5.2 Land Cover Classification

The classification scheme was divided between three coarse classes that represented land cover with unique hydrological function. The validation of the classification yielded very high accuracy results. The overall classification accuracy for

all catchments is greater than 90% with a mean of 94%. The producer's accuracy for fens is between 80% and 99% with a mean of 90%, and bogs are between 92% and 97% with a mean of 94.5%. This indicates the likelihood of land cover being correctly classified based on the ratio of classified and validation samples. The user's accuracy for fens is between 72% and 99% with a mean of 90.5%, and bogs are between 81% and 98% with a mean of 93%. This is the likelihood that a pixel is correctly classified based on the ratio of correct pixels and the sum of classified pixels.

The three validation metrics all provided high results that overestimate the performance of the classification procedure. This results from the selection procedure to establish the validation set. Validation objects (grouping of pixels) are manually selected from the imagery rather than being selected from field data. The quality of the validation set is therefore dependent on the user's knowledge and interpretation of the landscape from the imagery.

The quality of the validation set is considered acceptable based on the fact that bogs and fens can be readily distinguished within the imagery, thus facilitating the training set development. Fens appear darker in the imagery and are adjacent to the stream network. Bogs appear brighter in the imagery and are topologically disconnected from the stream network. However, the quality is diminished somewhat around transitional zones which are more difficult to interpret. Fortunately, transitional zones only account for small fraction of the landscape.

The OBIA approach with the neural network classifier approach provided a classification procedure that was easily reproducible and time efficient. However, neural networks are a black-box approach more suited for operational applications rather than research. Nevertheless, the purpose of the classification in this study was to partition the landscape to provide data for regionalization analysis. The approach satisfied this requirement.

5.3 Model Regionalization and Maximizing Predictive Value

The application of regionalization included nine methods in three approaches that directly transferred or estimated HBV model parameters. Each catchment was successively treated as an ungauged catchment, while the remaining catchments provided

model parameters and landscape information for regionalization. The initial Monte Carlo results ranged from 0.42 to 0.72 for NS and 0.52 to 0.76 for LNS. These results represent the optimal parameter set for each catchment. In addition, these results provide a benchmark to evaluate the performance of the regionalization methods by computing the difference. The regionalization methods were divided into three approaches. The first approach was regionalization methods that involved deriving regional parameter sets from descriptive statistics. The second approach was regionalization methods that directly transferred model parameters based on spatial proximity or physical similarity. The third approach was regionalization methods that estimated model parameters using trained statistical models. The following discusses each approach individually. Furthermore, the NNGC catchment was excluded due to poor results. The poor results are possibly due to the cone of depression or the area of the catchment being overestimated. The simulated results of NNGC are not comparable to the simulated results of the other catchments.

The first approach applied regional descriptive statistics to construct model parameters. The first comparison in section 4.4.3 was the performance of A1 and A2 or median versus mean values. A1 had a higher average NS value (0.48) than A2 (0.45), and a higher average LNS value (0.59) than A2 (0.57). The median derived parameter sets provided slightly higher results and was closer to the benchmark. The second comparison in section 4.4.3 was the performance of A3 and A4 or weighted mean of bogs versus fens. The average NS and LNS values of A3 were marginally higher than A4.

The basis for methods A3 and A4 was to relate model parameters to the percentage of fen and bog land cover. These methods were implemented because of the observed unique hydrologic function of fens and bogs (Quinton et al., 2003). The applicability of both A3 and A4 is determined on whether a relationship is observed between model performance and the portion of land cover at each catchment, meaning that a catchment with a greater portion of fen should demonstrate greater model performance with weighted mean fen (A4) than weighted mean bog (A3).

A comparison of the percentage of land cover in each catchment (Table 4.4-1) and the performance results of A3 and A4 (Table 4.4-4) did not support the use of the weighted mean method to derive parameter sets based on bog or fen. In order to justify

this approach a clear distinction must be observed between model performance and land cover.

Overall, the four regionalization methods used in the first approach provided satisfactory results near the benchmark. Method A1 had the best results using parameter sets established from median values. These results are important as they demonstrate the applicability of HBV in conjunction with simple statistical regionalization methods to efficiently calibrate an ungauged site without requiring topographical or other supporting data.

The second approach of regionalization methods directly transferred model parameters based on either spatial proximity and/or physical similarity. Comparing the three methods indicates a tie between spatial proximity (A5) and physical similarity (A6) due to only slight variations in results. In previous studies, spatial proximity appears to have been favoured (Merz & Bloschl, 2004; Parajka et al., 2005; Oudin et al., 2008) more often than physical similarity (Reichl et al., 2009). However, Reichl et al. (2009) demonstrated that adequately determining and weighing physical catchment attributes for regionalization had a significant impact on the results. The application of spatial proximity is supported by the notion that catchments that are in spatial proximity of each other are likely to share similar hydrological characteristics. The notion is the same for physical similarity, but based on physical catchment characteristics. Considering the basis of both methods, it is important to consider scale. The results from studies at a local scale may considerably differ than the results of studies at regional scales. In Oudin et al. (2008), they regionalized 913 catchments across France and observed an inconsistent spatial pattern in the performance of spatial proximity and physical similarity between catchments. This suggests that the application of either method is not ubiquitous, and the scale of the study site may influence the comparison of both methods.

Combining proximity + physical similarity (A7) was found to be an ineffective regionalization method in this landscape. In Zhang & Chiew (2009) the combination of both methods provided better results than spatial proximity alone. However, in this application the combined method had a much lower performance than the benchmark. The three regionalization methods in the second approach varied in performance. Both A5 and A6 demonstrated similar performance, and A7 had a notably poor performance.

The third approach of regionalization methods estimated model parameters using trained statistical models. A comparison of both A8 and A9 demonstrated a tie in performance. The majority of the catchments demonstrated equal performance for both methods, but a few catchments performed better with one method over the other. A previous comparison performed by Heuvelmans et al. (2006) demonstrated similar findings and that performance varied per catchment. The application of regression and artificial neural networks methods are both popular. They can be used to improve knowledge of the first-order controls on runoff generation by interpreting the relationships between physical landscape descriptors and parameter values.

The physical catchment descriptors selected to estimate model parameters are listed in Table 4.4-3. For each pair the *r* results varied from medium to high. Strong relationships were established between model parameters and physical catchment attributes. For example, drainage density was applied to estimate the BETA model parameter. The BETA model parameter determines the relative contribution of runoff. However, some of the relationships had questionable physical basis. An example of a questionable relationship is the minimum elevation value of a catchment and K1, the model parameter that is a storage/recession coefficient shaping the hydrograph. Another important observation is the relationship established for FC and PERC. FC and PERC are the most important model parameters, and yet they have the statistically least significant relationships.

The questionable relationships and the poor statistical significance of the two main parameters call into question the choice of catchment descriptors and the model parameterization approach. The FC parameter represents field capacity or the maximum soil moisture storage. The PERC parameter represents the maximum percolation rate between groundwater reservoirs. Both parameters generalize hydrological processes that may not be well represented by catchment descriptors that emphasize surface characteristics (Table 4.4-3). The model parameterization approach calibrates a model that is representative of the entire catchment. The catchments are divided between two hydrologically distinct land cover, bog and fen. A generalized parameterization of both bog and fen land cover may not be adequate.

The parameters in the snow routine were mostly estimated using average catchment slope or flow path gradient. There is a reasonable physical basis between the topographical metrics and the snow routine (Jost et al., 2007). However, it is uncertain whether the resolution of the DEM was sufficient to realistically capture those relationships.

The remaining parameters were often estimated based on the shape of the catchment. A catchments' shape is influential on the time of concentration and the shape of the hydrograph. The application of catchment shape to estimate model parameters is only reasonable for parameters in the response and routing routines that govern runoff in the model. The LP parameter in the soil response routine that controls evapotranspiration is unlikely to have physical basis to support its estimation based on the shape of a catchment. This baseless relationship may result from the lack of catchment descriptors that influence evapotranspiration, e.g. vegetation, soil properties.

Despite certain relationships being questionable, both methods provided good model performance, and performed only slightly below benchmark. There were twelve relationships established to estimate model parameters and at least eight were considered physically plausible.

Overall, the three regionalization approaches demonstrated some modest ability to calibrate the HBV model for ungauged catchments within this study region. However, the third approach using statistical models had the best model performance followed by the first approach, then the second approach. In previous studies, spatial proximity has often been the best method; outperforming physical similarity and regression models (Merz & Bloschl, 2004; McIntyre et al., 2005; Parajka et al., 2005; Oudin et al., 2008; Bao et al., 2012). There have been fewer studies that report regression-based regionalization outperforming spatial proximity or physical similarity (Kokkonen et al., 2003; Young 2006). This contrast in the optimal regionalization method warrants further examination of the differences and similarities between this study and the former studies listed. The following discussion focuses on three factors that might have contributed to these findings, justifying the use of empirical regionalization methods at this site.

The first factor to consider is the effect of scale and spatial heterogeneity on regionalization results. Many comparative regionalization studies were performed at a

large spatial scale across European countries: France (Oudin et al., 2008), Austria (Merz and Bloschl, 2004; Parajka et al., 2005), and the United Kingdom (McIntyre et al., 2005; Kay et al., 2006). It is important to consider the difference in heterogeneity at a range of spatial scales. For example, the application of the spatial proximity method (A5) at a large/regional scale in the comparative studies listed above likely demonstrated good performance because it involved comparing catchments on the basis of similar hydro-climatic properties like mean annual rainfall, PET, and streamflow, or geology, elevation, and other properties. These properties are likely to vary with distance when considered over such a broad scale (e.g. 100 - 500 km). The catchment closest to the ungauged catchment is likely to resemble the ungauged catchment more than the furthest catchment. However, at a more local scale (e.g. 1 - 100 km), as in the present study, all of the study catchments are likely to share the properties listed above. This reduces the applicability of the spatial proximity method (A5) for determining a suitable donor catchment.

The second factor to consider is the information available across the range of scales for regionalization. Studies at larger scales are unlikely to provide the same amount of information than those at smaller scales. The available information for regression-based regionalization has a significant impact on the outcome of the regionalization procedure. Furthermore, Goswami et al. (2007) demonstrated that ensuring regional homogeneity of physiographic and hydrologic conditions is important for regionalization, and including dissimilar catchments reduces the performance of the regionalization procedure. In Oudin et al. (2008) any catchment across France with a model performance above 0.70 NS was integrated into the regression model and very few topographic attributes were used in the analysis. In this study, regression-based regionalization was performed at a local scale within a homogeneous region with a greater number of topographic attributes. This provided the ideal conditions for performing regression-based regionalization. Considering the contrast between both studies and the observations by Goswami et al. (2007), Oudin et al's. (2008) approach to regression-based regionalization is not ideal.

The third factor to consider is the unique characteristics of each environment in regionalization studies. Goswami & O'Connor (2006) observed that the performance of

regionalization procedures is site-specific. As previously mentioned, James Bay Lowland peatlands have unique features such as a low-gradient and highly patterned nature of fen and bog complex. The results of the regionalization analysis presented are likely to have been influenced by three important factors: (1) differences in heterogeneity and the value of catchment descriptors vary at a range of scales, (2) the scale or magnitude of the study itself is an element that influences the acquisition of suitable catchment descriptors, and (3) different regionalization studies may yield different optimal regionalization method due to fundamental differences in landscape characteristics (e.g. the Victor Mine study site has an average gradient of 0.1%, compared to the mountainous Karkheh basin (Masih, et al., 2010)). These factors help to explain why the empirical regionalization methods were most successful, in contrast to other studies regarding the value of empirical regionalization methods.

In summary, nine regionalization methods from three different regionalization approaches were applied in a James Bay Lowland peatland complex. The first regionalization approach involved applying regional descriptive statistics to construct model parameter sets. The median and mean methods provided adequate results. However, the weighted mean method did not perform similarly to the previous two, nor did it support the application of bog and fen land cover percentage to construct parameter sets. The second regionalization approach involved the direct transfer of model parameters using several different strategies. Spatial proximity and physical similarity were the least favourable despite their successful applications in other studies. Finally, the third regionalization approach involved estimating model parameters using regression-based and artificial neural network statistical models. The two regionalization strategies used in this approach performed equally well, and were the best regionalization methods at this site. However, these results conflict with those from much larger regionalization studies, likely due to scale issues and lack of significant landscape or climate variability within the study site at Victor Mine. Nevertheless, the empirical regionalization methods demonstrated a significantly better performance for the lowland catchments in this study. As a result, both the HBV-Light model and the empirical regionalization methods are valuable tools to maximize the predictive value of

information acquired from landscape analysis for the purposes of rainfall-runoff modelling in this landscape.

Finally, there is a need to identify catchment descriptors for the FC and PERC model parameters for the HBV-Light. Progress in this area may provide insight into first-order controls on runoff generation in James Bay lowland catchments to better understand this environment.

5.4 Uncertainty in the Study

In any hydrological modelling effort there is always the issue of uncertainty throughout the entire workflow from the input data to validation of the model's performance. The initial uncertainty that is introduced and propagates throughout the modelling effort is input uncertainty. As previously defined, input uncertainty is the uncertainty in the model parameters that results from input data error (McMillan et al., 2010; Renard et al., 2010). In rainfall-runoff modelling the two variables of concern for uncertainty are streamflow and precipitation.

In this study, there is a degree of uncertainty in the streamflow data that warrants further discussion. The streamflow series were generated using a rating curve model calibrated from stage-discharge measurements. As Sikorska et al. (2013) indicated streamflow series generated from rating curve models naturally introduces uncertainty that influences the calibration process. In addition, gaps in the streamflow data were estimated using a multiple imputation technique that also introduces uncertainty. It is important to consider the potential impact of that uncertainty. However, in this study that uncertainty was not quantified making it difficult to understand how results would be affected. Similarly the precipitation dataset also has inherent uncertainties as a result of error in the measurement techniques, but is difficult to quantify for the purposes of this modeling exercise (Lanza & Stagi, 2008). Future work might benefit from sensitivity analysis to assess how plausible ranges in input errors might affect simulation and regionalization results.

It is sensible to suggest that input uncertainty from streamflow and precipitation datasets were a significant source of error and uncertainty in the simulated results. As discussed in section 5.1, components of the HBV model can be interpreted to capture bog

and fen in the studied catchments. This interpretation promotes its application in this environment. Also, the differences observed between the simulated and observed runoff in the hydrographs call into question the validity of some of the observation data, notably for the 2010 period. The observed and the simulated runoff differ significantly during this period, particularly for catchments SNGC (Figure 4.3-6) and Trib 5A (Figure 4.3-14). Differences between 2010 and other periods highlight potential issues with the 2010 observational streamflow and precipitation data.

Input uncertainty in both streamflow and precipitation propagated uncertainty throughout the remainder of the study. The input uncertainty impacts the model calibration process by making it difficult to capture the rainfall-runoff relationship. This inadequate representation of the rainfall-runoff relationship results in issues of *parameter identifiability*. Parameter identifiability is the capability to identify a unique set of parameters during the calibration process if the model structure is an adequate representation of the environment (Seibert, 1999; Wagener & Wheater, 2006). Difficulties in parameter identifiability lead to uncertainty in the regionalization results (Wagener & Wheater, 2006). As discussed in section 5.3, there was difficulty in establishing statistically significant relationships for the two main parameters, FC and PERC. Parameter identifiability may have been part of the issue.

The regionalization results are also subject to uncertainty due to other factors such as the spatial resolution of the DEM and the limited number of catchments. The spatial resolution of the DEM is a source of uncertainty in regionalization efforts (Muller et al., 2009). This has an impact on the delineation of the boundaries and the catchment descriptors generated from topography. The small number of catchments is also a source of uncertainty that requires a careful interpretation of the results (Wagener & Wheater, 2006). A more robust regionalization procedure would have assessed the performance of the regionalization methods on catchments located elsewhere in the James Bay Lowland. Additionally, a greater sample size for the empirical models in the third approach would have provided greater reliability in the results.

There are many sources of uncertainty throughout the study. However, the most important source of uncertainty to address is the streamflow and precipitation input uncertainty. The HBV model provided adequate results, but there are indications that its

performance could have been better. The quantification of the streamflow and precipitation input uncertainty is necessary to broaden the applicability of HBV and provide a better assessment in this environment.

Chapter 6: Conclusion

The aim of this study was to explore tools readily available to simulate rainfall-runoff by evaluating TOPMODEL and HBV and reduce dependency on costly and remote monitoring programs in a James Bay Lowland peatland complex by assessing regionalization methods.

The first objective involved a critical appraisal of the conceptual rainfall-runoff models, TOPMODEL and HBV for application in a James Bay Lowland peatland complex. HBV outperformed TOPMODEL with NS and LNS results ten to twenty percent higher than TOPMODEL's. TOPMODEL failed to capture a significant portion of the rainfall-runoff behaviour and was parametrically incapable of simulating both high and low flow conditions with one set of parameters. Unlike TOPMODEL, HBV was able to capture a significant portion of the rainfall-runoff behaviour. In addition, HBV's performance was similar to other models that require a greater number of parameters. Fewer model parameters facilitate model calibration and validation. Overall, the HBV model demonstrated adequate predicative capability, while TOPMODEL was ineffective in this James Bay Lowland peatland environment.

The second objective involved examining nine regionalization methods within three approaches to maximize the predictive value of information to enhance rainfall-runoff simulation in peatland catchments of the James Bay Lowland. The first approach focused on regional parameter sets to calibrate ungauged sites. The median value parameter set method provided the best results overall. The weighted mean parameter set method based on the percentage of fen and bog land cover did not perform as expected. Better results were expected in an attempt to relate the unique hydrologic function of fens and bogs to model parameters. The second approach focused on methods that directly transferred parameter values based on spatial proximity or physical similarity. The spatial proximity method and the physical similarity both demonstrated similar performance. The method that combined spatial proximity and physical similarity resulted in low

model performance. The third approach applied trained statistical models to estimate model parameters. Both regression-based and artificial neural network methods yielded similar results. The application of both methods required empirical relationships between model parameters and physical catchment attributes. Among the relationships, some of them relationships had a strong physical basis while others did not.

The statistical regionalization approach yielded the best results overall. The statistical approach was the method that maximized the predictive value of information to calibrate HBV for rainfall-runoff simulation. Both methods in this approach had NS and LNS results ten to twenty percent higher than the methods in the other two approaches. These results were in contrast to previous larger comparative regionalization studies.

Overall there are two important outcomes of this study: (1) the HBV model is a reliable tool for rainfall-runoff simulation in James Bay Lowland peatland complexes, and (2) statistical models to estimate HBV model parameters or regional median parameter sets can improve predictive capabilities for ungauged catchments in this environment. The HBV model structure applied in this study is conceptually representative of peatland catchments. Further efforts to improve its applicability should be directed towards quantifying streamflow and precipitation input uncertainty. The quantification of the input uncertainty is also beneficial for the regionalization efforts. However, efforts to improve regionalization should be directed towards obtaining topographical data with a finer spatial resolution and streamflow data for a greater number of catchments. In addition, efforts to improve regionalization by reducing the dependency on *in-situ* measurements to monitor components of the water balance are important. For example: examining the applicability of MODIS products for daily evapotranspiration estimates, or the applicability of numerically simulated precipitation datasets from NARR (North American Regional Reanalysis).

The findings reported in this study provide researchers with a methodological framework that can be readily applied to simulate rainfall-runoff in James Bay Lowland peatland complexes. Potential implications are the ability to improve monitoring efforts by providing reasonable estimates of streamflow to fill gaps in observed streamflow series, verify the quality of existing monitoring records, or provide data for an ungauged catchment. Also, a well calibrated model can be used to compare simulated and observed

streamflow to detect changes in the hydrological regime. Monitoring efforts in this environment are of critical importance as a result of current and future natural resource extraction projects in Northern Ontario. In the context of PUB, both rainfall-runoff modelling and regionalization studies have been limited in this environment. This study contributes towards PUB's main initiative to reduce uncertainty in hydrologic prediction.

References

Abdi, H., and Williams, L. 2010. Jackknife. Encyclopedia of Research Design. Thousand Oaks, CA. Sage.

AghaKouchak, A., Habib, E., and Bárdossy, A. 2010. Modeling radar rainfall estimation uncertainties: a random error model. Journal of Hydrologic Engineering. 15 (4): 265–274.

AghaKouchak, A., and Habib, E. 2010. Application of a conceptual hydrologic model in teaching hydrological processes. International Journal of Engineering Education. 26(4): 963-973.

Albregtsen, F. 2008. Statistical texture measures computed from gray level co-occurrence matrices. Image Processing Laboratory, Department of Informatics University of Oslo.

Allen, R. G., Pereira, L. S., Raes, D., and Smith, M. 1998. Statistical analysis of weather data sets. In Crop evapotranspiration - Guidelines for computing crop water requirements, FAO - Food and Agriculture Organization of the United Nations (Ed.), Annex IV, FAO Irrigation and drainage paper 56, Rome: FAO.

Alm, J., Talanov, A., Saarnio, S., Silvola, J., Ikkonen, E., Aaltonen, H., Nykänen, H., and Martikainen, P. 1997. Reconstruction of the carbon balance for microsites in a boreal oligotrophic pine fen, Finland. Oecologia. 110: 423–431.

Anderson, K., Bennie, J.J., Milton, E.J., Hughes, P.D.M., Lindsay, R., and Meade, R. 2010. Combining LiDAR and IKONOS Data for Eco-Hydrological Classification. Journal of Environmental Quality. 39:260-273.

Baatz, M., and Schape, A. 2000. Multiresolution segmentation: an optimization approach for high quality multi-scale image segmentation. Angewandte Geographische Informationsverarbeitung XII. Beiträge zum AGIT Symposium Salsburg 2000. Herbert Wichmann Verlag, Karlruhe, pp. 12-23

Baboo, S., and Devi, M.R. 2010. An Analysis of Different Resampling Methods in Coimbatore, District. Global Journal of Computer Science and Technology. 10(15): 61-66.

Bao, Z., Zhang, J., Liu, J., Fu, G., Wang, G., He, R., and Liu, H. 2010 Comparison of regionalization approaches based on regression and similarity for predictions in ungauged catchments under multiple hydro-climatic conditions. Journal of Hydrology. 466: 37-46.

Barling, R., Moore, I., and Grayson, R. 1994. A quasi-dynamic wetness index for characterizing the spatial distribution of zones of surface saturation and soil water content. Water Resources Research. 30(4): 1029-1044.

Bastolla, S., Ishidaira, H., and Takeuchi, K. 2008. Regionalisation of hydrological model parameters under parameter uncertainty: A case study involving TOPMODEL and basins across the globe. Journal of Hydrology. 357: 188-206.

Belyea, L. R., and Clymo, R. S. 2001. Feedback control of the rate of peat formation. Proceedings of the Royal Society of London: Biological Sciences. 268: 1315–1321.

Bendjoudi, H., and Hubert, P. 2002. Le coefficient Gravelius: Analyse critique d'un indice de courbes intensite-duree-frequence des precipitation. Academie Science Paris.

Bergström, S. 1976. Development and application of a conceptual runoff model for Scandinavian catchments. Department of Water Resources Engineering, Lund Institute of Technology, University of Lund. Lund, Sweden.

Bergström, S. 1995. The HBV model. *In* Computer models of watershed hydrology. *Edited by* V.P. Singh. Water Resources Publications, Highlands Ranch, Colorado. pp. 443-476.

Bernier, M., Ghedira, H., Magagi, R., Fillion, R., De Seve, D., Ouarde, T., Villeneuve, J., and Buteau, P. 2003. Détection et classification de tourbières ombrotrophes du Québec à partir d'images RADARSAT-1. Canadian Journal of Remote Sensing. 29(1): 88-98.

Beven, K. J., and Kirkby, M. J. 1979. A physically based variable contributing area model of catchment hydrology. Hydrological. Science Bulletin. 24: 43-69.

Beven, K. J. 1984. Infiltration into a class of vertically non-uniform soils. Hydrological Science Journal. 29: 425-434.

Beven, K.J., and Binley, A.M. 1992. The future of distributed models: model calibration and uncertainty prediction. Hydrological Processes. 6(3): 279–298.

Beven K.J. 1993. Prophecy, reality, and uncertainty in distributed hydrological modelling. Advance Water Resources. 16: 41-51.

Beven, K., Lamb, R., Quinn, P., Romanowicz, R., and Freer, J. 1995. TOPMODEL. *In* Computer models of watershed hydrology. *Edited by* V.P. Singh. Water Resources Publications, Highlands Ranch, Colorado. pp. 627-668.

Beven, K. J. 1997. TOPMODEL: A critique. Hydrological Processes. 11: 1069-1085.

Beven, K. 2000. Uniqueness of place and process representations in hydrological modelling. Hydrology and Earth Systems Science. 4(2): 203-2013.

Beven, K., and Freer, J. 2001. A Dynamic TOPMODEL. Hydrological Processes. 15: 1993-2011.

Beven, K.J., and Freer, J. 2001. Equifinality, data assimilation, and uncertainty estimation in mechanistic modelling of complex environmental systems. 249: 11–29.

Beven, K. 2006. A manifesto for the equifinality thesis. Journal of Hydrology. 320(2): 18-36.

Beven, K. 2009. Environmental Modelling: An Uncertain Future? An introduction to techniques for uncertainty estimation in environmental prediction. Routledge, New York.

Branham, J. 2013. Spatial variability of soil hydrophysical properties in Canadian sphagnum dominated peatlands. M.Sc. thesis, Department of Geography, University of Calgary, Calgary, AB.

Blöschl, G., and Sivapalan, M. 1995. Scale issues in hydrological modeling: a review. Hydrological Processes. 9: 251–290.

Blöschl, G. 2005. Rainfall–runoff modelling of ungauged catchments. *In* Encyclopedia of hydrological sciences Volume 3 Part 11. *Edited by* G. Anderson. Chichester: Wiley.

Bouhgton, W. 2007. Effect of data length on rainfall-runoff modelling. Environmental Modelling & Software. 22(3): 406-413.

Bocco, M., Willington, E., and Arias, M. 2009. Comparison of regression and neural networks models to estimate solar radiation. Chilean Journal of Agriculture Research. 70(3): 428-435.

Boehner, J., Koethe, R., Conrad, O., Gross, J., Ringeler, A., and Selige, T. 2002. Soil regionalization by means of the terrain analysis and process parameterization. Soil Classification. 7:213-222.

Bojanowski, J. 2013. Functions for calculating daily solar radiation and evapotranspiration. Sirad R package.

Bubier, JL., Moore, T., and Juggins, S. 1995. Predicting methane emissions from bryophyte distribution in northern Canadian peatlands. Ecology. 83: 403-420.

Burt, T. P. Butcher., D. P. 1985. Topographic controls of soil moisture distributions. Soil Science Society of America Journal. 36:469-486.

Chang, K., and Tsai, B. 1991. The effect of DEM resolution on slope and aspect mapping. Cartography and Geographic Information Systems. 18: 69–77.

Charrier, R., and Li, Y. 2012. Assessing resolution and source effects of digital elevation models on automated floodplain delineation: A case study from the Camp Creek Watershed, Missouri. Applied Geography. 34: 38-46.

Chen, M., Tucker, C., Vallabhaneni, P.E., Koran, J., Gatterdam, M., and Wride, D. 2003. Comparing Different Approaches of Catchment Delineation. Metropolitan Sewer District of Greater Cincinnati. Cincinnati, OH.

Chen, B., Jing, L., and Zhang, B. 2012. Investigation and modelling of subarctic wetland hydrology – A case study in the Deer River Watershed, Canada. *In* Management of Mountain Watersheds. *Edited by* J. Krecek, J. Martin, T. Hofer, and E. Kubin. pp. 56-82.

Cheng, L., Yaeger, M., Coopersmith, E., and Sivapalan, M. 2012. Exploring the physical controls of regional patterns of flow duration curves—part 1: insights from statistical analyses. Hydrology and Earth System Sciences. 16: 4435–4446.

Chiu, W. Y., and Couloigner, I. 2004. Evaluation of incorporating texture into wetland mapping from multispectral images. EARSeL eProceedings. 3(3): 363-371.

Congalton, R. 1991. A review of assessing the accuracy of classifications of remotely sensed data. Remote Sensing Environment. 37: 35-46.

Davidson, B., and Kamp, G.V.D. 2013. Low-Flows in Deterministic Modelling: A Brief Review. Canadian Water Resources Journal. 33(2): 181-194.

Devito, K., Hill, A., and Roulet, N. 1996. Groundwater-surface water interactions in headwater forested wetlands of the Canadian Shield. Journal of Hydrology. 181: 127-147.

Dey, V., Zhang, Y., and Zhong, M. 2010. A Review on Image Segmentation Techniques with Remote Sensing Perspective. ISPRS TC VII Symposium.

Di Febo, A. 2011. On developing an unambiguous peatland classification using fusion of IKONOS and LiDAR DEM terrain derivatives – Victor Project, James Bay Lowlands. M.Sc. thesis, Department of Geography, University of Waterloo. Waterloo, ON.

Digital Globe. ND. Data Sheet: Standard Imagery. Longmont, Colorado.

Dissanska, M., Bernier, M., and Payette, S. 2009. Object-based classification of very high resolution panchromatic images for evaluating recent change in the structure of patterned peatlands. 35(2): 189-215.

Dubreuil, P. 1974. Initiation à l'analyse hydrologique. Masson & Cie. et Orstom, Paris.

Eckhardt, R. 1987. Stan Ulam, John Von Neumann and the Monte Carlo Method. Los Alamos Science Special Issue.

Edward, P., and Bates, C.B. 2001. Regionalization of rainfall-runoff model parameters using Markov Chain Monte Carlo samples. Water Resources Research. 37(3): 731-739.

Engeland, K., and Hisdal, H. 2009. A comparison of low flow estimates in ungauged catchments using regional regression and the HBV-Model. Water Resources Management. 23: 2567-2586.

Environment Canada. 2003. Canadian Climate Normals or Averages 1971-2000. Environment Canada. http://climate.weatheroffice.gc.ca/ climateData/canada_e.html (Accessed 2013).

Franzen, L.G. 2006. Increased decomposition of subsurface peat in Swedish raised bogs: are temperate peatlands still net sinks of carbon?. Mires and Peat. 1(3).

GeoEye. 2010. GeoEye Product Guide V.2.

Glaser, P., Hansen, B., Siegel, D., Reeve, A., and Morin, P. 2004. Rates, pathways and drivers for peatlands development in the Hudson Bay Lowlands, northern Ontario, Canada. Journal of Ecology. 92: 1036-1053.

Gorham, E. 1991. Northern peatlands: role in the carbon cycle and probably responses to climatic warming. Ecological Applications. 1(2): 182-195.

Goswami, M., and O'Connor, K. M. .2006. Flow simulation in an ungauged basin: an alternative approach to parameterization of a conceptual model using regional data, in Large sample basin experiments for hydrological model parameterization. IAHS publication 307. Wallingford. pp.149–158.

Goswami, M., O'Connor, K., and Bhattarai, K. P. 2007. Development of regionalization procedures using a multi-model approach for flow simulation on an ungauged catchment. Journal of Hydrology. 333: 517–531.

Grenier, M., Labrecque, S., Garneau, M., and Tremblay, A. 2008. Object-based classification of a SPOT-4 image for mapping wetlands in the context of greenhouse gases emissions: the case of the Eastmain region, Québec, Canada. Canadian Journal of Remote Sensing. 34: 398-413.

Guntner, A., Uhlenbrook, S., Seibert, J., and Leibundgut, C. 1999. Multi-criteria validation of TOPMODEL in a mountainous catchment. Hydrological Processes. 13: 1603-1620.

Haan, C. T. 1977. Statistical Methods in Hydrology. The Iowa State University Press, Ames.

Haralick R.M., Shanmugam, K., and Dinstein, I. 1973. Textural features for image classification. IEEE Transactions on Systems, Man and Cybernetics. 3(6): 610-621.

Heikkinen, J., Maljanen, M., Aurela, M., Hargreaves, K., and Martikainen, P. 2002. Carbon dioxide and methane dynamics in a subarctic peatland in northern Finland. Polar Research. 21(1): 49-62.

Heuvelmans, G., Muys, B., and Feyen, J. Regionalization of the parameters of a hydrological model: Comparison of linear regression models with artificial neural nets. Journal of Hydrology. 319: 245-265.

Hornberger G.M., and Spear, R.C. 1981. An approach to the preliminary analysis of environmental systems. Journal of Environmental Management. 12: 7-18.

Hracchowitz, M., Savenije, H., Bloschl, G., McDonnell, J., Sivapalan, M., Pomeroy, J., Arheimer, B., Blume, T., Clark, M., Ehret, U., Fenicia, F., Freer, J., Gelfan, A., Gupta, H., Hughes, D., Hut, R., Montanari, A., Pande, S., Tetzlaff, D., Troch, P.A., Uhlenbrook, S., Wagener, T., Winsemius, H., Woods, R.A., Zehe, E., and Cudennec, C. 2013. A decade of Predictions in Ungauged Basins (PUB) – A Review. Hydrological Sciences Journal. 58(6): 1198-1255.

Hilbert, D. W., Roulet, N. T., and Moore, T. 2000. Modelling and analysis of peatlands as dynamical systems. Journal of Ecology. 88: 230–242.

Holden, J. 2005. Peatland hydrology and carbon release: why small-scale process matters. Philosophical Transactions of the Royal Society. 363: 2891-2913.

Huisman, J.A., Hubbard, S.S., Redman, J.D., and Anna, A.P. 2003. Measuring soil water content with ground penetrating radar: a review. Vadose Zone Journal. 2: 476–491.

Ingram, H. A. P. 1983. In Mires: Swamp, Bog Fen and Moor. Elsevier Scientific. 67-158.

IPCC. 1997. Stabilization of Atmospheric Greenhouse Gases: Physical, Biological and Socio-Economic Implications. Intergovernmental Panal on Climate Change. *Edited by* J. Houghton, L. Filho, D. Griggs, and K. Maskell.

Itasca Dever Inc. 2011. Dewatering of Victor Diamond Project, March 2011 update of March 2008 Groundwater flow model. Denver, CO.

Jakeman, G., and Hornberger, M. 1993. How much complexity is warranted in a rainfall-runoff model?. Water Resources Research. 29(8): 2637-2649.

Jenson, S.K., and Domingue, J.O. 1988. Extracting topographic structure from digital elevation data for geographic information system analysis. Photogrammetric Engineering and Remote Sensing. 54(11): 1593–1600.

Jin, X., Xu, C., Zhang, Q., and Chen, Y.D. 2009. Regionalization study of a conceptual hydrological model in Dongjiang basin, South China. Quaternary International. 208: 129-137.

Jing, L., Chen, B., and Zhang, B. 2010. A comparison study on distributed hydrological modelling of a subarctic wetland system. Energy Policy. 2: 1043-1049.

Jing, L., and Chen, B. 2011. Hydrological modeling of subarctic wetlands: comparison between SLURP and WATFLOOD. Environmental Engineering Science. 28(7): 521-533.

Jones, K.L., Poole, G., O'Daniel, S.J., Mertes, L.A.K., and Stanford, J.A. 2008. Surface hydrology of low-relief landscapes: assessing surface water flow impedance using LIDAR-derived digital elevation models. Remote Sensing of Environment. 112(11): 4148–4158.

Jost, G., Weiler, M., Gluns, D., and Alila, Y. 2007. The influence of forest and topography on snow accumulation and melt at the watershed-scale. Journal of Hydrology. 347: 101-115.

Kay, A. L., Jones, D. A., Crooks, S. M., Calver, A., and Reynard N. S. 2006. A comparison of three approaches to spatial generalization of rainfall-runoff models. Hydrological Processes. 20: 3953 – 3973.

Kazuo, O., Noda, K., Yoshida, K., Azechi, I., Maki, M., Homma, K., Hongo, C., and Shirakawa, H. 2013. Development of an Environmentally Advanced Basin Model in Asia. *In* Agricultural and Biological Sciences Crop Production. *Edited by* A.Goyal and M. Asif. InTech Open Sciences, Crotia.

Kenny, F., and Matthews, B. 2005. A methodology for aligning raster flow direction data with photogrammetrically mapped hydrology. Computers and Geoscience. 31(6): 768-779.

Kim, K.Y., Kim, B.J., and Yi, G.S. 2004. Reuse of imputed data in microarray analysis increases imputation efficiency. BMC Bioinformatics. 5(160): 1-9.

Kirchner, J. 2006. Getting the right answers for the right reasons: Linking measurements, analyses, and models to advance the science of hydrology. Water Resources Research. 42(3).

Kirkby, M., and Weyman, D. 1974. Measurements of contributing area in very small drainage basins. Seminar Series B, No. 3. Department of Geography, University of Bristol, Bristol, UK.

Kirkby, M. J. 1975. Hydrograph modelling strategies. Process in Physical and Human Geography. Heinemann, London. pp. 69-90.

Kleeberg, H.-B. 1992. Regionalisierung in Der Hydrologie Ergebnisse Von Rundgesprachen Der Deutschen. Wiley-VCH.

Kleinen, T., Brovkin, V., and Schuldt, R. 2012. A dynamic model of wetland extent and peat accumulation: results for the Holocene. Biogeosciences. 9:235-248.

Klemes, V. 1986. Operational testing of hydrological simulation models. Journal of Hydrological Sciences. 31: 13-24.

Kokkonen, T. S., Jakeman, J., Young, P.C., and Koivusalo, H. J. 2003. Predicting daily flows in ungauged catchments: model regionalization from catchment descriptors at the Coweeta Hydrologic Laboratory, North Carolina. Hydrological Processes. 17: 2219-2238.

Konrad, C.P., and Voss, F.D. 2012. Analysis of streamflow-gaging network for monitoring stormwater in small streams in the Puget Sound basin, Washington. USGS Scientific Investigation Report. WA.

Kotsiantis, S., Kostoulas, A., Lykoudis, S., Argiriou, A., and Menagias, K. 2006. Filling missing temperature values in weather data banks. 2nd IEE International Conference on Intelligent Environments. 1: 327-334.

Kouwan, N., Soulis, E., Pietroniro, A., Donald, J., and Harrington, R. 1993. Grouped response units for distributed hydrologic modelling. ASCE Journal of Water Resources Planning and Management. 119: 289–305.

Krause, S., and Bronstert, A. 2005. An advanced approach for catchment delineation and water balance modelling within wetlands and floodplains. Advances in Geosciences. 5: 1-5.

Krause, S., Boyle, D.P., and Base, F. 2005. Comparison of different efficiency criteria for hydrological model assessment. Advances in Geosciences. 5: 89-97.

Kuczera, G., Raper, G.P., Brah, N.S., and Jayasuriya, M.D.A. 1993. Modelling yield changes following strip thinning in a mountain ash catchment: An exercise in catchment model validation. Journal of Hydrological Sciences. 150: 433-457.

Kuczera, G., and Parent, E. 1998. Monte Carlo assessment of parameter uncertainty in conceptual catchment models: the Metropolis algorithm. Journal of Hydrology. 211(1-4): 69-85.

Lane, S.N., Brookes, C.J., Kirkby, M.J., and Holden, J. 2004. A network-index-based version of TOPMODEL for use with high-resolution digital topographic data. Hydrological Processes. 18(1): 191-201.

Lane, S.N., Reaney, S.M., and Heathwaite, A.L. 2009. Representation of landscape hydrological connectivity using a topographically driven surface flow index. Water Resources Research. 45(8).

Lang, S., Albrecht, F., and Blaschke, T. ND. Introduction to Object-based Image Analysis OBIA – Tutorial. Rochester, NY.

Lee, H., McIntyre, N., Wheater, H., and Young, A. 2005. Selection of conceptual models for regionalisation of the rainfall-runoff relationship. Journal of Hydrology. 312(1-4): 125-147.

Lanza, L.G., and Stagi, L. 2008. Certified accuracy of rainfall data as a standard requirement in scientific investigations. Advances in Geosciences. 16: 43-48.

Legates, D. R., and McCabe, G.J. 1999. Evaluating the use of "goodness-of-fit" measures in hydrologic and hydroclimatic model validation. Water Resources Research. 35(1): 233-241.

Lewis, C., Albertson, J., Xu, X., and Kiely, G. 2011. Spatial variability of hydraulic conductivity and bulk density along a blanket peatland hillslope. Hydrological Processes. 26(10): 1527-1537.

Lu, D., and Weng, Q. 2007. A survey of image classification methods and techniques for improving classification performance, International Journal of Remote Sensing. 28(5):823-870.

Lunt, I.A., Hubbard, S.S., and Rubin, Y. 2005. Soil moisture content estimation using ground-penetrating radar reflection data. Journal of Hydrology. 307: 254–269.

Lyon, S., Nathanson, M., Spans, A., Grabs, T., Hjalmar, L., Temnerud, J., Bishop, K., and Seibert, J. 2012. Specific discharge variability in a boreal landscape. Water Resources Research. 48(8).

Ma, J., Lin, G., Chen, J., and Yang, L. 2010. An improved topographic wetness index considering topographic position. Geoinformatics.

Maidment, D.R. 2002. Arc Hydro: GIS for water resources. ESRI Press Inc. Redlands, CA. pp. 208.

Matei, D. 2012. Runoff modeling using GIS. Application in torrential basins in the Apuseni Mountains. Ph.D. thesis, Department of Physical and Technical Hydrology, University Babeş-Bolyai, Cluj-Napoca, Romania.

McGuire, K. J., McDonnell, J. J., Weiler, M., Kendall, C., McGlynn, B. L., Welker, J. M., and Seibert, J. 2005. The role of topography on catchment-scale water residence time. Water Resources Research. 41.

McIntyre, N., Lee, H.,Wheater, H.,Young, A., and Wagener T. 2005. Ensemble predictions of runoff in ungauged catchments. Water Resources Research. 41.

McMillan, H., Jackson, B., Clark, M., Kavetski, D., and Woods, R. 2010. Input Uncertainty in Hydrological Models: An Evaluation of Error Models for Rainfall. Journal of Hydrology. 400(1-2): 83-94.

Mahoney, M. L., Hanson, A. R., and Gilliland, S. 2007. An evaluation of a methodology for wetland classification and inventory for Labrador. Department of Environment Canada. 480: 1 – 29.

Marshall, L., Nott, D., and Sharma, A. 2004. A comparative study of Markov chain Monte Carlo methods for conceptual rainfall-runoff modeling. Water Resources Research. 40(2).

Marechal, D., and Holman, I.P. 2005. Development and application of a soil classification based conceptual catchment scale hydrological model. Journal of Hydrology. 312: 277–293.

Masih, I., Uhlenbrook, S., Maskey, S., and Ahmad, M.D. 2010. Regionalization of a conceptual rainfall‐runoff model based on similarity of the flow duration curve: A case study from the semi-arid Karkheh basin, Iran. Journal of Hydrology. 391(1-2): 188-201.

Merz, R., and Bloschl, G. 2004. Regionalisation of catchment model parameters. Journal of Hydrology. 287: 95–123.

Mazvimavi, D., Meijerink, A.M.J., and Stein, A. 2004. Prediction of base flows from basin characteristics: a case study from Zimbabwe. Hydrological Sciences Journal. 49 (4): 703–715.

Mazvimavi, D., Meijerink, A.M.J., Savenije, H.H.G., and Stein A. 2005. Prediction of flow characteristics using multiple regression and neural networks: a case study in Zimbabwe. Phyics and Chemistry of the Earth. 30(11-16): 639–647.

McCuen, R. 2005. Hydrological Analysis and Design. Pearson Prentice Hall. New Jersey: Upper Saddle River.

Metcalfe, R.A., and Buttle, J.M. 2001. Soil partitioning and surface store controls on spring runoff from a boreal forest peatland basin in north-central Manitoba, Canada. Hydrological Processes. 15: 2305-2324.

Metropolis, N. Ulam, S. 1949. The Monte Carlo Method. Journal of American Statistical Association. 44(247).

Miller, R. 1974. The jackknife – a review. Biometrika. 61(1): 1-15.

Ministry of Natural Resources. 2012. Technical Release Ontario Integrated Hydrology Data: Elevation and Mapped Water Features for Provincial Scale Hydrology Applications. Peterborough, ON.

Ministry of Natural Resources. 2013. Water Resources Information Program: Provincial Digital Elevation Model (DEM). Peterborough, ON.

Moriasi, D., Arnold, J., Van Liew, M., Bingner, R., Harmel, T., and Vieth, T. 2007. Model evaluation guidelines for systematic quantification of accuracy in watershed simulations. American Society of Agriculture and Biological Engineers. 50(3): 885-900.

Morris, S.E., Cobby, D.C., Donovan, B. 2011. Developing indicators to detect changes in the seasonality, frequency and duration of medium and high river flows. Water Environment Journal. 26: 38-46.

Muller, C., Hellebrand, H., Seeger, M., and Schobel, S. 2009. Identification and regionalization of dominant runoff processes – a GIS-based and a statistical approach. Hydrology and Earth Systems Sciences. 13: 779-792.

Nourani, V., Roughani, A., and Gebremichael, M. 2011. TOPMODEL capability for rainfall-runoff modelling of the Ammameh watershed at different time scales using different terrain algorithms. Journal of Urban and Environmental Engineering. 5(1): 1-14.

Oudin, L., Andréassian, V., Perrin, C., Michel, C., and Le Moine, N. 2008. Spatial proximity, physical similarity, regression and ungauged catchments: A comparison of regionalization approaches based on 913 French catchments. Water Resources. Research. 44(3).

Oudin, L. Kay, A. Andreassian, V. Perrin, C. 2010. Are seemingly physically similar catchments truly hydrologically similar? Water Resources Research. 46.

Ozesmi, S. L., and Bauer, M. E. 2002. Satellite remote sensing of wetlands. Wetlands Ecology and Management. 10:381-402

Pallard, B., Castellarin, A., and Montanari, A. 2009. A look at the links between drainage density and flood statistics. Hydrology and Earth System Sciences. 13: 1019–1029.

Parajka, J., Merz, R., and Blöschl, G. 2005. A comparison of regionalisation methods for catchment model parameters. Hydrology and Earth System Sciences. 9: 157–171.

Parajka, J., and Blöschl, G. 2006. Validation of MODIS snow cover images over Austria. Hydrology and Earth System Sciences. 10: 679–689.

Parajka, J., and Blöschl, G. 2008. Spatio-temporal combination of MODIS images—potential for snow cover mapping. Water Resources Research. 44.

Parker, J., Kenyon, R., and Troxel, D. 1983. Comparison of interpolating methods for image resampling. IEEE Transactions on Medical Imaging. 2(1): 31-39.

Pastor, J., Solin, J., Bridgham, S., Updegraff, K., Harth, C., Weishampel, P., and Dewey, B. 2003. Global Warming and the export of dissolved organic carbon from boreal peatlands. Oikos. 100: 380-386.

Peel, M., Chiew, F., Western, A., and McMahon, T. 2000. Extension of unimpaired monthly streamflow data and regionalization of parameter values to estimate streamflow in ungauged catchments. National Land and Water Resources Audit. Centre for Environmental Applied Hydrology The University of Melbourne.

Pilgrim, D. H. 1983. Some problems in transferring hydrological relationships between small and large drainage basins and between regions. Journal of Hydrology. 65: 49-72.

Price, J. S., and Maloney, D. A. 1994. Hydrology of a Patterned Bog-Fen Complex in Southeastern Labrador Canada. Geography. 25(5): 313-330.

Price, J.S., and Schlotzhauer S.M. 1999. Importance of shrinkage and compression in determining water storage changes in peat: the case of a mined peatland. Hydrological Processes. 13: 2591–2601

Price, J.S. 2003. Role and character of seasonal peat soil deformation on the hydrology of undisturbed and cutover peatlands. Water Resources Research. 39(9): 1241.

Price, J., Branfireun, B., Waddington, M., and Devito, K. 2005. Advances in Canadian wetland hydrology, 1993-2003. Hydrological Processes. 19: 201-214.

Swanson, D. 2007. Interaction of mire microtopography, water supply, and peat accumulation in boreal mires. Finnish Peatland Society. 58(2): 37-47.

Pietroniro, A., Prowse, T., Hamlin, L., Kouwen, N., and Soulis, R. 1996. Application of a grouped response unit hydrological model to a northern wetlands region. Hydrological Processes. 10: 1245–1261.

Pomeroy, J., Spence, C., and Whitfield, P. 2013. Chapter 1 Putting Prediction in Ungauged Basins into Practice in Putting Prediction. *In* Ungauged Basins into Practice. *Edited by* J. Pomeroy, C. Spence, and P. Whitfield. Canadian Water Resources Association.

Popper, K. R. 1963. Conjectures and Refutations: The Growth of Scientific Knowledge. Routledge Classics.

Quinton, W., and Roulet, N. 1998. Spring and summer runoff hydrology of a subarctic patterned wetland. Arctic and Alpine Research. 30(3): 285-294.

Quinton, W. L., Hayashi, M., and Pietroniro, A. 2003. Connectivity and storage functions of channel fens and flat bogs in northern basins. Hydrological Processes. 17(18): 3665-3684.

Razavi, T., and Coulibaly, P. 2013. Streamflow prediction in ungauged basins: review of regionalization methods. Journal of Hydrologic Engineering. 18(8): 958-975.

Raghavendra, J., and Mohanty, B. 2012. On topographic controls of soil hydraulic parameters scaling at hillslopes scales. Water Resources Research. 48.

Reichl, J., Western, A., McIntyre, N., and Chiew, F. 2009. Optimization of a similarity measure for estimating ungauged streamflow. Water Resources Research. 45.

Renard, B., Kavetski, D., Kuczera, G., Thyer, M., and Franks, S. 2010. Understanding predictive uncertainty in hydrologic modeling: The challenge of identifying input and structural errors. Water Resources Research. 46 (5).

Richardson, M., Mitchell, C., Branfireun, B., and Kolka, R. 2010. Analysis of airborne LiDAR surveys to quantify the characteristic morphologies of northern forested wetlands. Journal of Geophysical Research. 115.

Richardson, M., Ketcheson, S., Whittington, P., and Price, J. 2012. The influence of catchment geomorphology and scale on runoff generation in a northern peatland complex. Hydrological Processes. 26(12): 1805-1817.

Riley, J.L. 2011. Wetlands of the Ontario Hudson Bay Lowland: A Regional Overview, Nature Conservancy of Canada, Toronto, ON.

Riley, S. J., DeGloria, S. D., and Elliot, R. 1999. A terrain ruggedness index that quantifies topographic heterogeneity. Intermountain Journal of Sciences. 5: 1-4.

Rodhe, A. Seibert, J. 1999. Wetland occurrence in relation to topography: a test of topographic indices as moisture indicators. Agriculture and Forest Meteorology.

Scanlon, T., Raffensperger, J., and Hornberger, G. 2000. Shallow subsurface storm flow in a forested headwater catchment: Observations and modeling using a modified TOPMODEL. Water Resources Research. 36(9): 2575-2886.

Schiff, S., Aravena, R., Mewhinney, E., Elgood, R., Warner, B., Dillon, P., and Trumbore, S. 1998. Precambrian Shield Wetlands: Hydrologic control of the sources and export of dissolved organic matter. Climatic Change. 40: 167-188.

Schumann, G., Matgen, P., Cutler, M., Hoffmann, L., and Pfister, L. 2008. Comparison of remotely sensed water stages from LiDAR, topographic contours and SRTM. ISPRS Journal of Photogrammetry and Remote Sensing. 63(3): 283–296.

Seibert, J., Bishop, K., and Nyberg, L. 1997. A test of TOPMODEL's ability to predict spatially distributed groundwater levels. Hydrological Processes. 11: 1131-1144.

Seibert, J. 1997. Estimation of parameter uncertainty in the HBV model. Nordic Hydrology. 28(4-5): 247-262.

Seibert, J. 1999. Regionalisation of parameters for a conceptual rainfall-runoff model. Agriculture and Forest Meteorology. 98(99): 279-293.

Seibert, J. 1999. Conceptual runoff models - fiction or representation of reality. Ph.D. thesis, Department of Earth Sciences, Uppsala University. Uppsala, Sweden.

Seibert, J. 2005. HBV light Version 2 User's Manual. Stockholm University Department of Physical Geography and Quaternary Geology.

Seibert, J. 2014. HBV-Light-GUI Documentation. Department of Geography, University of Zürich. Zürich, Switzerland.

Siegel, D. 1983. Groundwater and the evolution of patterned mires, glacial lake Agassiz peatlands, northern Minnesote. Journal of Ecology. 71: 913-921.

Sikorska, A.E., Scheidegger, A., Banasik, K., and Rieckermann, J. 2013. Considering rating curve uncertainty in water level predictions. Hydrology and Earth System Sciences. 17: 4415-4427.

Sivapalan, M., Takeuchi, K., Franks, S., Gupta, C., Karambiri, H., Lakshmi, V., Lian, X., McDonnell, J., Mendiondo, M., O'Connell, P., Oki, T., Pomeroy, J., Schertzer, D., Uhlenbrook, S., and Zehe, E. 2003. IAHS Decade on Predictions in Ungauged Basins (PUB), 2003–2012: Shaping an exciting future for the hydrological sciences. Hydrological Sciences Journal. 48(6).

Sivapalan, M. 2006. Pattern, Process, and Function: Elements of a Unified Theory of Hydrology at the Catchment Scale. *In* Encyclopedia of Hydrological Sciences.

Smith, L. C., MacDonald, G. M., Velichko, A. A., Beilman, D. W., Borisova, O. K., Frey, K. E., Kremenetski, K. V., and Sheng, Y. 2004. Siberian peatlands a net carbon sink and global methane source since the early Holocene. Science. 303: 353-356.

Sorensen, R., Zinko, U., and Seibert, J. 2006. On the calculation of the topographic wetness index: evaluation of different methods based on field observations. Hydrology and Earth System Sciences. 10: 101-102.

Spear, R.C., and Hornberger, G.M. 1980. Eutrophication in Peel Inlet, II, Identification of critical uncertainties via generalized sensitivity analysis. Water Resources Research. 14: 43-49.

Spence, C., and Woo M. 2003. Hydrology of subarctic Canadian shield: soil-filled valleys. Journal of Hydrology. 279: 151-166.

Spence, C., Whitfield, P., Pomeroy, J., Pietroniro, A., Burn, D. ,Peters, D., and St-Hilaire, A. 2013. A review of the Prediction in Ungauged Basins (PUB) decade in Canada. Canadian Water Resources Journal. 38(4): 253-262.

Sivapalan, M., Takeuchi, K., Franks, S.W., Gupta, V.K., McDonnell, J.J., Mendiondo, E.M., O'Connell, P.E., Oki, T., Pomeroy, J.W., Schertzer, D., Uhlenbrook, S., and Zehe, E. 2003. IAHS 25 decade on predictions in ungauged basins (PUB), 2003–2012: Shaping an exciting future for the hydrological sciences. Hydrological Sciences. 48(6):867–880.

Strack, M. 2008. Peatlands and climate change. *Edited by* Maria Strack. International Peat Society.

Tarboton, D.G. 1997. A new method for the determination of flow directions and upslope areas in grid digital elevation models. Water Resources Research. 33(2): 309-319.

Teegavarapu, R.,Viswanathan, C., and Ormsbee, L. 2006. Effect of Digital Elevation Model (DEM) Resolution on the Hydrological and Water Quality Modeling. World Environmental and Water Resource Congress 2006. 1-8.

Tomkins, K.M. 2014. Uncertainty in streamflow rating curves: methods, controls and consequences. Hydrological Processes. 28(3): 464-481.

Trimble. 2011. eCognition Developer 8.64.1 User Guide. Germany, Munich.

Trujillo, R., Ramirez, J., and Elder, K. 2007. Topography meteorologic and canopy controls on the scaling characteristics of the spatial distribution of snow depth fields. Water Resources Research. 43.

Vaze, J., Teng, J., and Spencer, G. 2010. Impact of DEM accuracy and resolution on topographic indices. Environmental Modeling and Software. 25.

Vogel, R.M., and Sankarasubramanian, A. 2003. Validation of a watershed model without calibration. Water Resources Research. 39(10).

Vrugt, J., Diks, C., Gupta, H., Bouten, W., and Verstraten, J. 2005. Improved treatment of uncertainty in hydrologic modeling: Combining the strengths of global optimization and data assimilation. Water Resources Research. 41(1).

Vrugt, J., Braak, C., Clark, M., Hyman, J., and Robinson, B. 2008. Treatment of input uncertainty in hydrological modeling: Doing hydrology backward with Markov chain Monte Carlo simulation. Water Resources Research. 44(12).

Waddington, J.M., and Roulet, N.T. 2000. Carbon balance of a boreal patterned peatland. Global Change Biology. 6: 87–97.

Wagener, T., McIntyre, N., Lees, M.J., Wheater, H.S., and Gupta, H.V. 2003. Towards reduced uncertainty in conceptual rainfall-runoff modelling: Dynamic identifiability analysis. Hydrological Processes. 17: 455-476.

Wagener, T., and Wheater, H.S. 2006. Parameter estimation and regionalization for continuous rainfall-runoff models including uncertainty. Journal of Hydrology. 320: 132-154.

Wagener, T., and Kollat, J. 2007. Numerical and visual evaluation of hydrological environmental models using the Monte Carlo analysis toolbox. Environmental Modelling & Software. 22(7): 1021-1033.

Wagener, T., Sivapalan, M. Troch, P. Woods, R. 2007. Catchment classification and hydrologic similarity. Geography Compass.1(4): 901-931.

Walter, T., Steenhuis, T., Mehta, V., Thongs, D., Zion, M., and Schneiderman, E. 2002. Refined conceptualization of TOPMODEL for shallow subsurface flows. Hydrological Processes. 12: 2041-2046.

Wilson, J.P., and Gallant, J.C. 2000. Terrain Analysis – Principles and applications. John Wiley & Sons, New York.

Whitfield, P., St-Hilaire, A., and Van Der Kamp, G. 2009. Improving hydrological predictions in peatlands. Canadian Water Resources Journal. 34: 467-478.

Whitfield, P. 2013. Exploring the statistical consequences of infilling missing observations in environmental data. Bridging Environmental Science, Policy and Resource Management Conference. SK: Saskatoon. Willmott, C. J. 1981. On the evaluation of model performance in physical geography. Physical Geography. 2: 184-194.

Whittington, P., and Price, J. 2012. Effect of mine dewatering on peatlands of the James Bay Lowland: the role of bioherms. Hydrological Processes. 26: 1818-1826.

Whittington, P. 2013. The Impacts of Diamond Mining to Peatlands in the James Bay Lowlands. Doctoral Dissertation, Department of Geography. Waterloo, ON.

Worrall, F., Burt, T., and Adamson, J. 2006. The rate and controls upon DOC loss in a peat catchment. Journal of Hydrology. 321: 311-325.

Yeh, P., and Eltahir, E. 1998. Stochastic analysis of the relationship between topography and the spatial distribution of soil moisture. Water Resources Research. 34(5): 1251-1263.

Young, A. R. 2006. Stream flow simulation within UK ungauged catchments using a daily rainfall-runoff model. Journal of Hydrology. 320: 155-172.

Yu, Z. 2012. Northern peatland carbon stocks and dynamics: a review. Biogeosciences Discussion. 9: 5073-5107.

Zhang, Y., and Chiew, F. 2009. Relative merits of different methods for runoff predictions in ungauged catchments. Water Resources Research. 45.

Appendices

Appendix A Analysis of Meteorological Variables

A.1 Comparison of Precipitation Cumulative Distributions

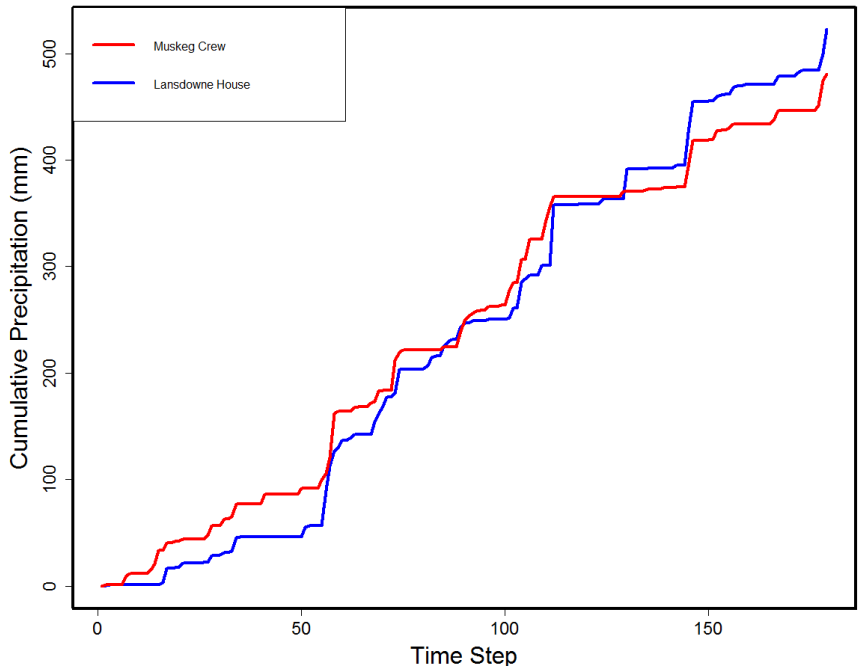

Comparison of precipitation cumulative distribution between Muskeg Crew and Lansdowne House.

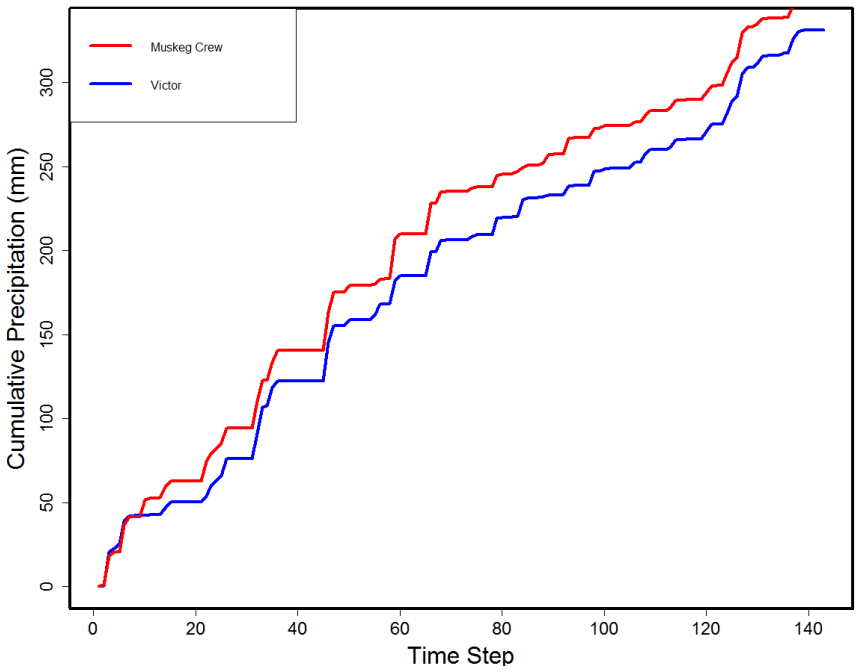

Comparison of precipitation cumulative distribution between Muskeg Crew and Victor.

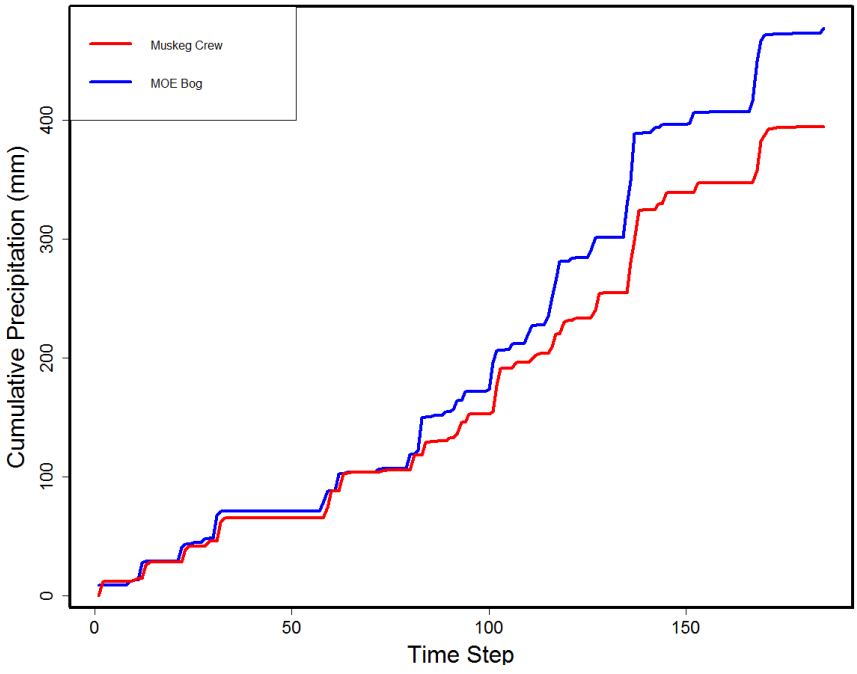

Comparison of precipitation cumulative distribution between Muskeg Crew and MOE Bog.

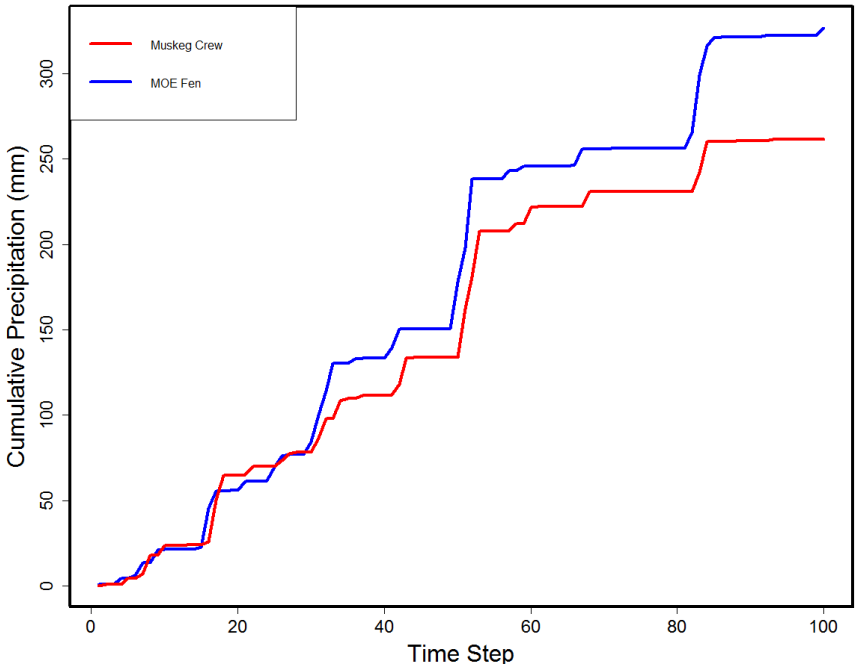

Comparison of precipitation cumulative distribution between Muskeg Crew and MOE Fen.

A.2 Homogeneity Comparison of Precipitation

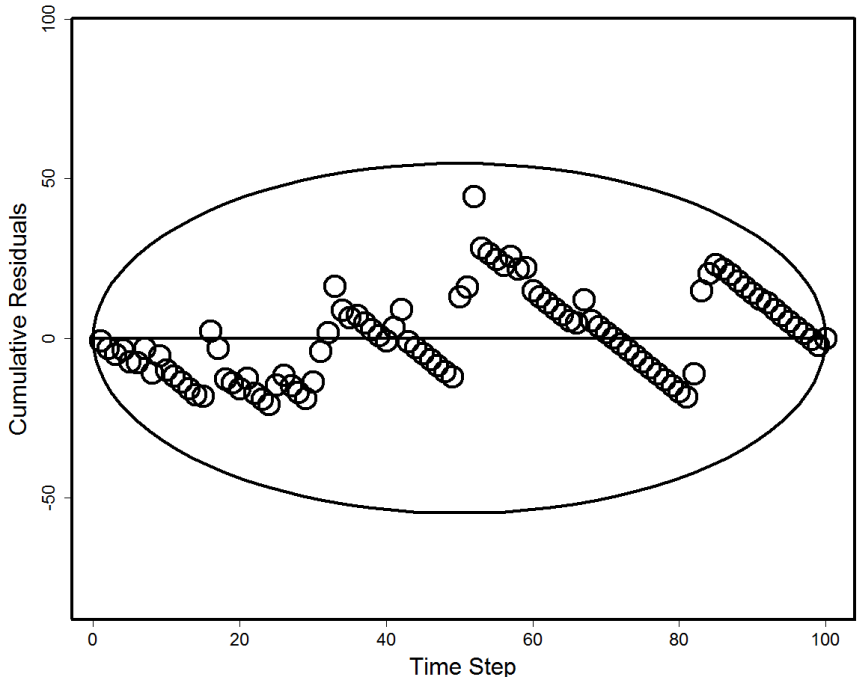

Homogeneity comparison of precipitation between Muskeg Crew and MOE Fen.

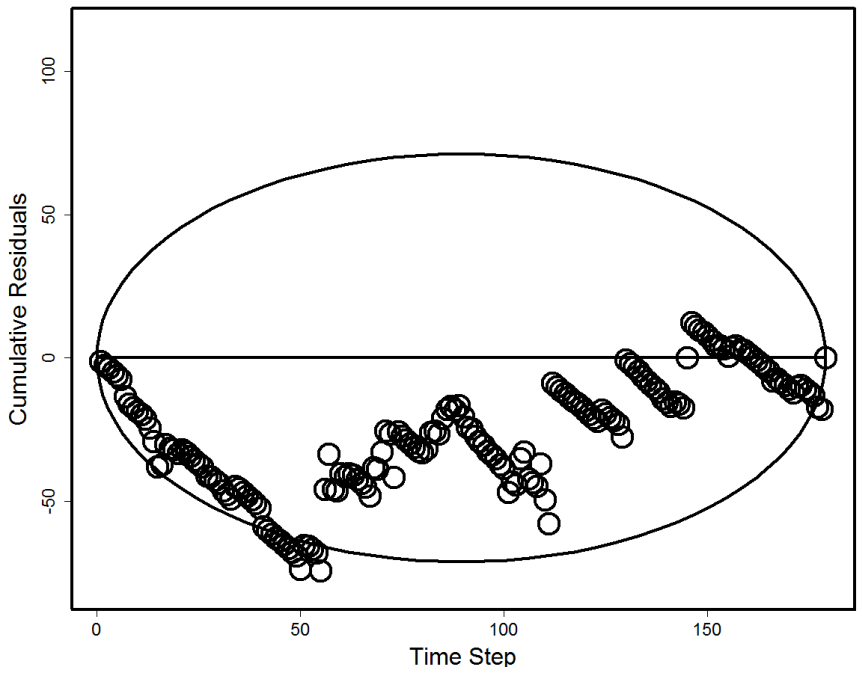

Homogeneity comparison of precipitation between Muskeg Crew and Lansdowne House.

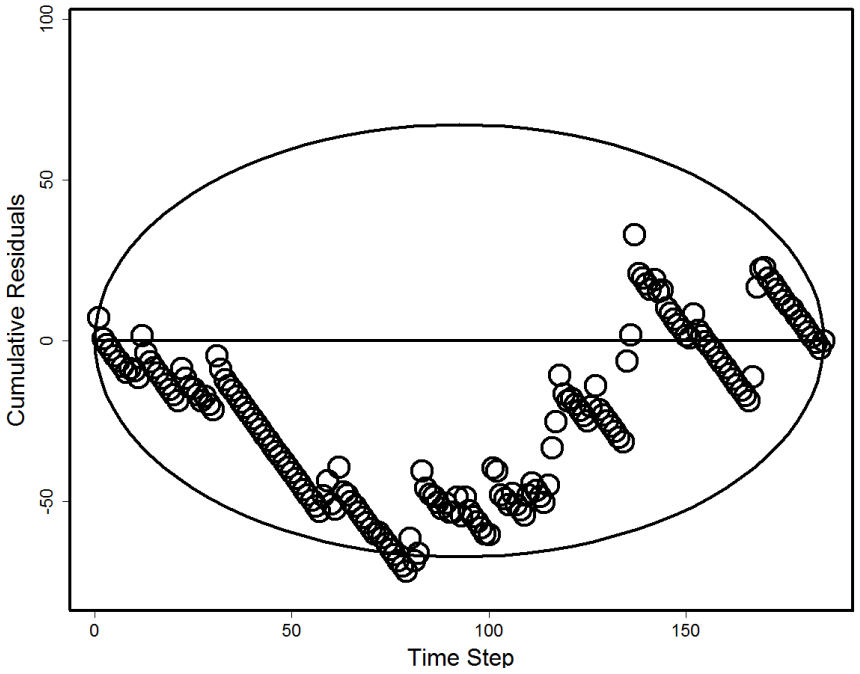

Homogeneity comparison of precipitation between Muskeg Crew and MOE Bog

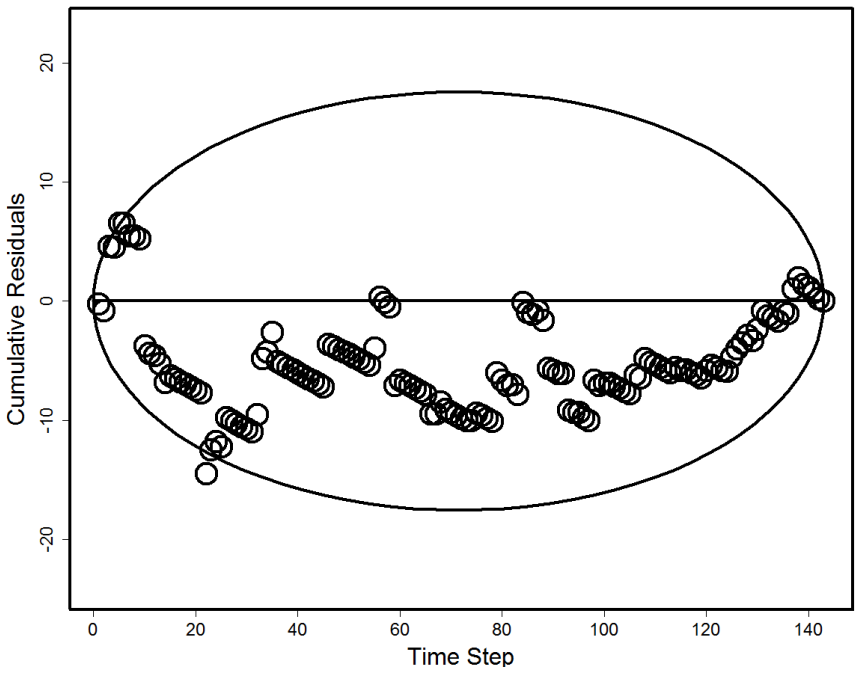

Homogeneity comparison of precipitation between Muskeg Crew and Victor

A.3 Homogeneity Comparison of Net Radiation

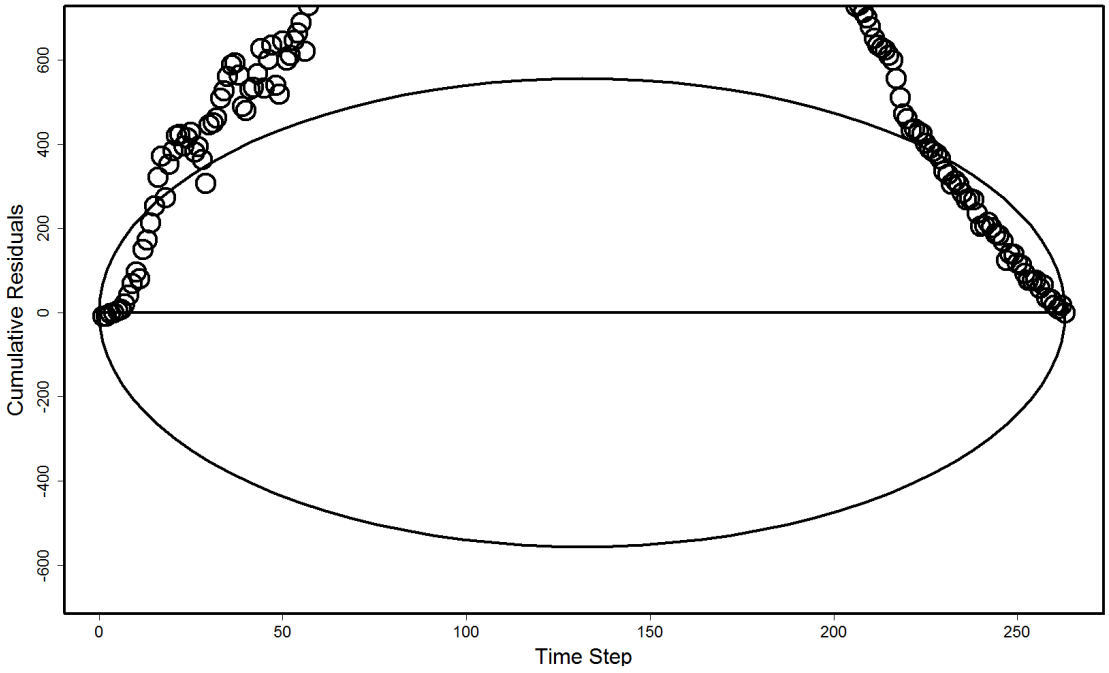

Homogeneity comparison of net radiation between Muskeg Crew and MOE Bog.

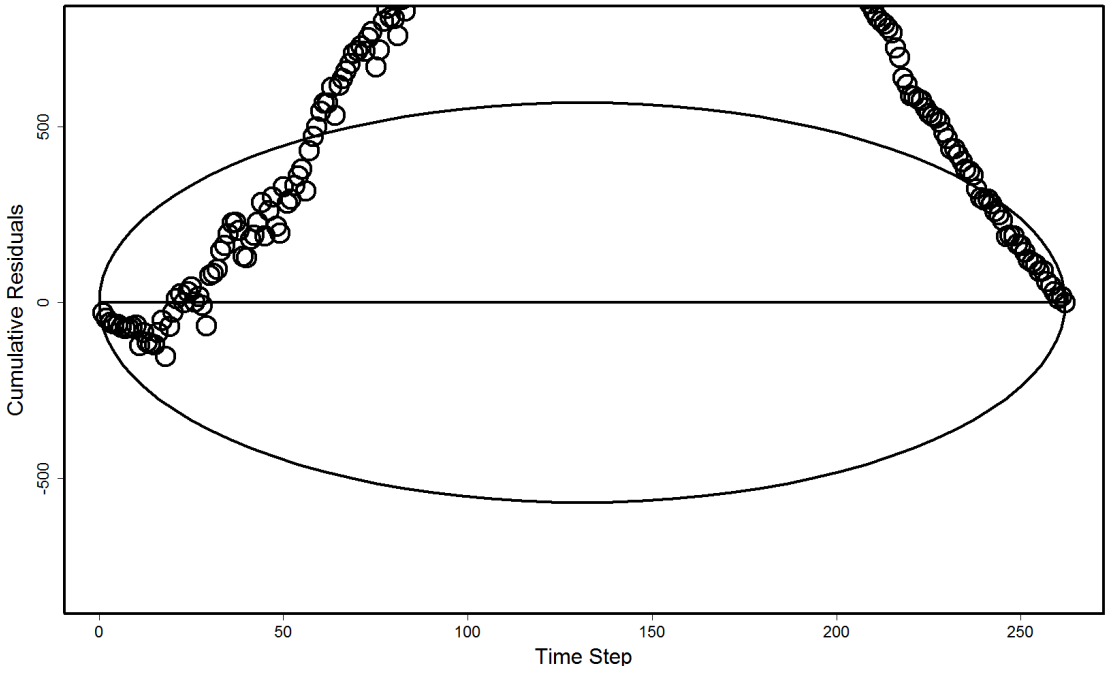

Homogeneity comparison of net radiation between Muskeg Crew and MOE Fen.

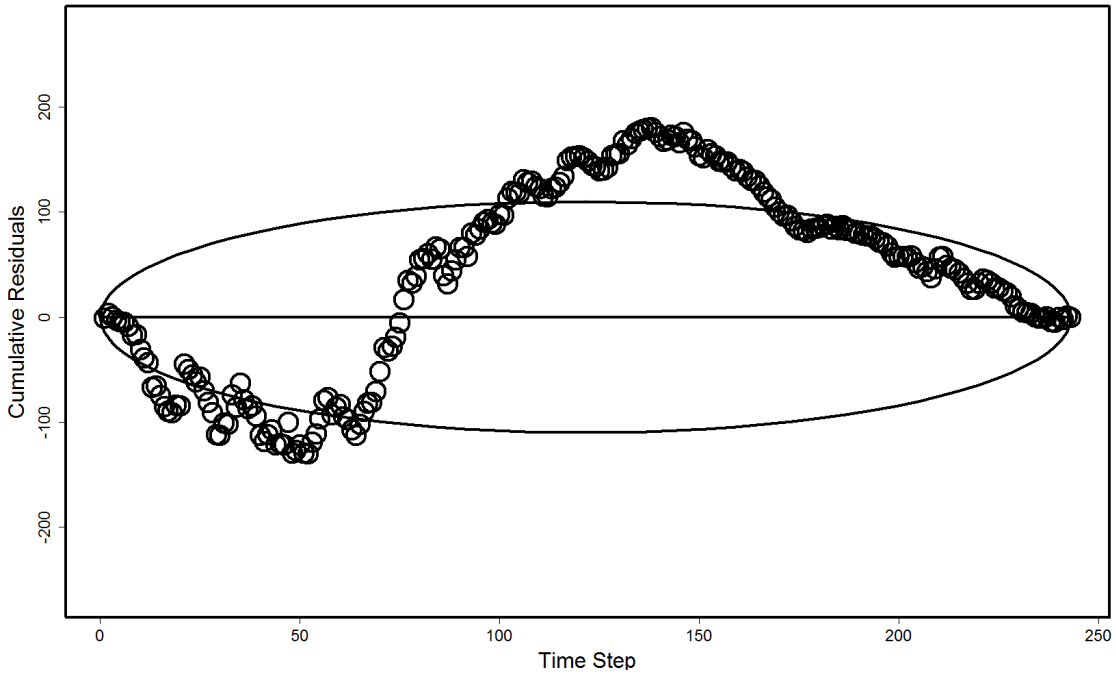

Homogeneity comparison of net radiation between Muskeg Crew and Victor.

A.4 Homogeneity Comparison of Temperature

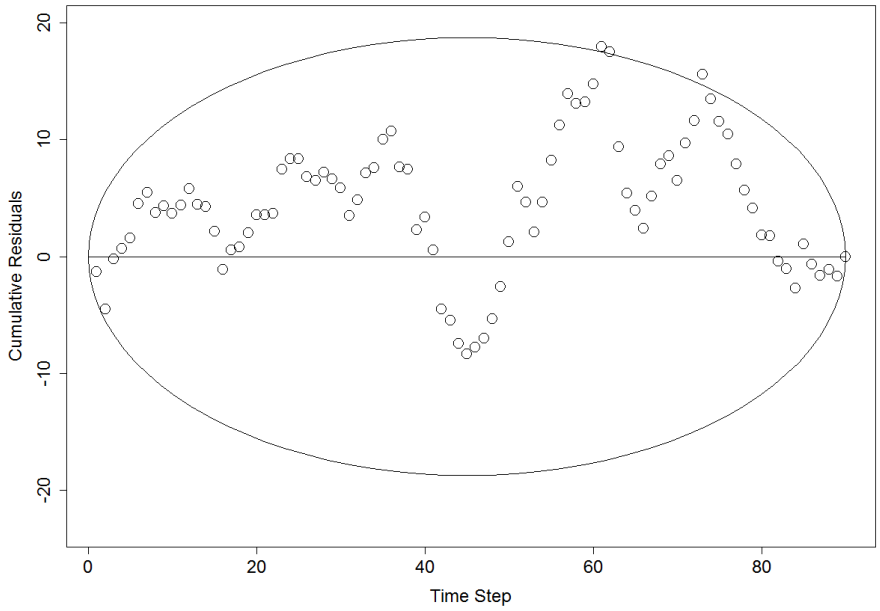

Homogeneity comparison of fall temperature between Muskeg Crew and Lansdowne House.

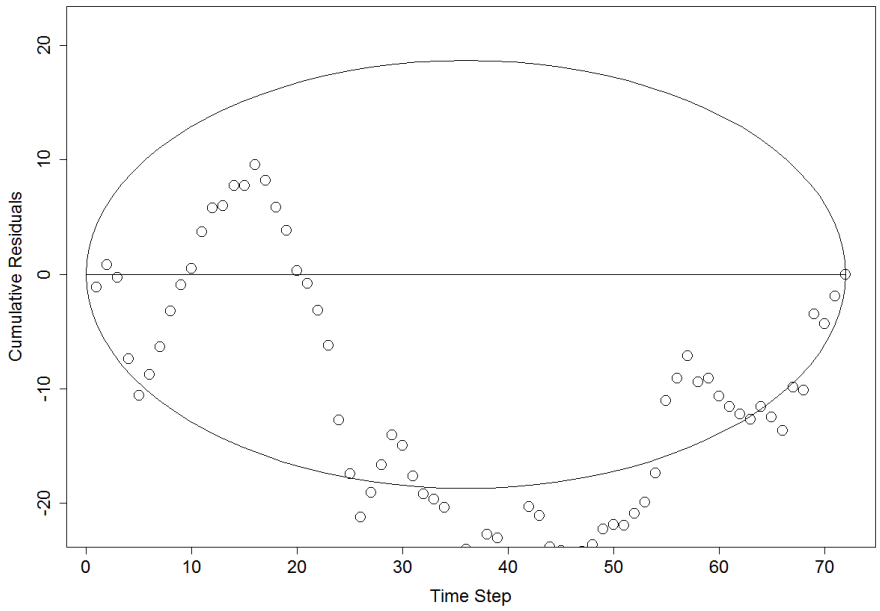

Homogeneity comparison of spring temperature between Muskeg Crew and Lansdowne House.

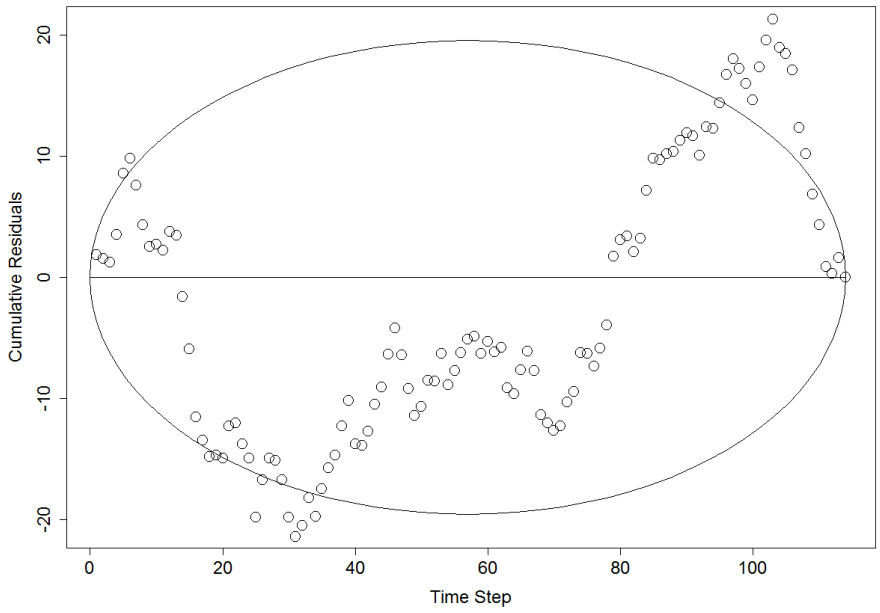

Homogeneity comparison of summer temperature between Muskeg Crew and Lansdowne House.

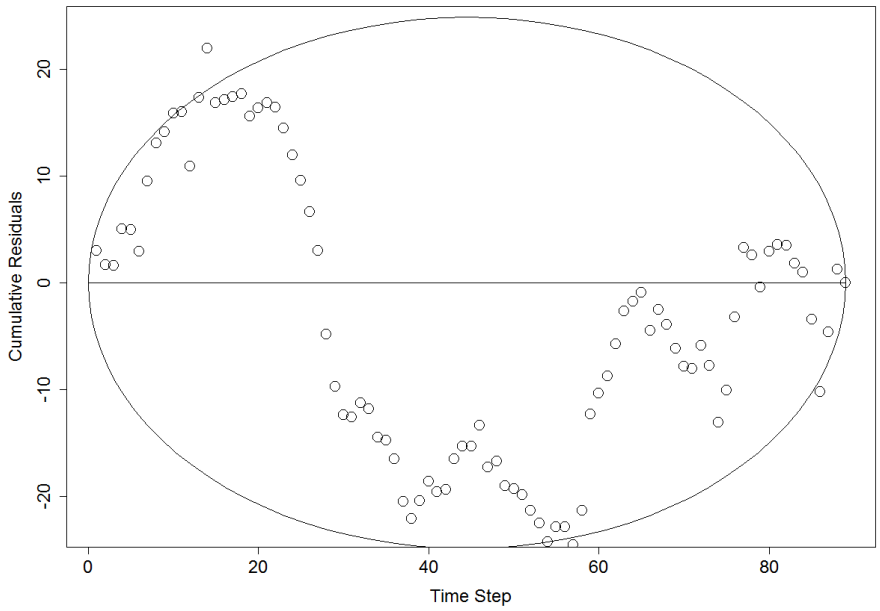

Homogeneity comparison of winter temperature between Muskeg Crew and Lansdowne House.

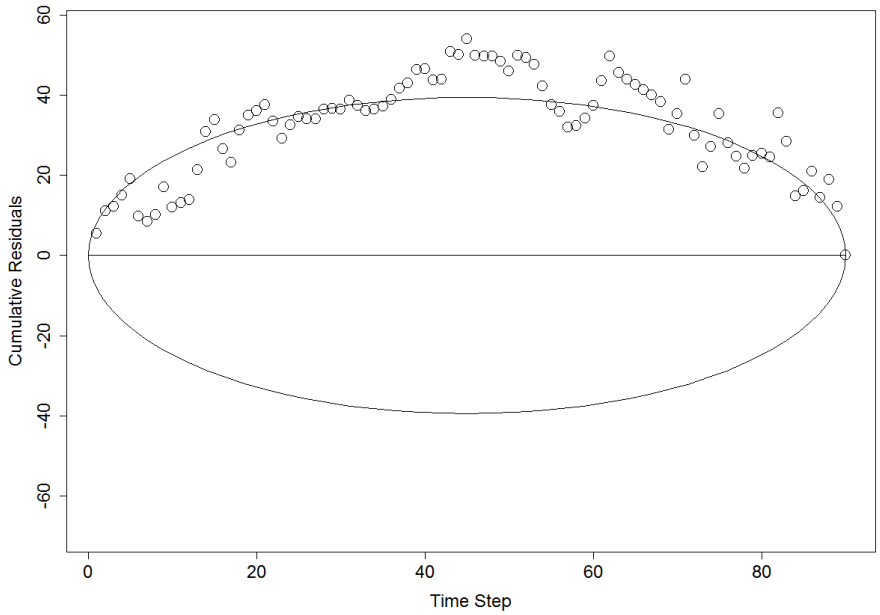

Homogeneity comparison of fall temperature between Muskeg Crew and MOE Bog.

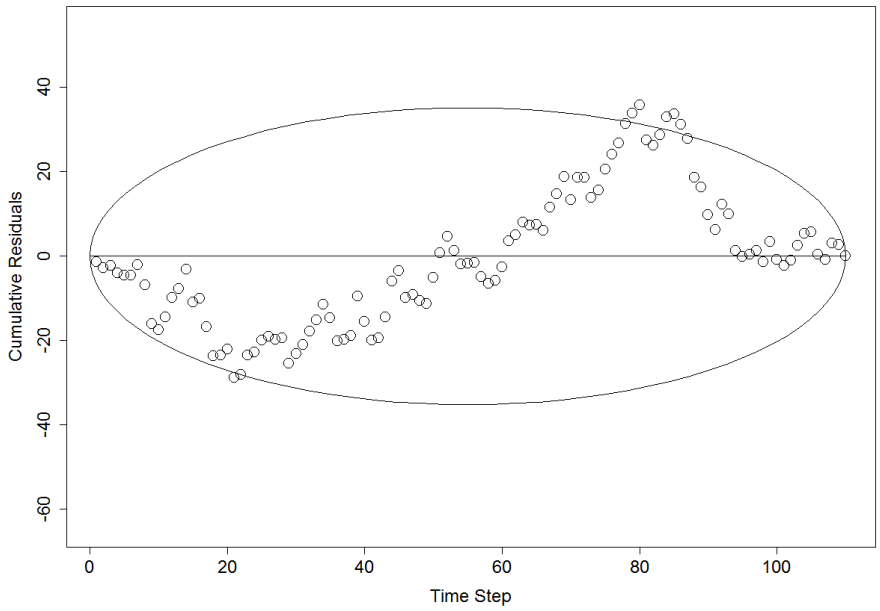

Homogeneity comparison of spring temperature between Muskeg Crew and MOE Bog.

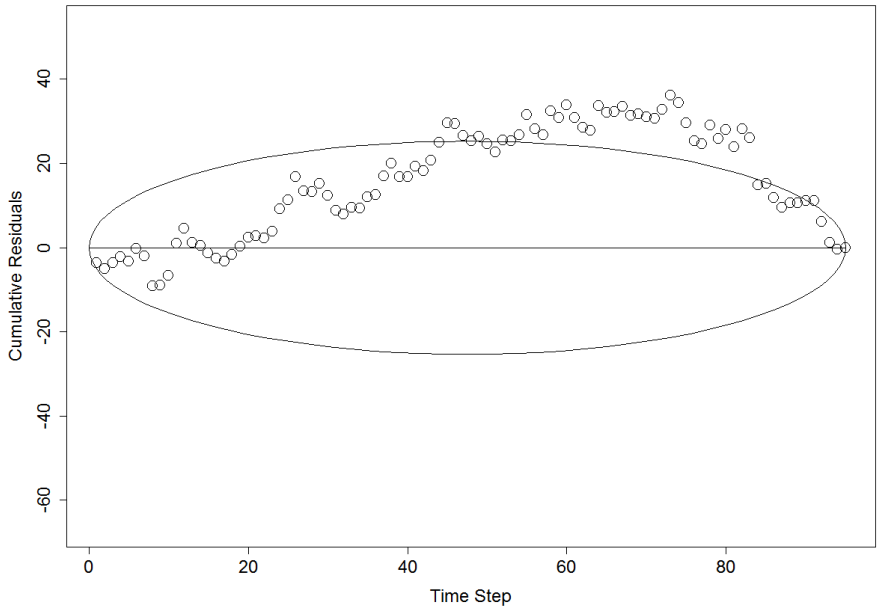

Homogeneity comparison of summer temperature between Muskeg Crew and MOE Bog.

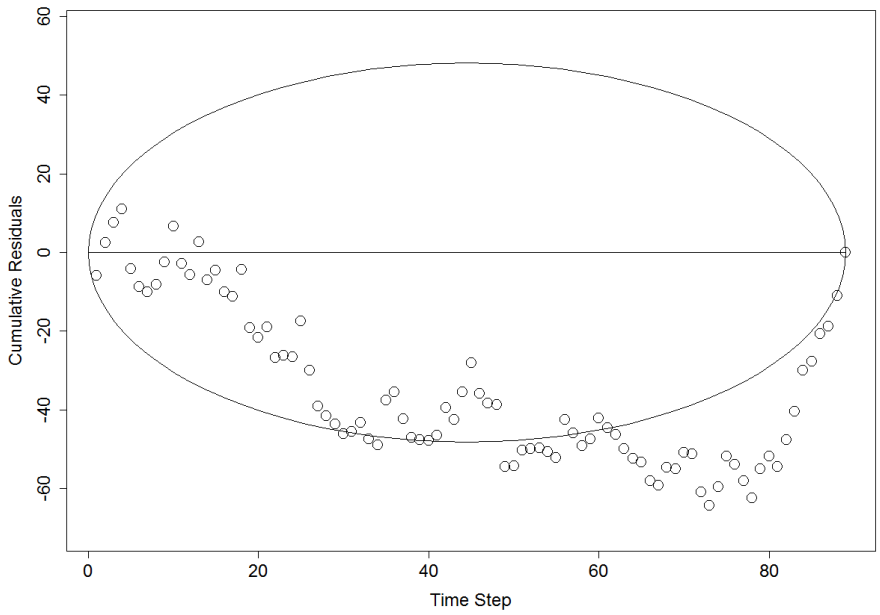

Homogeneity comparison of winter temperature between Muskeg Crew and MOE Bog.

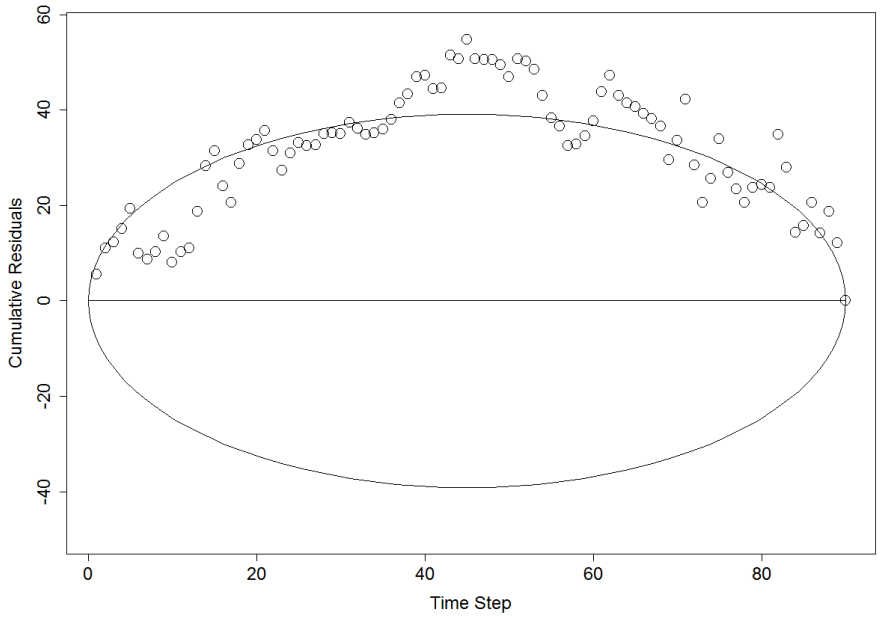

Homogeneity comparison of fall temperature between Muskeg Crew and MOE Fen.

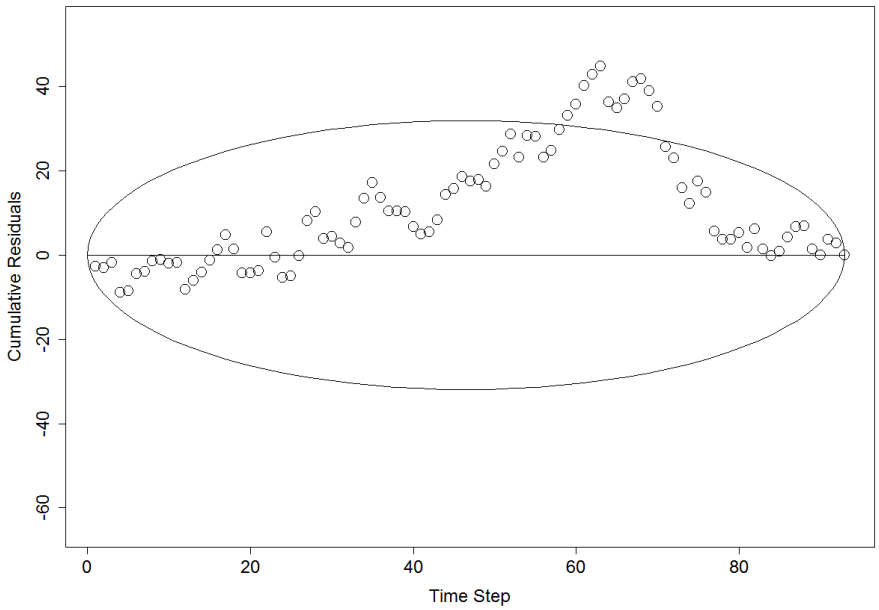

Homogeneity comparison of spring temperature between Muskeg Crew and MOE Fen.

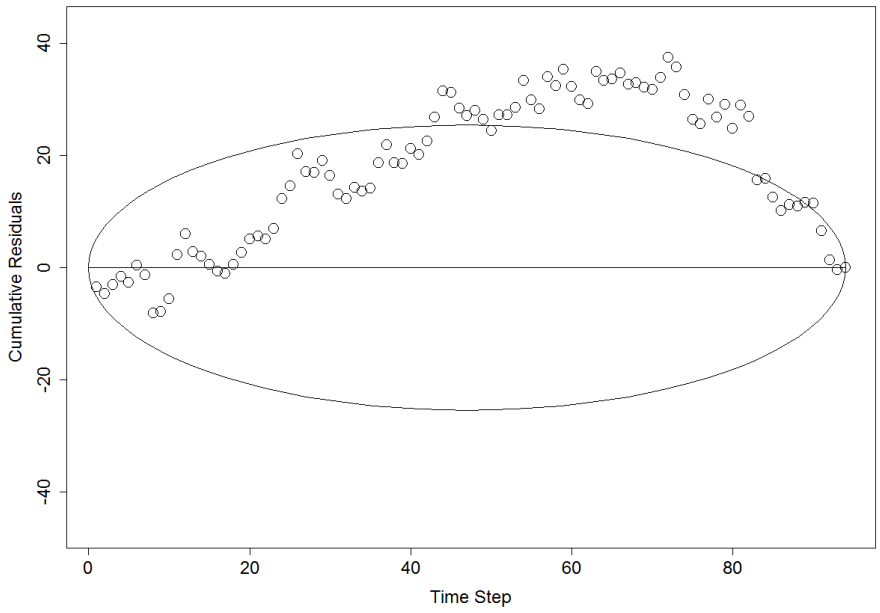

Homogeneity comparison of summer temperature between Muskeg Crew and MOE Fen.

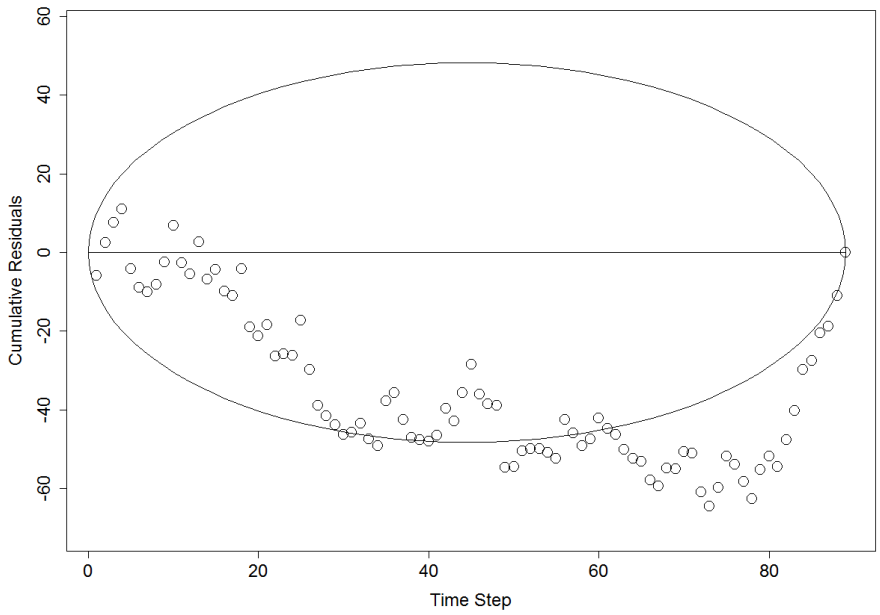

Homogeneity comparison of winter temperature between Muskeg Crew and MOE Fen.